Vol. 11 No. 2 (2022)

JTL

www.teknolabjournal.com

Vol. 11 No. 2 (2022)

CONTENT

JURNAL TEKNOLOGI LABORATORIUM

Vol. 11 No. 2 (2022)

JTL 11 (2) December 2022
Page: 52-59

Contents list available at Jurnal Teknologi Laboratorium

JURNAL TEKNOLOGI LABORATORIUM

Journal Homepage: www.teknolabjournal.com
ISSN 2580-0191(Online) I ISSN 2338 – 5634(Print)

Original Research

The wound healing effect of Morinda citrifolia leaf extract and biomolecular analysis on inflammation and proliferation stages in Wistar rats

Grace Noviyanthi Sinambela[1], **Erny Tandanu**[2], **Refi Ikhtiari**[1*]

[1] Department of Biomedical Sciences, Faculty of Medicine, Universitas Prima Indonesia, Medan, Indonesia
[2] Department of Medicine, Faculty of Medicine, Universitas Prima Indonesia, Medan, Indonesia.

Abstract: Noni leaves (Morinda citrifolia L.) are empirically used to heal wounds traditionally. The active ingredients of the leaves have benefits as antibacterial, anti-inflammatory, antioxidant, antiviral etc. This research aims to evaluate the wound healing effect of noni's leaf extract (*Morinda citrifolia L.*) based on phytochemical analysis, the number of fibroblast cells, wound diameter, healing time, TNF-α and IL-1 at inflammation stage, PDGF and TGF-β at proliferation stage. This study is a true experimental with a post-test-only control group design. We divided 25 male Wistar rats into five groups; positive control (with povidone-iodine), negative control (with no treatment), treated by NLEE 20%, 25%, and 30%. NLEE has good physical characteristics based on the value of ethanol soluble extract, water-soluble extract, water content, ash content, and acid insoluble ash content. GCMS analysis showed bioactive compounds such as N-ethyl hydrazine carbothioamide (31.57%), 2-furancarboxaldehyde 5-hydroxymethyl (15,64%), 2E-3,7,11,15-tetramethyl-2-hexadecene-1-of (7.08%), 3,5-dihydroxy-6-methyl-2,3-dihydro-4H-pyran-4-one (4.29%), D:C-friedooleana-7,9(11)-dien-3-ol,3 beta (4.04%), while the rest are considered as the decanoic acids methyl ester, piperazine (3%) and vitamin E (1%). We observed the slight effects of NLEE 20%, 25%, and 30% on the number of fibroblasts, wound diameter, healing time, TNF-α, IL-1, PDGF, and TGF-β. The optimum concentration of NLEE at any treatment was 20%. However, there were no significant differences between groups based on a two-way ANOVA analysis. This research implies a potential utilization of noni leaves as the alternative for wound healing treatments.

Keywords: Morinda citrifolia; Wound healing; Inflammation; Proliferation

INTRODUCTION

Physical and chemical trauma can cause injury [1] and disruption of skin integrity [2,3]. The side effect of commercial medicine is one of the reasons to continue the research on herbal therapy that effective and safe for wound healing application [4]. Hence, we studied a Noni leaf extract (*Morinda citrifolia L*) which was previously reported for its antibacterial, antiinflammation, antioxidants, antivirus, etc [5,6]. The potential bioactivities were supposed due to the presence of secondary metabolites; alkaloids for antibacterial, flavonoids for antiinflammation, saponins for antiseptic, tannins, and triterpenoids for antioxidants [7].

Previous studies reported that hydro alcohol extract [8], ethanol extract [9], hexane fraction [10], and cream of ethanol extract [11] have positive effects on wound healing, even though no significant effect on the healing of rat oral mucosal ulceration. A significant difference in fibroblast cells of Wistar rats was reported

Corresponding author.
E-mail address: refiikhtiari@unprimdn.ac.id (Refi Ikhtiari)
DOI: 10.29238/teknolabjournal.v11i2.369
Received 21 July 2022; Received in revised form 07 August 2022; Accepted 06 December 2022

between the cream's extract of 10% and control as well as paste's extract could reduce the inflammation of the carrageenan-induced rat paw edema [12].

The comprehensive research covering phytochemical analysis and biomarkers investigation on inflammation and proliferation stage on wound healing treated with noni's leaves ethanol extract (NLEE) is not reported yet. In this study, we report the phytochemical analysis by using GCMS then followed by wound healing evaluation based on the number of fibroblasts, wound diameter, healing time, TNF-α and IL-1 at inflammation stage, PDGF and TGF-β at proliferation stage. Data obtained were evaluated by SPSS with analysis of variance (ANOVA).

MATERIAL AND METHOD

The noni's leaves were obtained from the university's garden and then washed and dried. Noni leaves were determined in Herbarium Universitas Sumatera Utara. Simplicia powder was prepared by using a mixer, then macerated with ethanol 96% for 1 day, 3 times. After rotary evaporation, noni's leaves ethanol extracts (NLEE) were varied by 20, 25, 30 (% w/w) concentrations. Laboratory tools used were rotary evaporator (B-One), separating funnel (Schott Duran), and Waterbath (memmert). Solvents and reagents used were aquadest, ethanol 96%, chloralhydrate, ethanol 96%, ethyl acetate, methanol, chloroform, n-hexane, FeCl, bourchardat reagent, Mayer's reagent, NaOH, H_2SO_4, aquadest, and dragendor's reagent.

This study is a true experimental with a post-test-only control group design. About 25 male Wistar rats (2-3 months,150-200 g) were acclimatized for one week and selected according to the completely randomized design method. The animal experiment procedure has been approved by Ethics Committee (KEPK UNPRI) No. 029/KEPK/UNPRI/X/2021.

The animal groups are:

K- : Negative control, with no treatment.
K+ : Positive control, with Povidone Iodine.
PI : treated with NLEE 20%
PII : treated with NLEE 25%
PIII : treated with NLEE 30%

The animals hair were shaved and then anesthetized with lidocaine. The incision was made on the back using a sterile scalpel 2 cm long. The wound was smeared with NLEE 2 times per day at 08.00 am and 05.00 pm from day 1st to day 14th. Wound observations were carried out visually every day by measuring the diameter of the wound, and calculating the average reduction in wound diameter and healing days. Wounds are considered healed if the diameter of the wound is zero. Wounds closure formula was referred to Guo et.al., 2020. Each group was evaluated by the number of fibroblasts at 400 magnifications, and immunohistochemistry expression of TNFα, IL-1, TGFβ , and PDGF on days 3rd, 7th, and 14th.

Statistical analysis has been employed to determine the normality of data obtained by using the *Kolmogorov-Smirnov* test ($p > 0.05$) and the homogeneity by *Levene* methods. Then two-way *ANOVA* was applied ($p < 0.05$), followed by the *Post Hoc Tukey HSD* test to determine the significant differences between groups.

RESULTS AND DISCUSSION

NLEE contains 44.72% ethanol soluble extract, 15.32% water soluble extract, 8.64% water content, 8.56% ash content, and 1.26% acid insoluble ash content. A qualitative phytochemical method showed that NLEE has a positive reaction with all reagents indicating that NLEE contains alkaloids, flavonoids, glycosidic, saponins, tannins, triterpenoids/steroids. Quantitatively, NLEE has 10.88 mgQE/g of flavonoid content.

GCMS analysis showed that NLEE mostly contained n-ethyl hydrazine carbothioamide (31.57%), 2-furancarboxaldehyde 5-hydroxymethyl (15,64%), 2e-3,7,11,15-tetramethyl-2-hexadecene-1-ol (7.08%), 3,5-dihydroxy-6-methyl-2,3-dihydro-4H-pyran-4-one (4.29%), D:C-friedooleana-7,9(11)-dien-3-ol,3beta (4.04%). The rest compounds are decanoic acids methyl ester, piperazine (3%), and vitamin E (1%). The specific numbers of the GCMS spectrum as shown in Figure 1.

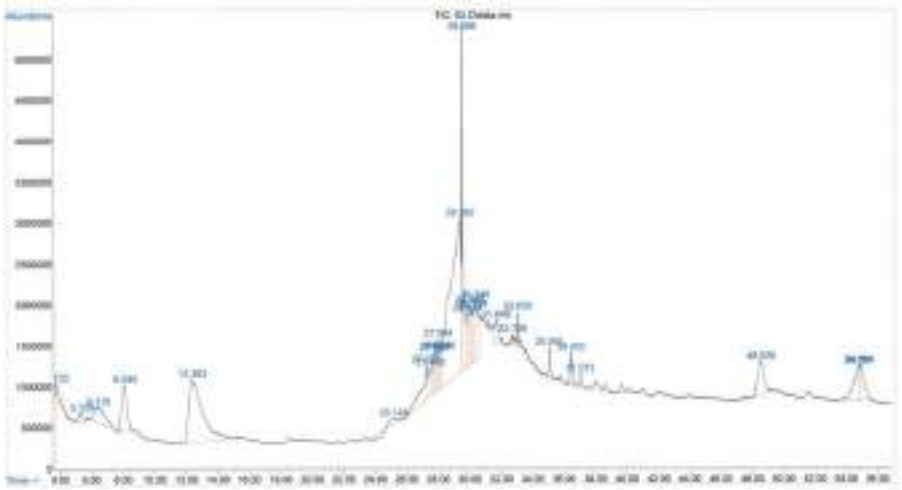

Fig 1. GCMS spectra of NLEE

Literature studies showed that hexanoic acid (3.02%) and tetradecanoic acid (1.36%) were saturated fatty acids with potential as antioxidants anticancer and antihistamines [13]. The 2-furancarboxaldehyde 5-hydroxymethyl (15,64%) and 3,5-dihydroxy-6-methyl-2,3-dihydro-4H-pyran-4-one (4.29%) were phenolic compounds that reported as antimicrobial, anti-inflammatory and antiproliferative [14]. Vitamin E is the popular antioxidant as well as the piperazine known as anthelmintic.

Kolmogorov-Smirnov test showed that the number of fibroblasts, wound diameter, healing time, TNFα, IL-1, TGFβ, and PDGF data are normal ($p > 0.05$). *Levene* test showed that the regression model meets the assumption of homogeneity ($p > 0.05$).

The number of fibroblast cells with hematoxylin staining produced on a variety of NLEE is shown in Figure 2.

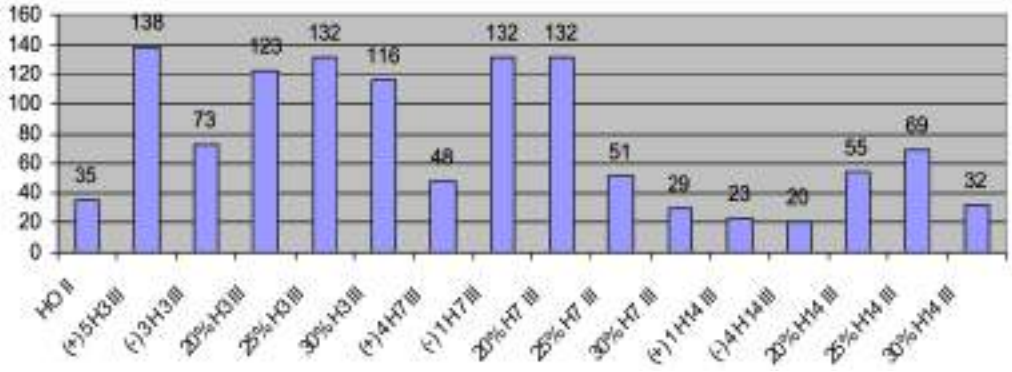

Fig.2 Effect of NLEE on the number of fibroblast cells on day 3rd,7th, and 14th between positive control (+), negative control (-), NLEE 25%, 25%, and 30%.

Figure 2 indicates that the variety of NLEE had no significant effect on the number of fibroblast cells. Even though there were changes in the number of fibroblasts but no significancies showed by two-way ANOVA (sig 0.885, α 5%).

This result is in line with a report that showed no significant effect of noni's extract against the number of fibroblast cells[6]. In their report, the number of fibroblasts in the control group was higher than in all treatment groups, although it was not statistically significant. This indicates that the proliferation of fibroblast cells in all treatment groups has decreased earlier than in the control group.

This phenomena could be explained that occurrence of fibrosis was subjected to the inflammatory response classified as acute and chronic inflammation, which differs from their vascular reactions, cells involved, and duration [6]. Another report also showed that a remodelling phase of wound healing, fibroblast cell proliferation decreases as collagen fibres are synthesized [12].

The wound diameter and healing time on a variety of NLEE are shown in Fig 3.

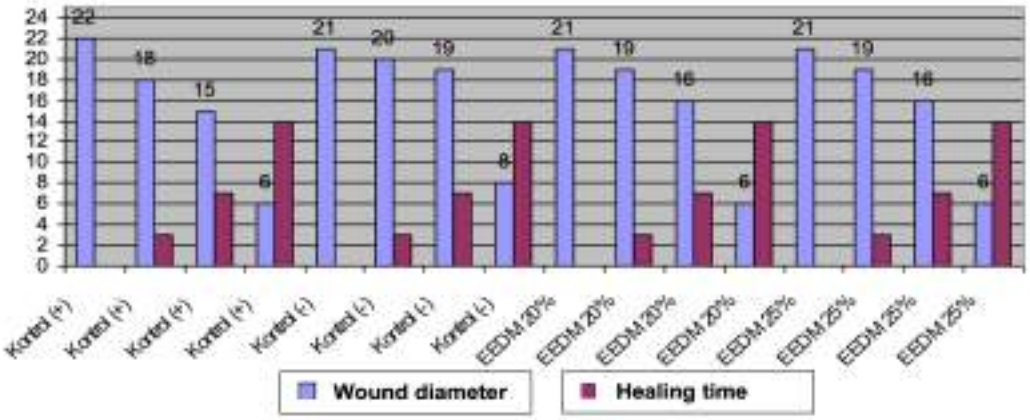

Fig.3 Effect of NLEE on the wound diameter and healing time on the day 3rd,7th, and 14th between positive control (+), negative control (-), NLEE 25%, 25%, and 30%

Figure 3 indicates that the variety of NLEE had no significant effect on the wound diameter and healing time. Even though there were but no significancies showed by two-way ANOVA (sig 0.997 and 1.000 with α 5% for wound diameter and healing time respectively). Our result was the same as the report by [15]. This phenomenon explained that wound healing in the skin is a complex process involving blood clotting, inflammation, new tissue formation, and tissue remodelling [16].

The effects of NLEE on TNFα and IL-1 were shown in Figures 4 and 5 respectively.

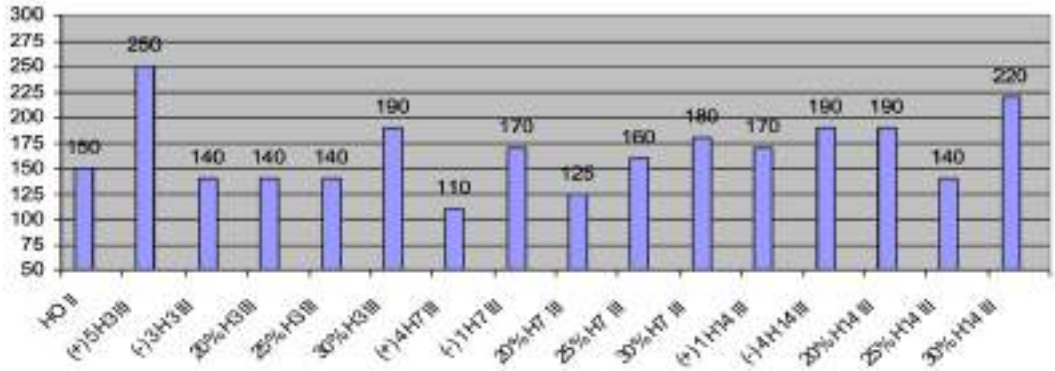

Fig.4 Effect of NLEE on the TNFα on the day 3rd,7th, and 14th between positive control (+), negative control (-), NLEE 25%, 25%, and 30%.

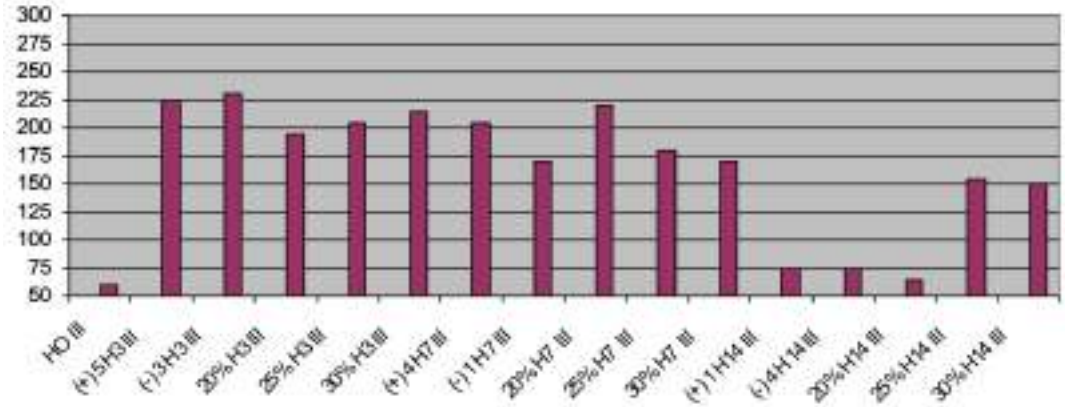

Fig.5 Effect of NLEE on the IL-1 on the day 3rd,7th, and 14th between positive control (+), negative control (-), NLEE 25%, 25%, and 30%.

Figure 4 showed that the variety of NLEE had no significant effect on the TNFα by two-way ANOVA (sig 0.541 with α 5%) nor the IL-1 (sig 0.949 with α 5%) as shown in Figure 5.

A previous report showed that the variety of noni's leaf extract did not have a significant effect on the expression of TNF-a and IL-1 [17]. In their report, noni's extract showed maximal inhibition of IL-1β production (79%) at 750 g/ml, which was not statistically different from the maximal inhibition produced by dexamethasone (97% at 3.92 g/ml), indomethacin (70% at 3.58 g/ml), and rutin (90% at 48.84 g/ml). A comparison of IC_{50} values revealed that the inhibitory potential of IL-1β production from the extract (294 g/ml) was much lower than that of rutin (30.2 g/ml), dexamethasone (0.93 g/ml), and indomethacin (1.50 g/ml). This can be explained by that TNF-α plays a key role in the induction and perpetuation of inflammation and up- regulation of other pro-inflammatory cytokines and endothelial adhesion molecules[18]. The production of TNF-α increases the release of IL-1β [19,20].

The effects of NLEE on TGFβ and PDGF were shown in Figures 6 and 7 respectively.

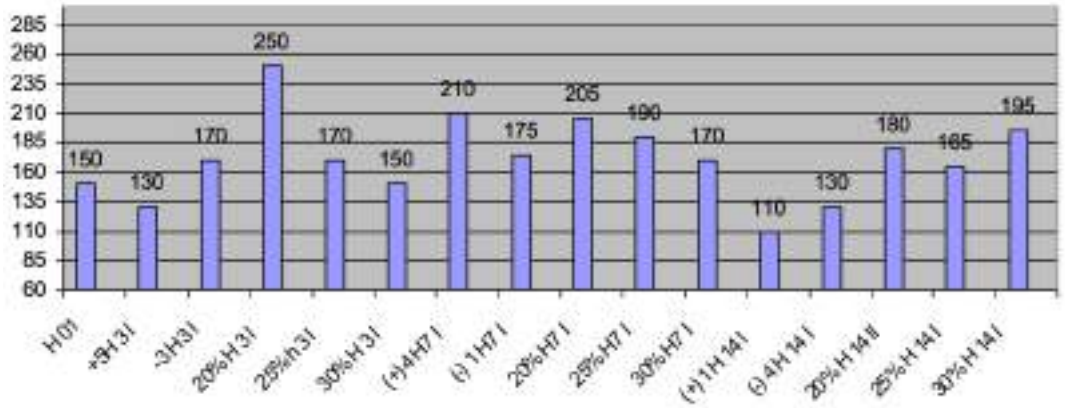

Fig.6 Effect of NLEE on the TGFβ on the day 3rd,7th, and 14th between positive control (+), negative control (-), NLEE 25%, 25%, and 30%.

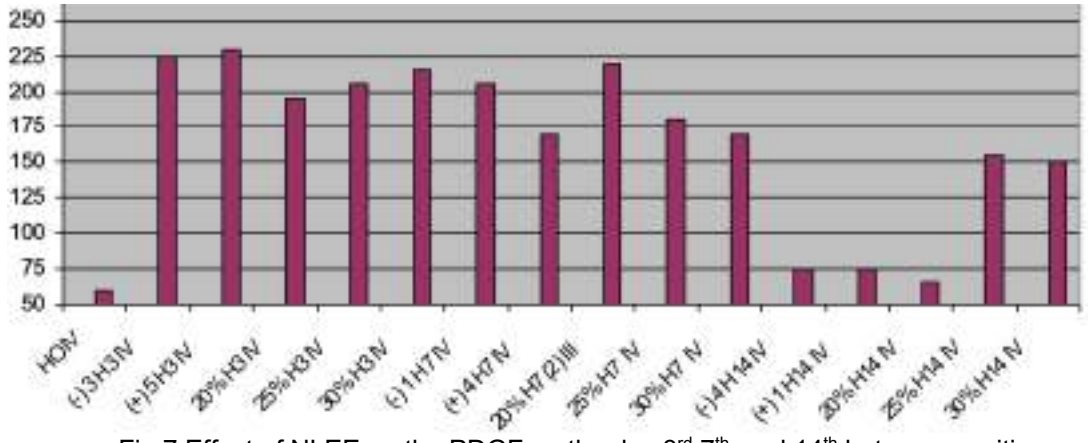

Fig.7 Effect of NLEE on the PDGF on the day 3rd,7th, and 14th between positive control (+), negative control (-), NLEE 25%, 25%, and 30%.

Figure 6 showed that the variety of NLEE had no significant effect on the TGFβ by two-way ANOVA (sig 0.510 with α 5%) nor the PDGF (sig 0.997 with α 5%) as shown in Figure 7. Based on data shown in Figures 2-7, the descriptive analysis showed that the optimum condition was at NLEE 20% with a mean value of 1.9625 (sig. 0.310 α 5%). During the inflammation stage in the first three-days injury, the wound healing effect is related to the degradation of cytokine activity released by macrophages; TNF-α, IL-1, PDGF dan TGF-β [21]. Afterward, during the proliferation stage, the PDGF and TGF-β will be secreted after injury immediately. PDGF can increase fibroblast proliferation and then produce an extracellular matrix whereas the PDGF-BB gene-modified human Dental Pulp Stem Cells (hDPSCs) can continuously secrete the PDGF-BB protein and that the overexpression of PDGF-BB can significantly enhance hDPSC proliferation[22]. TGF-β also plays an important role to increase fibroblasts, and cell chemotaxis, and modulates collagen and collagenase expression, which in turn produces matrix-producing cells for the rapid deposition of the new connective tissue[23]. In adult mammals, high levels of TGFβ1 and TGFβ2, and low levels of TGFβ3 facilitate scar-forming healing, while in fetal mammals, high levels of TGFβ3 and low levels of TGFβ1 and TGFβ2 favour scar-free healing[24]. The multifunctional cytokine plays a central role in tissue repair. Initially after wounding, TGF-β is secreted by platelets, and serves as a chemoattractant for parenchymal cells and leukocytes, which in turn enhance production of TGF-β. This mechanism leads to restoration of tissue architecture in normal wound repair, although overproduction may lead to fibrosis [25].

CONCLUSION

Simplicia of noni's leaf extract has several bioactive compounds based on GCMS data. Quantitatively, NLEE has 10.88 mgQE/g of flavonoid content. Some phenolic compounds and saturated fatty acid methyl ester, piperazine, and vitamin E are the bioactive compounds that play a role in the wound healing effect in Wistar rats. We observed the slight effects of NLEE 20%, 25%, and 30% on the number of fibroblasts, wound diameter, healing time, TNF-α, IL-1, PDGF, and TGF-β. The optimum concentration of NLEE at any treatment was 20%. However, there were no significant differences between groups based on a two-way ANOVA analysis. These results suggest a diverse variety of concentrations to capture a better understanding of the wound healing potential of NLEE treatments in Wistar rats.

AUTHORS' CONTRIBUTIONS

All authors contributed equally to this work.

ACKNOWLEDGEMENT
Author thanks to Pharmacy Laboratory, Universitas Sumatera Utara, for their facilities and materials during this research.

FUNDING INFORMATION
This research did not receive any specific grant from funding agencies

DATA AVAILABILITY STATEMENT
The utilized data to contribute to this investigation are available from the corresponding author on reasonable request.

DISCLOSURE STATEMENT
The views and opinions expressed in this article are those of the authors and do not necessarily reflect the official policy or position of any affiliated agency of the authors. The data is the result of the author's research and has never been published in other journals.

REFERENCE
1. Pebri IG, Rinidar, Amiruddin. Pengaruh Pemberian Ekstrak Daun Binahong (Anredera cordifolia) Terhadap Proses Penyembuhan Luka Insisi (Vulnus incisivum) Pada Mencit (Mus musculus). *J Ilm Mhs Vet*. 2017;2(1):1-11.
2. Abdo JM, Sopko NA, Milner SM. The applied anatomy of human skin: A model for regeneration. *Wound Med*. 2020;28(January):100179. doi:10.1016/j.wndm.2020.100179
3. Chhabra S, Chhabra N, Kaur A, Gupta N. Wound Healing Concepts in Clinical Practice of OMFS. *J Maxillofac Oral Surg*. 2017;16(4):403-423. doi:10.1007/s12663-016-0880-z
4. Pereira LOM, Vilegas W, Tangerina MMP, et al. Lafoensia pacari A. St.-Hil.: Wound healing activity and mechanism of action of standardized hydroethanolic leaves extract. *J Ethnopharmacol*. 2018;219(2367):337-350. doi:10.1016/j.jep.2018.02.038
5. Setyani W, Setyowati H. Phytochemical investigation of noni (Morinda citrifolia L.) leaves extract applicated for sunscreen product. *Malaysian J Fundam Appl Sci*. 2018;14(1-2):164-167. doi:10.11113/mjfas.v14n1-2.996
6. Sabirin IPR, Yuslianti ER. Effect of Topical Noni (*Morinda citrifolia* L.) Leaf Extract Paste in Carrageenan-induced Paw Edema on Wistar Rats. *Glob Med Heal Commun*. 2019;7(2):116-122. doi:10.29313/gmhc.v7i2.4087
7. Torres MAO, de Fátima Braga Magalhães I, Mondêgo-Oliveira R, de Sá JC, Rocha AL, Abreu-Silva AL. One Plant, Many Uses: A Review of the Pharmacological Applications of Morinda citrifolia. *Phyther Res*. 2017;31(7):971-979. doi:10.1002/ptr.5817
8. Melo MB De, Araújo-neto I, Bruno T, et al. Effect of nanostructured extract morinda citrofolia l. (noni) in infected wounds in rats. *Int J Dev Res*. 2017;7(6):13501-13507.
9. Senja RY, Hidayati NR, Setyaningsih I. "Uji Efektivitas Salep Ekstrak Daun Mengkudu (Morinda Citrifolia L.) Terhadap Luka Sayat Pada Kelinci Jantan (Oryctolagus cuniculus) and Activities of Ethanol Extract Noni Leaf (Morinda Citrifolia L.) Ointment For Wound Healing In Male Rabbits (Oryctolagus. *ojsstffmuhammadiyah cirebon*. 2017:100-107.
10. Palu A, Su C, Zhou BN, West B, Jensen J. Wound healing effects of noni (Morinda citrifolia L.) leaves: A mechanism involving its PDGF/A2A receptor ligand binding and promotion of wound closure. *Phyther Res*.

2010;24(10):1437-1441. doi:10.1002/ptr.3150

11. Parmadi A. Formulation Development qnd Physical Test of Leaf Ethanol Extract Cream Noni (Morinda Citrifolia L) As A Wound Healer. *J Farm (Journal Pharmacy)*. 2018;1(1):20-26. doi:10.37013/jf.v1i1.59
12. Sabirin IPR, Yuslianti ER. Benefits of Ethanolic Extract Paste of Noni (Morinda citrifolia L.) Leaves on Oral Mucosa Wound Healing by Examination of Fibroblast Cells. *J Dent Indones*. 2016;23(3):59-63. doi:10.14693/jdi.v23i3.980
13. Farid MM, Hussein SR, Ibrahim LF, et al. Cytotoxic activity and phytochemical analysis of Arum palaestinum Boiss. *Asian Pac J Trop Biomed*. 2015;5(11):944-947. doi:10.1016/j.apjtb.2015.07.019
14. Shalini K, Ilango K. Preliminary phytochemical studies, gc-ms analysis and in vitro antioxidant activity of selected medicinal plants and its polyherbal formulation. *Pharmacogn J*. 2021;13(3):648-659. doi:10.5530/pj.2021.13.83
15. Haestidyatami VL, Sugiritama IW, Linawati NM. Pengaruh ekstrak krim Morinda citrifolia terhadap jumlah fibroblas pada penyembuhan luka tikus Wistar. *Intisari Sains Medis*. 2019;10(3):679-683. doi:10.15562/ism.v10i3.487
16. Beldon P. Basic science of wound healing. *Surgery*. 2010;28(9):409-412. doi:10.1016/j.mpsur.2010.05.007
17. Saraphanchotiwitthaya A, Sripalakit P. Anti-inflammatory effect of Morinda citrifolia leaf extract on macrophage RAW 264.7 cells. *ScienceAsia*. 2015;41(1):5-11. doi:10.2306/scienceasia1513-1874.2015.41.005
18. Ceramit BBAC. The Biology of Cachectin/TNF- A Primary Mediator of The Host Response. *AnnRevImmunol*. 9189;7(625):55. doi:10.1016/s0168-7069(02)08018-7
19. Molloy RG, Mannick JA, Rodrick ML. Cytokines, sepsis and immunomodulation. *Br J Surg*. 1993;80(3):289-297. doi:10.1002/bjs.1800800308
20. West MA, Seatter SC, Bellingham J, Clair L. Mechanisms of reprogrammed macrophage endotoxin signal transduction after lipopolysaccharide pretreatment. *Surgery*. 1995;118(2):220-228. doi:10.1016/S0039-6060(05)80327-7
21. Ritsu M, Kawakami K, Kanno E, et al. Critical role of tumor necrosis factor-α in the early process of wound healing in skin. *J Dermatology Dermatologic Surg*. 2017;21(1):14-19. doi:10.1016/j.jdds.2016.09.001
22. Zhang M, Jiang F, Zhang X, et al. The Effects of Platelet-Derived Growth Factor-BB on Human Dental Pulp Stem Cells Mediated Dentin-Pulp Complex Regeneration. *Stem Cells Transl Med*. 2017;6(12):2126-2134. doi:10.1002/sctm.17-0033
23. Baranoski S, AAyello EA. *Wound Care Essentials: Practice Principles*. Vol 4. New York: Wolters Kluwer; 2557.
24. Gilbert RWD, Vickaryous MK, Viloria-Petit AM. Signalling by transforming growth factor beta isoforms in wound healing and tissue regeneration. *J Dev Biol*. 2016;4(2). doi:10.3390/jdb4020021
25. Glim JE, Van Egmond M, Niessen FB, Everts V, Beelen RHJ. Detrimental dermal wound healing: What can we learn from the oral mucosa? *Wound Repair Regen*. 2013;21(5):648-660. doi:10.1111/wrr.12072.

JTL 11 (2) December 2022
Page: 60-64

Contents list available at Jurnal Teknologi Laboratorium

JURNAL TEKNOLOGI LABORATORIUM

Journal Homepage: www.teknolabjournal.com
ISSN 2580-0191(Online) I ISSN 2338 – 5634(Print)

Case Study

A simple and quick isolation method to obtain a huge number of fibroblasts like mesenchymal stem cells from human umbilical cord

Sudhir Bhatia
Genekam Biotechnology AG, Duissernstr. 65a, 47058 Duisburg, Germany

Abstract: In this publication, we have developed a simple and quick isolation method of stem cells from umbilical cord. Usually, umbilical cord is a waste product during the child delivery procedure, but the umbilical cords contain valuable stem cells called mesenchymal stroma stem cells (also called MSCs), which can be basis for different applications e.g., testing effect of therapeutic compounds as well as development of therapeutic applications for cure of degenerative diseases like bone and cartilage related. These stem cells can be used to create new artificial organs too. The umbilical cord was cut with sterile scissors into small pieces (1-2 mm size) and these pieces were placed on 6 well culture plates. The cell culture media was added to these plates after 5-10 minutes placing these plates in CO_2 incubator. The successful growth of cells was observed after 7 days in wells, where pieces of umbilical cord were implanted. Microscopic observations show how the cells are oozing out from these pieces. These cells were isolated and passaged further. These adhere on the plastic surface, were fibroblast shaped and isolated successfully in different experiments.

INTRODUCTION

The plastic adherent and fibroblast like cells were isolated from bone marrow in late eighties[1,2]. These cells were called mesenchymal stem cells (MSCs). These cells are in position to differentiate in different lineages like osteogenic, chrondrogenic, adipogenic, myogenic and many others in vitro experiments[3]. MSCs express different markers like CD105, CD90, CD73, but do not CD45, CD34 and HLA-DR markers. MSCs are known to have immunomodulatory effects, hence they may be candidate for allogenic clinical therapies e.g., transplantation in cancer patients as well as autoimmune disorders. MSCs are to be subjected for the possibilities to regenerate bones and cartilages along with non-skeletal tissue applications e.g., generation of cardiomyocytes, spinal cord tissue, pancreatic and hepatic tissue etc, which can lead to cure the many chronic diseases of society. Usually, these MSCs can be isolated from different sources like bone marrow, adipose tissue, joint tissue, dental pulp and other sources[4]. Umbilical cord is one of the waste products during the delivery of a child and usually it is thrown away, but it offers also a good source of MSCs, therefore we develop a simple method to isolate the MSCs in laboratory[5,6].

MATERIAL AND METHOD

The umbilical cord was transferred to laboratory under the cooling condition after consent of donors and it was stored for one day at 4 °C. The whole procedure was conducted under sterile conditions and with sterile instruments. The umbilical cord was cut with sterile scissor in 2-3 cm pieces in such way that blood vessels were avoided and placed in a sterile petri disc. (Picture 1) If there were blood

Corresponding author.
E-mail address: anfrage@genekam.de (Sudhir Bhatia)
DOI: 10.29238/teknolabjournal.v11i2.385
Received 16 November 2022; Received in revised form 17 December 2022; Accepted 28 December 2022

vessels, they were punctured with forceps or scissor to remove the blood. The 2-3 cm piece was washed in PBS (Lonza, USA) twice to remove the blood and other fluids. After that piece of umbilical cord was placed in fresh petri dish in 2-3 ml PBS and cut into small pieces of 2 to 4 mm. (Picture 2) These were collected in 50 ml tubes and treated with 2ml trypsin/EDTA solution (Promocell, Germany) for 30 minutes. A part of pieces was kept untreated. (Picture 3) They were filtered through a retainer to get the pieces at the top of 50 ml tube. The treated and non-treated pieces were placed in wells of 6 well cell culture plate as well as 50 ml cell culture flasks with the help of sterile forceps. These plates without cell culture media were placed in CO_2 inoculator for 5 minutes at 37°C, so that pieces of umbilical cords adhere to the plastic surface of the plate or flask. This step is very important, otherwise pieces of umbilical cord will float in the cell culture media and there will be no stem cells, therefore it is important that umbilical pieces adhere to the plastic surface before the media was added. Each well has only 3-5 pieces only. After this, 5 ml cell culture media DMEM (Lonza, USA) with 1% Streptopenicillin and 1% Glutamine containing 10% fetal calf serum (Biochrome, Germany) were added to each well. This whole above-mentioned procedure took around 60-75 minutes to finish.

The plates and flasks were kept at 37 °C very carefully and gently in CO_2 incubator so that pieces of umbilical cord do not start floating in the media. They were observed under the microscope daily and changed the media on 3rd day. On day 7, there was growth of fibroblast like cells coming out from these pieces and these cells adhere to the plastic surface. On day 14, these cells are removed with trypsin I EDTA treatment and washed in PBS to get the pellet. They were counted under the microscope with Neubauer Chamber with trypan blue dye (Biochrome, Germany). A part of the pellets was passaged in 6 well cell culture plates and 50 ml flasks. The rest pieces of umbilical cord and stem cells were frozen in freezing media (Genekam, Germany) containing DMSO for later use. They were analyzed for expression of specific markers.

Picture 1 shows a piece of umbilical cord is being washed in PBS. The deep red colored spot is a blood vessel in this. Second pete dish shows washed pieces of umbilical cord, which were cut into small pieces to isolate the stem cells.

Picture 2 shows that umbilical cord is cut in small pieces of 1-2 mm in two petri dishes

RESULTS AND DISCUSSION

There was successful growth of fibroblast like cells in cell culture wells and flasks. The pictures are showing that the cells were oozing out from the small pieces of human umbilical cords. (Picture 4 and 5) Trypsin/EDTA treated umbilical cord pieces provided more fibroblast like cells, which adhere to the plastic surface. Such cells were also observed in plates in non-treated umbilical cord pieces. There was need of only 3 to 5 pieces of umbilical cord in each well and in the flasks. (Picture 6) It shows that umbilical cord is huge source of MSCs because 3 cm piece has generated huge number of cells. From 3 cm piece of umbilical cord, we were able to get 2 plates with 6 wells and 3 Flasks. A part of small pieces was stored in freezing media for later use.

Cutting of umbilical cord needed some patience and good scissors as it slips, hence this care must be taken in order to avoid the loss of umbilical cord with this mistake. The small blood vessels in umbilical cord made empty in order to remove the blood cells including erythrocytes because they may be disturbing

factor during the isolation process. Multiple PBS washings were done to remove them.

The counting of stem cells shown that number of cells obtained per well was about one million in treated population, where number of cells obtained from non-treated pieces (trypsin/EDTA) was less. The growth was observed in 12 wells and 3 flasks. No growth was observed, where the pieces were floating in media. (Data not shown)

The passaging of the cells was done after the trypsin/EDTA treatment. Once these fibroblast-like cells were treated with trypsin, it was found that they can be easily removed from the plastic surface for further passaging. The cells were able to passage up to 7 passages. After the 7th passage, they lost their activity to redivide and they change their shapes, which become irregular.

They were tested for the presence of biomarkers like CD90, CD73 and CD105 and It was found that they were positive for these. The presence of CD90 marker was used to isolate these cells with magnetic beads along with CD105 marker.

In this research work, we have shown a simple method to isolate the fibroblast stem cells called MSCs in different setting (treated and non-treated). As there is a need of large number of stem cells to conduct the studies, umbilical cord offers a huge source of stem cells. We are able to get one million cells per well as well as per flask, hence there may be many million cells from the whole umbilical cord, which may be solution for a large number of stem cells needed for different therapeutic applications. Average size of human umbilical cord is 55 cm; hence user can isolate many million cells because in this research, 3 cm pieces of umbilical cord were used. These stem cells can be stored for long term for repeated applications. The industry can also isolate these stem cells from umbilical cord and provide to research institutes at discounted prices with constant quality instead each institute is going to isolate them, hence this can result in new research fields. MSCs can be obtained from other sources like adipose tissue and bone marrow, but one cannot obtain such a large number of cells. Moreover, umbilical cord is a waste product and it is discarded after the child delivery. This publication and other research work show that umbilical cord can be a big source of MSCs[3]. Our method opens door to many laboratories around the world to isolate the MSCs in large number to do research in 2D as well as 3D applications using biomaterials for development of new therapies[7]. The stem cells are slowly growing cells, therefore many times, it is very difficult to have the sufficient number as single population to conduct the studies, this shortage of homogenous population may be solved through this method. We have shown in another publication that these cells can be isolated with the help of CD90 magnetic beads and can be passaged from the plates as well as flasks after the trypsin treatment[8].

The supernatant from MSCs is being tested as potential therapeutic option for many diseases e.g., joint disorders because it has immunomodulating properties[9]. The studies are conducted in 2D and 3D applications to find the therapeutic potential on corneal wound[10]. MSCs generated through our method offers an excellent supernatant source in large volume for research community to conduct further studies.

The method presented in this research work is simple and easy to be carried in any laboratory against the method presented in a video publication and other publications[11]. Different methods of isolations in literature show that user needs a lot of time to isolate the stem cells from umbilical cord against our method, which can be finished within 60-75 minutes (around one hour) and a number of plates or flasks can be cultivated with umbilical cord pieces to generate huge number of stem cells[12].

Picture 3 shows that 1-2mm pieces of umbilical cords are treated with trypsin in 50ml tubes. Tube 1 is treated and tube 2 is non treated.

Picture 4 shows under microscope that fibroblast like stem cells are oozing out from pieces of umbilical cord.

Picture 5 shows under microscope that fibroblast like stem cells are oozing out from pieces of umbilical cord.

Picture 6 shows that there are 5-8 pieces (1-2 mm size) of umbilical cord in 50 ml flask, from them the growth of stem cells were observed under microscope.

CONCLUSION

The cells were tested for the presence of biomarkers like CD90, CD73 and CD105 and it was found that they were positive for these. The average size of human umbilical cord is 55 cm and the stem cells can be stored for long term for repeated applications. The industry can also isolate these stem cells and provide them to research institutes at discounted prices with constant quality. MSCs can be obtained from other sources like adipose tissue and bone marrow, but they are a waste product and discarded after the child delivery. The method opens door to many laboratories around the world to isolate the MSCs for research in 2D and 3D applications using biomaterials.

DATA AVAILABILITY STATEMENT

The utilized data to contribute to this investigation are available from the corresponding author on reasonable request.

DISCLOSURE STATEMENT

The views and opinions expressed in this article are those of the authors and do not necessarily reflect the official policy or position of any affiliated agency of the authors. The data is the result of the author's research and has never been published in other journals.

REFERENCE

1. Friedenstein AJ, Chailakhyan RK, Gerasimov UV. Bone marrow osteogenic stem cells: in vitro cultivation and transplantation in diffusion chambers. *Cell Prolif*. 1987;20(3):263-272. doi:10.1111/j.1365-2184.1987.tb01309.x
2. Friedenstein AJ, Latzinik NW, Grosheva AG, Gorskaya UF. Marrow microenvironment transfer by heterotopic transplantation of freshly isolated and cultured cells in porous sponges. *Exp Hematol*. 1982;10(2):217-227.
3. Mishra S, Sevak JK, Das A. Umbilical cord tissue is a robust source for mesenchymal stem cells with enhanced myogenic differentiation potential

compared to cord blood. *Sci Rep*. 2020;10:18978. doi:10.1038/s41598-020-75102-9
4. Bari D.C. TP Dell´Accio F, F. LP. Multipotent Mesenchymal Stem Cells From Adult Synovial Membrane. *Arthritis Rheum*. 2001;44(8). doi:10.1002/1529-0131(200108)44:8
5. Atala A, Lanza R, Thomson JA, Nerem R. *Principles of Regenerative Medicine*. Elsevier; 2011. doi:10.1016/C2009-0-61040-0
6. Gazit Z, Pelled G, Sheyn D, Yakubovich DC, Gazit D. Principles of regenerative medicine. Published online 2019.
7. De Bartolo L, Bader A, eds. *Biomaterials for Stem Cell Therapy: State of Art and Vision for the Future*. CRC Press; 2013.
8. Bhatia S. A simple method for isolation of rest of trypsinized stem cells with magnetic beads. *J Teknol Lab*. 2021;10(1):01-02. doi:10.29238/teknolabjournal.v10i1.268
9. Kay AG, Long G, Tyler G. Mesenchymal Stem Cell-Conditioned Medium Reduces Disease Severity and Immune Responses in Inflammatory Arthritis. *Sci Rep*. 2017;7:18019. doi:10.1038/s41598-017-18144-w
10. Carter K, Lee HJ, Na KS, et al. Characterizing the impact of 2D and 3D.
11. N. B, C. M, A. A, et al. Isolation and Characterization of Mesenchymal Stromal Cells from Human Umbilical Cord and Fetal Placenta. *JoVe J*. Published online 2017. doi:10.3791/55224
12. Stefańska K, Sibiak R, Dompe C, et al. Overview of methods of isolation, cultivation and genetic profiling on human umbilical cord stem cells. *Med J Cell Biol*. 2019;7(4):170-174. doi:10.2478/acb-2019-0023

JTL 11 (2) December 2022
Page: 65-72

Contents list available at Jurnal Teknologi Laboratorium

JURNAL TEKNOLOGI LABORATORIUM

Journal Homepage: www.teknolabjournal.com
ISSN 2580-0191(Online) I ISSN 2338 – 5634(Print)

Original Study

Identification of Pathogenic Bacteria in Blood Cockle (Anadara granosa) using 16S rRNA Gene

Meutia Srikandi Fitria[1*], Aprilia Indra Kartika[2], Ana Hidayati Mukaromah[2], Nurfi Ismatul Unasiah[2]

[1] Department of Medical Laboratory Technology, Faculty of Nursing and Health Science, Universitas Muhammadiyah Semarang, Indonesia
[2] Magister Study Program of Medical Laboratory Science, Universitas Muhammadiyah Semarang, 50273, Indonesia

Abstract: Blood cockle (*Anadara granosa*) is one of the marine resources in Indonesia that contains protein. Processing of blood cockles that are not perfect or raw will be contaminated with pathogenic bacteria that live in the waters. Pathogenic bacteria cause foodborne disease, which is a disease in humans caused by food. Several bacterial pathogens that cause foodborne disease are *Escherichia* sp. *Pseudomonas* sp., and *Vibrio* sp. Pathogenic bacteria in blood cockle should be identified using 16S rRNA as molecular identification. Samples were isolated using BAP, HIA, and BHI media. Bacteria from BHI media were isolated. Isolation DNA was isolated using the phenol-CIAA method. The DNA isolates were amplified by the PCR method based on the 16S rRNA target gene, then visualized the DNA with 2% agarose gel electrophoresis and sequencing. Bacterial colonies produced from BAP media for isolates BVA1, BVA9, and BVA10 were ß-hemolysis. Visualization of hemolytic bacterial DNA in blood cockle culture amplified about 1500 bp. Whereas the results of the sequencing analyzed by BLAST on the NCBI database and the Mega X program for BVA1 and BVA10 isolates showed similarity to *Vibrio* sp. bacteria, whereas BVA9 isolates showed similarity to Bacterium whose species still unknown. The conclusion showed that blood cockle had close simililarity with with *Vibrio* sp. and Bacterium.

Keyword: *Anadara granosa;* Pathogenic bacteria*;* 16S rRNA gene

INTRODUCTION

Pathogenic bacteria are the cause of food poisoning in both raw and processed foods, one of which is blood cockle (*Anadara granosa*). It is one type of shellfish has a high economic value and generally as a source of seafood in Southeast Asia region especially in Indonesia[1]. Blood cockle (*A. granosa*) have high protein content and potential to be contaminated with pathogenic bacteria due to the way they consume food is a filter feeder that is filtering water to acquire food. The presence of pathogenic bacteria can cause foodborne diseases[2]. Identification of pathogenic bacteria is required to find out what type of bacteria that live in blood cockle and to provide information concerning the hygiene of blood cockle when consumed raw. Microbiological identification of bacterial is known as the gold standard for detecting pathogenic bacteria, however it takes a long time[3]. Therefore, the molecular identification is needed. Molecular identification was

Corresponding author.
E-mail address: meutia@unumus.ac.id (Meutia Srikandi Fitria)
DOI: 10.29238/teknolabjournal.v11i2.364
Received 16 November 2022; Received in revised form 17 December 2022; Accepted 28 December 2022

carried out by sequencing analysis of the 16S rRNA gene, this method has high level of sensitivity, specificity and takes a less time[4]. The 16S rRNA gene is a marker gene for bacterial identification. The 16S rRNA gene used as a universal primer used in PCR (Polymerase Chain Reaction) and the nucleotide sequence can be determined through sequencing[5].

Several bacteria that cause foodborne disease such as *Escherichia* sp., *Pseudomonas* sp. and *Vibrio* spp. Whereas blood cockle reported to have bacterial contamination, such as those from the species of *Klebsiella* spp. and *Bacillus* spp, *E. coli*, *Pseudomonas* spp., *Staphylococcus* spp., and *Micrococcus* spp. Bacterial infections in humans are often associated with improper processing or raw consumption[6]. Bacterial identification from blood cockle found in the south coast of Thailand are have contamination with *V. parahaemolytticus*[7]. The study regarding in Tanah Merah Kupang Tengah state that blood cockle had *V. harveyi* contamination[8]. Another study showed that blood cockle were contaminated with *Salmonella* sp. and *Vibrio* sp[9]. In addition to bacteria in blood cockle, endoparasite and microplastics were also discovered[10,11].

The study related to the identification of pathogenic bacteria that cause foodborne disease in *A. granosa* has limited research. It is needed to do research it because it can help related to the correct food processing and hygiene of the food. Therefore, it is necessary to conduct research on the molecular identification of pathogenic bacteria in *A. granosa* by sequencing analysis of the 16S rRNA gene.

MATERIAL AND METHOD

The type of the research is descriptive explorative. The sample of *A. granosa* obtained from Sayung Market, Demak. The research was conducted from Januari to April 2021. Pure bacterial isolation was carried out at Microbiology Laboratory. Therefore, DNA isolation and amplification at Molecular Biologi, Medical Laboratory Technology, University of Muhammadiyah Semarang. Sequencing analysis of 16S rRNA gene was carried out at PT. Genetika Science, Indonesia.

Research stages

Pure Bacterial Isolation of *A. granosa* Culture

Three grams of *A. granosa* were put in a clean and dry place to be mashed. Then one tablespoon of *A.* granosa was diluted into 5 ml of Physiological NaCl and homogenized. Isolation was carried out by culturing *A. granosa* on Nutrient agar then incubated at 37°C for 24 hours. Later the bacteria were isolated again on BAP media at 37°C for 24 hours. Then hemolysis formed was observed on BAP (Blood Agar Plate) media against a bright light background. Colonies on BAP media which contained a full clear zone and a clear green zone were inoculated on HIA (Heart Infusion Agar) fertilizing media for 24 hours at 37°C then colonies from HIA were cultured on BHI (Brain Heart Infusion) agar for 48 hours at 37°C in the incubator.

DNA isolation of A. granosa bacteria

A. granosa bacterial colonies from HIA media was implated in 5ml BHI media, then incubated at 37°C for 24 hours. The colonies were centrifuged at 12000 rpm for 10 minutes at 4°C. The pellet required for the isolation was added with 750 µl of lysis buffer then vortexed for a few seconds. Then added 20 µl of proteinase K, the solution shaken for 15 minutes using a rotator. Then the solution incubated at 55°C for 30 minutes. Later centrifuged for 10 minutes at 12000 rpm at 4°C.

The supernatant solution transferred to a 1.5 ml microtube and 700 µl of phenol CIAA was added, stirred slowly for 30 minutes, then centrifuged at 12000 rpm for 10 minutes at 4°C. The top part was transferred to microtube, then in a 1:1 ratio 96% ethanol was added, the solution needed to mix gently until fine threads were visible, then centrifuged at 12000 rpm for 10 minutes at 4°C. The supernatant solution was eliminated from microtube, and the pellet was washed with 70% cold ethanol, then centrifuged at 12000 rpm for 10 minutes at 4°C for three times. The supernatant solution was removed from the pellets then air dried. Then 200 µl of

TE solution was added to dissolve the bacterial DNA so that it could be visible in the 1 % agarose gel electrophoresis.

DNA isolate concentration and purity was measured using nanodrop spectrophotometer. Two µl was pipetted in nanodrop at a 260/280 nm wavelength. The limit ratio of DNA purity is between 1.8 – 2.0.

Amplification of *A. granosa* bacteria

The compositon of mixed PCR was 12.5 µl of taq polymerase enzyme, 7.5 µl of Nuclease Free Water, 2µl each of forward and reverse primers, and 1µl of DNA samples were added to the PCR microtube. The PCR microtube is inserted into the PCR, then the temperature is set at the initial denaturation stage (pre-denaturation) at 95°C for 6 minutes, the denaturation stage at 95°C for 30 seconds, then the annealing stage at 55°C for 30 seconds. The extension at 72°C for 2 minutes. The final extension stage at 72°C for 10 minutes and the cooling down stage at 4°C for 6 minutes. The results of PCR amplification and markers were read using 2% agarose gel electrophoresis. PCR amplification using 16S rRNA forward and reverse primers has a target area about 1500 bp.

Data analysis

The further processing to the sequencing analysis stage of PCR product is sent to PT Genetics Science Indonesia. The nucleotide sequences obtained were then used for comparison with the sequence data in Gebank through the BLAST (Basic Local Alignment Search Tool) program at the National Center for Biotechnology Information (NCBI), National Institute for Health, USA on the Website https://blast.ncbi.nlm.nih.gov/. The results from the sequencing were aligned and a phylogenetic tree was created using the Mega X program[12].

RESULTS AND DISCUSSION

Bacterial colonies were cultured on BAP media to see the nature of the bacteria in hemolyzing red blood cells. The bacterial culture of *A. granosa* obtained three colonies of bacteria capable of lysing red blood cells so that it is harmful to humans. The three bacterial colonies (BVA1, BVA9, and BVA10) produced ß-hemolysis colonies with the characteristics of forming a transparent zone around the colony (Figure 1).

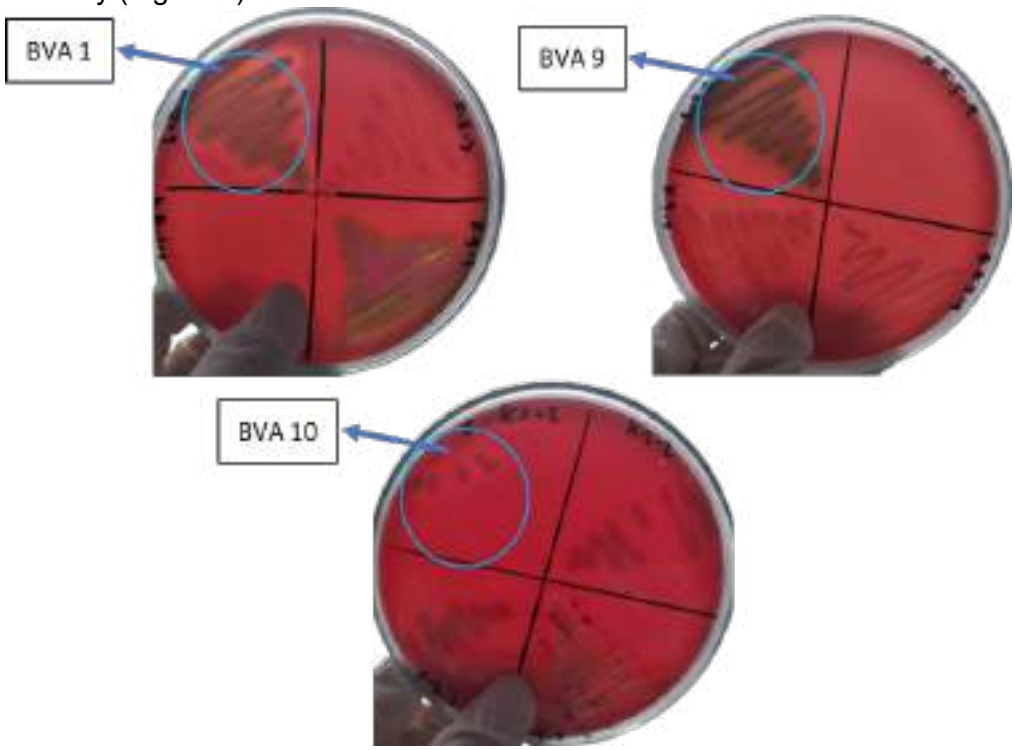

Figure 1. Bacterial colonies of *A. granosa* isolates in BAP media

Each colony was taken, and gram stain was performed to see the characteristic of the bacteria. The three colonies such as isolates BVA1, BVA9, and BVA10 were Gram-negative bacteria. They were basil or rod-shaped and the color were red. ß-hemolysis bacteria have the ability to multiply faster than α-hemolysis. The production of enterotoxin from α-hemolysis and ß-hemolysis, can lead to pathogenicity. ß-hemolysis strains can last longer than α-hemolysis[13].

Each bacterial colony was inoculated on HIA media, then instilled on BHI media for DNA isolation. DNA isolation was conducted using the phenol-CIAA method and then the 16S rRNA gene was amplified by the PCR method. The PCR product of each isolate then visualized with 2% agarose electrophoresis (Figure 2).

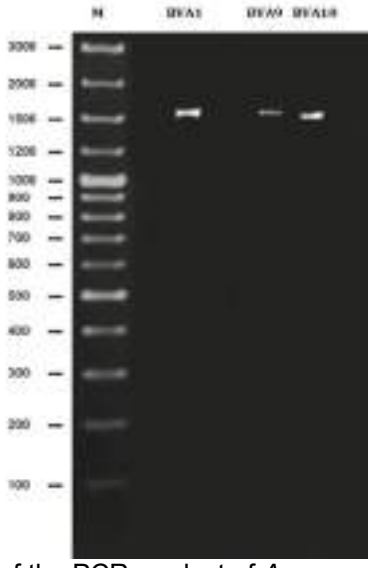

Figure 2. Visualization of the PCR product of *A. granosa* bacterial isolates

BVA1, BVA9, and BVA10 isolates had PCR products about 1500 bp due to the 16S rRNA gene has a size of about 1550 base pairs and about 500 bases at the end is a hypervariable region[4]. The hypervariable region in the 16S rRNA gene is used to identify bacteria or determine the characteristics of a bacteria[5]. The PCR products of the three isolates (BVA1, BVA9, and BVA10) were then sequenced.

The results of the sequencing were compared with the data in Genbank through the BLAST program and then aligned and made a phylogenetic tree with the Mega X program. Based on the results from the Mega X program, three phylogenetic trees were obtained from the three isolates. BVA1 and BVA10 isolates obtained phylogenetic tree as follows (Figures 3 and 4).

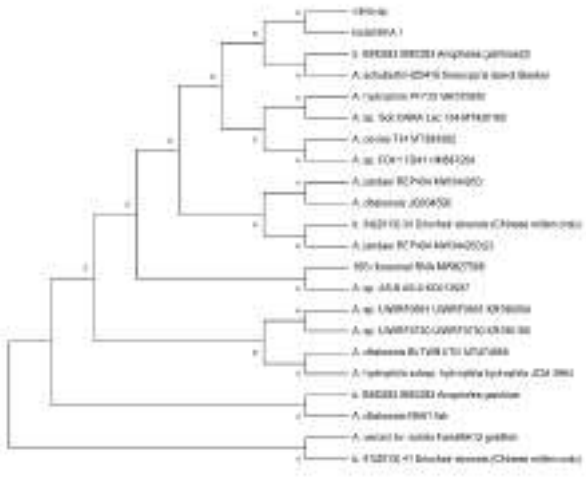

Figure 3. Phylogenetic tree analysis of BVA1 isolates that were similar to *Vibrio* sp.

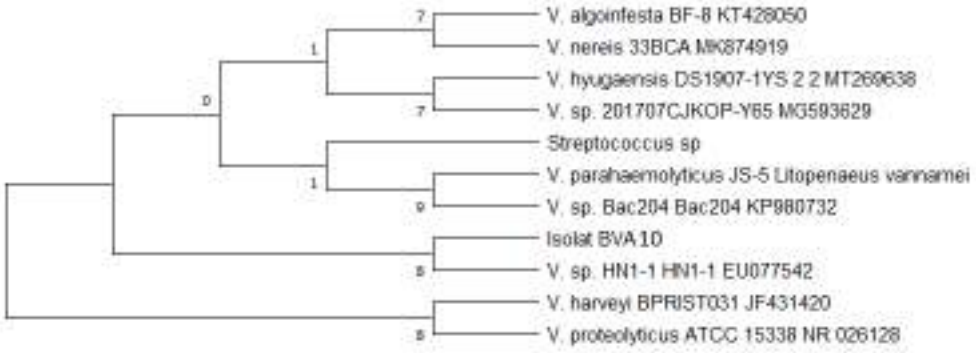

Figure 4. Phylogenetic tree analysis of isolates BVA10 has similarities with *Vibrio* sp.

Based on the results of the phylogenetic tree analysis (Figures 3 and 4), it was shown that the isolates BVA1 and BVA10 had similarities with *Vibrio* sp. It is Gram-negative bacteria that are single-celled with short curved (comma) or straight rods. The length of the *Vibrio* sp. is about 1.4-50 nm and the wide is about 0.3-1.3 nm, motile and have polar flagella[14]. The genome of *Vibrio* sp is divided into two chromosomes, which are formed by recombination and horizontal gene transfer (HGT; acquisition of genetic material by transfer from another organism). Although these pathogens may be diverse in genomic, the bacteria came from aquatic and marine environments. *Vibrio* sp. prefer warm environments and salty waters[15]. The presence of *Vibrio* sp. in traditional seafood processed products should be a concern because these products are ready to eat and can be a source of disease caused by food[16]. It responsible for most human diseases caused by the natural microbiota of aquatic environments and seafood. The most common bacterial pathogenic species are *Vibrio cholerae*, *Vibrio parahaemolyticus*, *Vibrio vulnificus*, and *Vibrio alginolyticus*[9].

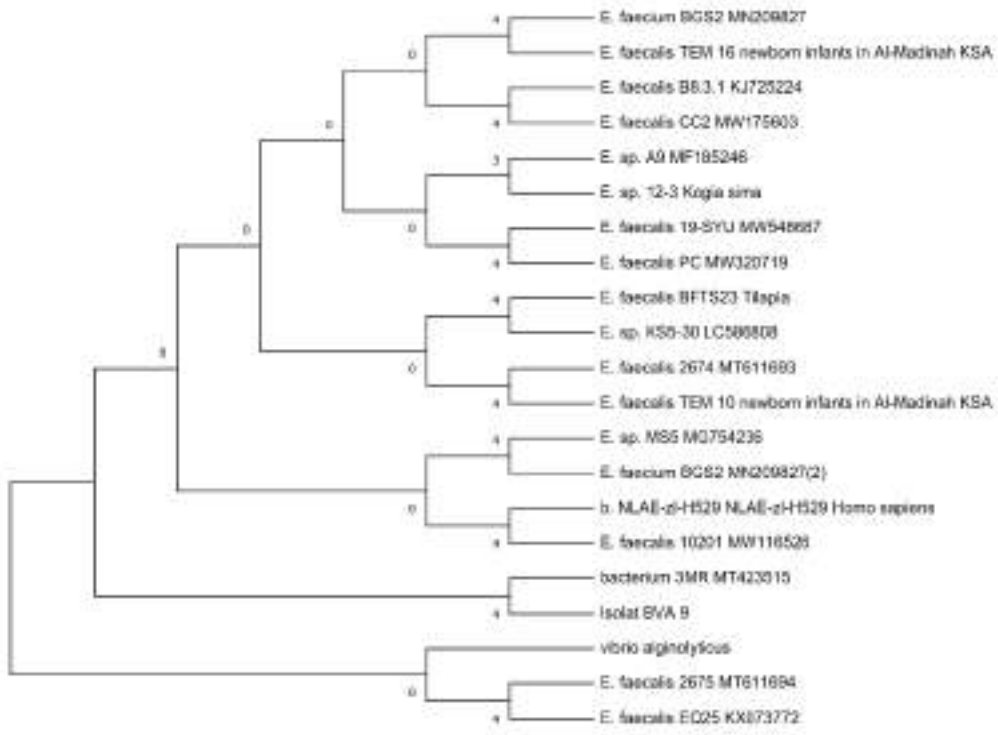

Figure 5. Phylogenetic tree analysis of BVA9 isolates were similar to Bacterium.

The sequence of BVA9 isolates were similar to Bacterium 3MR MT423515 because the sequence of BVA9. Bacterium 3MR MT423515 is a type of bacteria whose species has not been decided. This bacterium was also discovered by Gao from China, but the journal about Bacterium has not been published[17].

A. granosa is a species that lives in muddy coastal waters, but it can also be found in mangroves and seagrass. Bacterial contamination in the cultivation of blood clams is influenced by human activities around. Human activities can produce household waste that pollutes waters if it contains pathogenic bacteria, so it can affect the quality of blood cockle because they are filter feeders (filtering water to get food)[18].

The foodborne disease is closely related to bacterial pathogenic factors, the ability to attack tissues, the speed of pathogen proliferation, colonization, and the host's defense system against pathogens. The hemolytic activity of bacteria makes bacterial defense factors attack the host's defenses by lysing the host's blood cells. Bacteria that can survive will enter the bloodstream so that they spread to all host body cells and target organs[19]. Target organs can be animal organs such as blood cockles or from humans. *Vibrio* sp. can infect animals and humans due to imperfect food processing.

The presence of *Vibrio* sp. in aquaculture waters such as blood cockles and other seafood are also influenced by physical and chemical parameters. The chemical parameters that affect are the levels of ammonia and organic matter in cultivation. Another studies showed that poor physical and chemical parameters are the cause of the abundance of *Vibrio* sp. in vaname shrimp rearing water[20,21].

CONCLUSION

The bacterial isolate BVA1 and BVA10 in *A. granosa* were similar to *Vibrio* sp. Therefore isolate bacteria BVA9 had similarity with Bacterium. *Vibrio* sp. has often been found in aquacultured seafood, while for Bacterium the species has not yet been determined. Blood cockle with imperfect processing may still contain *Vibrio* sp. and can cause foodborne disease.

AUTHOR'S CONTRIBUTION STATEMENT

Meutia Srikandi Fitria carried out the DNA extraction, PCR and compiling publication manuscript, Aprilia Indra Kartika performed analyzing sequencing data, Ana Hidayati Mukaromah measured the concentration and purity DNA, Nurfi Ismatul Unasiah carried out the bacteria culture, NA, BAP, and BHI.

FUNDING INFORMATION

This research received Dosen Pratama Grant from LPPM University of Muhammadiyah Semarang, Indonesia

DATA AVAILABILITY STATEMENT

The utilized data to contribute to this investigation are available from the corresponding author on reasonable request.

DISCLOSURE STATEMENT

The views and opinions expressed in this article are those of the authors and do not necessarily reflect the official policy or position of any affiliated agency of the authors. The data is the result of the author's research and has never been published in other journals.

REFERENCE

1. Eoh CB. Tinjauan Ekonomi Kerang Darah (Anadara granosa) Konsumsi Produsen Ramah Lingkungan di Desa Oebelo. *J Bahari Papadak*. 2021;2(2):62-71.

2. Devi AR, Susilowati A, Setyaningsih R. Enumerasi dan uji patogenitas Vibrio sp . yang terdapat pada kerang darah (Anadara granosa) di kawasan pantai wisata Yogyakarta. *Biodiversitas*. 2019;20(10):2980-2896. doi:10.13057/psnmbi/m050138
3. Radji M, Puspaningrum A, Sumiati A. Deteksi Cepat Bakteri Escherichia coli Dalam Sampel Air dengan Metode Polymerase Chain Reaction Menggunakan Primer 16E1 dan 16E2. *Makara Sains*. 2010;14(1):39-43. doi:10.7454/mss.v14i1.474.
4. Riananda T. Analisis Sekuensing 16S rRNA Di Bidang Mikrobiologi. *J Kedokt Syiah Kuala*. 2011;11:172-177.
5. Yang B, Wang Y, Qian PY. Sensitivity and correlation of hypervariable regions in 16S rRNA genes in phylogenetic analysis. *BMC Bioinformatics*. 2016;17:1-8. doi:10.1186/s12859-016-0992-y
6. Kanjanasopa D, Pimpa B, S C. Occurrence of Vibrio parahaemolyticus in cockle (Anadara granosa) harvested from the south coast Thailand. *Songklanakarin J Sci Technol*. 2011;33(3):295-300.
7. Zarkasi KZ, Sheng KF, Nazari TF, Muhammad NA, Abdullah AA. Bacterial Community Diversity with Blood Cockle (Anadara granosa) in Penang, Malaysia. *Sci Bruneiana*. 2017;16(2):41-47. doi:10.46537/scibru.v16i2.64
8. Hoar YS, Y., Santoso P. Identifikasi Parasit dan Bakteri Vibrio pada Kerang Darah (Anadara granosa) di Perairan Tanah Merah, Kecamatan Kupang Tengah. *J Aquat*. 2020;3(2):57-66.
9. Ekawati ER dan YSNH. Detection of Salmonella sp., Vibrio sp. In: *And Total Plate Count Bacteria on Blood Cockle (Anadara Granosa). International Symposium on Food and Agro-Biodiversity (ISFA*. ; 2017. doi:10.1088/1755-1315/102/1/012086
10. Fitri S, Patria. Microplastic contamication on Anadara granosa Linnaeus 1758 in Pangkal Babu Mangrove Forest Area, Tanjung Jabung Barat District, Jambi. In: *Sriwijaya International Conference on Basic and Applied Science 1282*. ; 2019. doi:10.1088/1742-6596/1282/1/012109.
11. Putra DF, Ramadina S, Mellisa S, Abbas MA, He-he X. Endoparasite Infection in Blood Cockle (Anadara granosa) in Aceh Besar Waters, Indonesia. *J Kedokt Hewan*. 2021;15(3):97-102. doi:doi: https://doi.org/10.21157/
12. Kumar S, Stecher G, Li M, Knyaz C, Tamura K. MEGA X: Molecular Evolutionary Genetics Analysis across Computing Platforms. *Mol Biol Evol*. 2018;35:1547-1549. doi:10.1093/molbev/msy096.
13. Hikmawati F, Susilowati A, Setyaningsih R. Colony Morphology and Molecular Identification of Vibrio spp. on Green Mussels (Perna viridis) in Yogyakarta, Indonesia Tourism Beach Areas. *Biodiversitas*. 2019;20(10):2891-2899. doi:10.13057/biodiv/d201015
14. Felix F, Nugroho TT, Silalahi S, Octavia Y. Screening of Indonesian Original Bacterial Vibrio sp. as a Cause of Shrimp Disease Based on 16S Ribosomal DNA Technique. *Trop Mar Sci Technol J*. 2011;3(2):85-99. doi:10.29244/jitkt.v3i2.7824
15. Baker-Austin C, Oliver JD, Alam M, et al. Vibrio spp. *Infect Nat Rev Dis Primer*. 2018;4:1-19. doi:10.1038/s41572-018-0005-8
16. Pramono H, Noor HM, Fatimah SS, Harahap NA, Selia AA. Isolation and Identification of Vibrio sp. from Traditional Seafood Products of Eastern Surabaya City Area. *J Ilm Perikan Dan Kelaut*. 2015;7(1):25-29. doi:10.20473/jipk.v7i1.11223
17. N.C.B.I. Bacterium strain 3MR 16S ribosomal RNA gene, partial sequence. Published online 2021. https://www.ncbi.nlm.nih.gov/nuccore/1837382530.
18. Pratiwi FD dan S, E. Evaluasi Depurasi Total Bakteri Pada Kerang Darah dari Perairan Desa Sukal, Kabupaten Bangka Barat. *J Fish Mar Res*. 2019;3(3):308-314. doi:10.21776/ub.jfmr.2019.003.03.4

19. Fitriatin E, Manan A. Examination of Viral Nervous Necrosis (VNN) in Fish with the Polymerase Chain Reaction (PCR) Method. *Fish Mar Sci J*. 2015;7(1):2088-5842. doi:10.20473/jipk.v7i2.11198
20. Kharisma A dan A, M. Kelimpahan Bakteri Vibrio Sp. Pada Air Pembesaran Udang Vaname (Litopenaeus vannamei) Sebagai Deteksi Dini Serangan Penyakit Vibriosis. *J Ilm Perikan Dan Kelaut*. 2012;4(2). doi:10.20473/jipk.v4i2.11563
21. M.F. M, Bunga M, Achmad M. Penggunaan Probiotik untuk Menekan Populasi Bakteri Vibrio sp. Pada Budidaya Udang Vaname (Litopenaeus vannamei. *ToraniJournal Fish Mar Sci*. 2019;2(2):69-76. doi:10.35911/torani.v2i2.7056

JTL 11 (2) December 2022
Page: 73-77

Contents list available at Jurnal Teknologi Laboratorium

JURNAL TEKNOLOGI LABORATORIUM

Journal Homepage: www.teknolabjournal.com
ISSN 2580-0191(Online) I ISSN 2338 – 5634(Print)

Original Study

Effect of fetal bovine serum concentration towards vero cells growth on culture in DMEM medium

Bella Niken Ikasari[1,2], Salman Alfarizi[1], Shifa Fauziyah[3], Puspa Wardhani[3,4], Aryati[3,4], Soegeng Soegijanto[3], Teguh Hari Sucipto[3,*]

1 Internship student, Research Center on Global Emerging and Re-emerging Infectious Diseases, Institute of Tropical Desease, Universitas Airlangga, Indonesia
2 Chemistry Department, Faculty of Science and Technology, Universitas Airlangga, Indonesia
3 Dengue Study Group, Institute of Tropical Disease, Universitas Airlangga, Indonesia
4 Clinical Pathology Department, Faculty of Medicine, Universitas Airlangga, Indonesia

Abstract: Cell culture requires a suitable medium and environment for in vivo conditions. Conditions are created by regulating temperature, pH, oxygen, CO_2, osmotic pressure, surfaces to adhere to cells, nutrients, and vitamins, protection against toxic substances, hormones, and growth factors that regulate cell growth and differentiation. In general, good cell growth occurs at a pH of 7.0 - 7.6. Fetal Bovine Serum (FBS) is one of the supplement media to support cell growth. The purpose of this study was to determine the effect of using FBS supplementation with various concentrations on Vero cell culture media on DMEM (Dulbecco's modified eagle medium) media. Vero cell culture on DMEM media has been successfully carried out using FBS by observing its growth for 14 days. Vero cell culture process begins with the manufacture of media consisting of DMEM and FBS. The cell density of each well at 5% and 10% concentration media was 1017 cells/well. By varying the concentration of FBS in the culture medium, the difference in the number of cells produced can be observed under the microscope. The results showed that the number of Vero cells produced from DMEM media with 10% FBS concentration was higher than 5% FBS concentration. Thus, this study proves that the higher the concentration of FBS in the medium, the more it supports the cell growth process in the Vero cell culture process.

Keyword: *Vero cells; DMEM; FBS*

INTRODUCTION

Vero cells are cells that were first taken from the kidney of an adult African green monkey Cercopithecus aethiops, Vero cells are one of the most common mammalian continuous cell lines used in research[1,2,3]. It is used as a positive control that represents normal cells in the human body and is often used in toxicity test studies because of its easy handling, unlimited replication capability, and easy replacement of frozen stock in case of contamination[4]. Cell culture relates to a mode of reproduction of dispersed cells. Cell culture requires a suitable medium and environment for in vivo conditions. Conditions are created by regulating temperature, pH, oxygen, CO_2, osmotic pressure, the surface to adhere to cells,

Corresponding author.
E-mail address: teguhharisucipto@staf.unair.ac.id (Teguh Hari Sucipto)
DOI: 10.29238/teknolabjournal.v11i2.313
Received 30 November 2021; Received in revised form 10 November 2022; Accepted 28 December 2022

nutrients, and vitamins, protection against toxic substances, hormones, and growth factors that regulate cell growth and differentiation.

The serum is a biological fluid that is proven to support cell growth outside the body[5]. Fetal Bovine Serum (FBS) is one of the IVM medium supplements derived from fetal bovine blood which was frozen and collected aseptically. It is used to stimulate the growth of large amounts of tissue culture cells. Serum concentrations are needed to support cell growth. For best cell growth a concentration of 5% is usually used. The function of FBS as a growth factor, penicillin as an antibiotic, and fungizon as an antifungal. Generally, good cell growth occurs at a pH of 7-7.6. The growing medium also requires a buffer because of two conditions: the use of an open flask causing the entry of O2 which can increase the pH, and a high concentration of cells causing the production of CO2 and lactic acid, which causes a decrease in the pH. Both of these conditions are faced by providing a buffer into the medium and the incubator CO2 flows from outside. The condition culture consisting of a medium, Growth Hormone concentration and use of CO2 incubator (old culture time) supports growth from follicular culture[6].

MATERIAL AND METHOD

Research materials and tools

Vero cell purchased from The European Collection of Authenticated *Cell* Cultures (*ECACC*). Dulbecco's modified eagle medium (DMEM) purchased from Gibco that contains 4.5 g/L D-glucose, L-glutamine, and sodium pyruvate. FBS purchased from Gibco, and *trypsin-ethylenediaminetetraacetatic acid* (Trypsin-EDTA).

Medium Preparation and Cell Culture

The Vero cell culture process begins with the making of a medium consisting of DMEM and FBS. In this study, variations in the concentration of FBS were 5% and 10% in 100 mL medium volume. Vero cells in the initial medium were observed to ensure their presence. Normal vero cells are like small leaves attached to the bottom of the flask, while dead cells are round and do not stick[7].

Figure 1. Vero Cell (Misra et al., 2010)

After the presence of Vero cells was observed, the initial medium was removed and trypsin-EDTA was added to exfoliate the cells from the vial it is called the passage process[8]. The medium was added again to neutralize trypsin-EDTA then centrifuged to separate the Vero cell with other substances. The cells are taken a slight to be counted using a counting chamber and microscope which aims to determine the amount of cell dilution in a new medium. Finally, a new medium was added with concentrations of FBS is 5% and 10%[9]. *Cell culture is the most popular method of virus propagation because of its high sensitivity. However, the need for high cost liquid nitrogen for cell line storage is one of the main limiting factors for its widespread use in developing countries. Freezer at -85ºC can be used as an alternative to liquid N2 for cell line preservation*[10]. Respectively, then it was saved in a 6-well culture cell and incubated in a cell incubator. The cell density of each well in 5% and 10% concentration media were 1017 cells/well. Cells in the medium were incubated to observe cell growth for 14 days. To reduce the risk of contamination, almost all activities above are carried out a sterile, laminar flow

hood, make sure all equipment and solutions that come into contact with the cells are sterile, and use proper sterile technique when working in the hood.

RESULTS AND DISCUSSION

Vero cell growth in this study was observed on days 5, 7, 12, and 14 by comparing the approach to the number of Vero cells produced between the medium with 10% and 5% FBS. Cells can be in 3 states, namely being dividing (proliferative cycle), in a resting state (not dividing), and not dividing permanently. Vero cells that are dividing are found in several phases, namely mitosis (M), postmitotic (G1), DNA synthesis phase (S), and premitotic phase (G2) (Campbell and Farrell, 2003; Johnson dan Walker, 1999). At the end of the G1 phase there is an increase in RNA followed by the S phase which is the time of DNA replication[11,12]. After the S ends, the cell enters the premitotic phase (G2) with the following characteristics: the cell is tetraploid, contains twice as much DNA as other cells, and continues to synthesize RNA and proteins. During mitosis (phase M), protein and RNA synthesis decreases abruptly, and division into 2 cells occurs. After that, cells can enter interphase to re-enter the G1 phase, when cells proliferate or enter a resting phase (G0)[13,14]. Cells in the G0 phase that still have the potential to proliferate are called peak cells. So that the increase in the number of cells is cells that are in the proliferation cycle and G0 phase. The addition of serum will induce cells to reenter the cell cycle to the point of restriction for the next process[15]. The results of cell observation using a microscope are shown in figure 2.

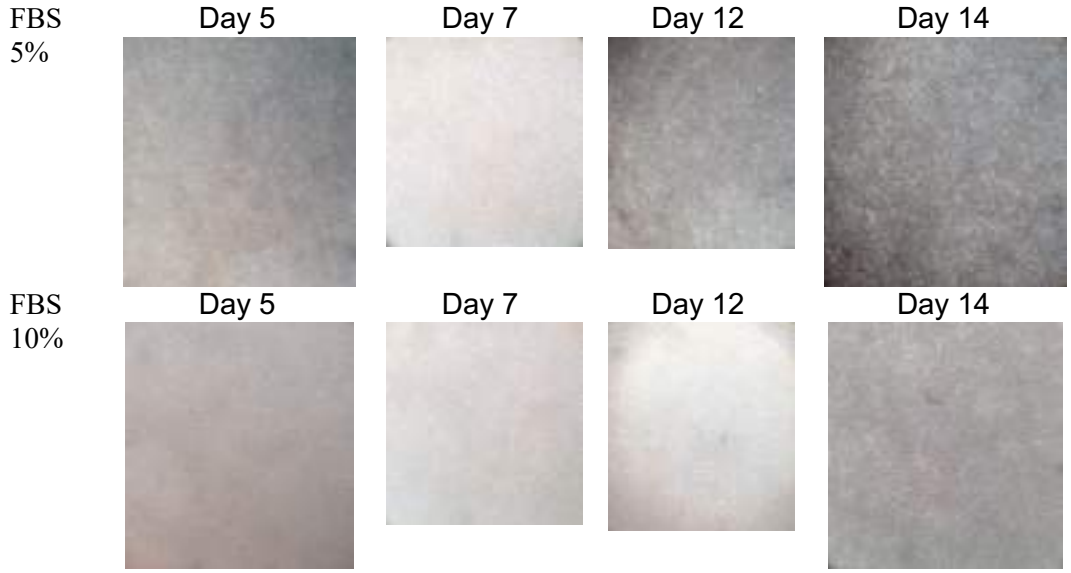

Figure 2. Vero cell development at day 5, 7, 12 and 14.

The figure shows that the more days, the number of cells contained in the medium are getting much and dense. Furthermore, there were differences in the approach number of cells produced from cultures with 10% and 5% FBS medium in DMEM. Vero cells produced by medium containing 10% FBS more than 5% FBS medium. This proves that the higher the concentration of FBS in the medium will support the growth of Vero cells in the culture process.

CONCLUSION

Based on the research, it can be concluded that the use of FBS in DMEM medium with concentrations of 5% and 10% effect the number of Vero cells produced in the culture process. Observations on cell growth on days 5, 7, 12, and 14 using a microscope, proved that the number of cells increased day by day. Thus, from this study, it was reported that FBS 10% produced the most cells.

AUTHOR'S CONTRIBUTION STATEMENT

all authors have equal responsibility in the research and preparation of the manuscript.

FUNDING INFORMATION

-

DATA AVAILABILITY STATEMENT

The utilized data to contribute to this investigation are available from the corresponding author on reasonable request.

DISCLOSURE STATEMENT

The views and opinions expressed in this article are those of the authors and do not necessarily reflect the official policy or position of any affiliated agency of the authors. The data is the result of the author's research and has never been published in other journals.

REFERENCE

1. Ammerman NC, Beier-Sexton M, Azad AF. Growth and Maintenance of Vero Cell Lines. *Curr Protoc Microbiol*. 2008;11(1). doi:10.1002/9780471729259.mca04es11
2. Cao S, Dong G, Tang J, et al. Development of a Vero cell DNA reference standard for residual DNA measurement in China. *Hum Vaccines Immunother*. 2013;9(2):413-419. doi:10.4161/hv.22699
3. Listyawati S, Sismindari S, Mubarika S, Murti YB, Ikawati M. Anti-Proliferative Activity and Apoptosis Induction of an Ethanolic Extract of Boesenbergia pandurata (Roxb.) Schlecht. against HeLa and Vero Cell Lines. *Asian Pac J Cancer Prev*. 2016;17(1):183-187. doi:10.7314/APJCP.2016.17.1.183
4. Nor YA, Sulong NH, Mel M, Salleh HM, Sopyan I. The Growth Study of Vero Cells in Different Type of Microcarrier. *Mater Sci Appl*. 2010;01(05):261-266. doi:10.4236/msa.2010.15038
5. Han ZB, Lan GC, Wu YG, et al. Interactive effects of granulosa cell apoptosis, follicle size, cumulus–oocyte complex morphology, and cumulus expansion on the developmental competence of goat oocytes: a study using the well-in-drop culture system. *Reproduction*. 2006;132(5):749-758. doi:10.1530/REP-06-0055
6. GOTO K, TAKUMA Y, OOE N, OGAWA K. In vitro development of bovine oocytes collected from ovaries of individual cows after in vitro fertilization. *Jpn J Anim Reprod Jpn*. Published online 1990.
7. Marbawati D, Sarjiman S. Konsentrasi Aman Kurkumin dan PGV-0 terhadap Sel Vero Berdasarkan Hasil Uji Sitotoksik. *J Kefarmasian Indones*. 5(2):2015.
8. Indonesia Society for Cancer Chemoprevention. Protokol In Vitro. Published online 2017.
9. Comşa Ş, Cîmpean AM, Raica M. The Story of MCF-7 Breast Cancer Cell Line: 40 years of Experience in Research. *Anticancer Res*. 2015;35(6):3147-3154.
10. Mishra A, Chandiraseharan V, Jose N, Sudarsaman T. Chlorantraniliprole: An unusual insecticide poisoning in humans. *Indian J Pathol Microbiol*. 53(4):742. doi:10.4103/0972-5229.195718
11. Rang HP, Dale MM, Rang HP, eds. *Pharmacology*. 5. ed. Churchill Livingstone; 2003.
12. Dorée M, Hunt T. From Cdc2 to Cdk1: when did the cell cycle kinase join its cyclin partner? *J Cell Sci*. 2002;115(12):2461-2464. doi:10.1242/jcs.115.12.2461
13. Murti H, Boediono A, Setiawan B, Sandra F. Regulasi Siklus Sel : Kunci Sukses Somatic Cell Nuclear Transfer. *Cermin Dunia Kedoktera*. 2007;34(6).

14. Qu Z, MacLellan WR, Weiss JN. Dynamics of the Cell Cycle: Checkpoints, Sizers, and Timers. *Biophys J*. 2003;85(6):3600-3611. doi:10.1016/S0006-3495(03)74778-X
15. Jones SM, Kazlauskas A. Growth factor-dependent signaling and cell cycle progression. *FEBS Lett*. 2001;490(3):110-116. doi:10.1016/S0014-5793(01)02113-5

JTL 11 (2) December 2022
Page: 78-94
Contents list available at Jurnal Teknologi Laboratorium

JURNAL TEKNOLOGI LABORATORIUM

Journal Homepage: www.teknolabjournal.com
ISSN 2580-0191(Online) I ISSN 2338 – 5634(Print)

Original Study

Isolation and identification of an alkaloid compound from Bebuas leaves (Premna serratifolia) as an anti-inflammatory in white rats (Rattus norvegicus)

Muhammad Irhash Shalihin[1*], Muhaimin[1,2], and Madyawati Latief[1]

[1] Department of Mathematics and Natural Science, University of Jambi, Indonesia
[2] Department of Pharmacy, University of Jambi, Indonesia

Abstract: Bebuas (*Premna serratifolia*) is traditionally used by Malay people as a traditional medicine to restore health. This indicates it contains chemicals that potentially have an anti-inflammatory activity. The phytochemical screening showed that the ethanol extract contained phenolics, alkaloids, flavonoids, steroids and saponins. Meanwhile, hexane extract contained steroids only. Anti-inflammatory activity evaluation on crude extracts showed that the ethanol extract was more active than the hexane extract. Therefore, the isolation was carried out to ethanol extract with the targeted compound was an alkaloid. The extraction was conducted by using acid-base and partition techniques to give the alkaloids fraction (EaBW). EaBW was then further separated by liquid vacuum column technique using gradual polarity elution, with eluent of ethyl acetate - methanol and 5 fractions were obtained. The isolate was obtained from F.3. The isolate showed it had anti-inflammatory activity with ED_{50} = 5.45 mg/kgbw. The UV-Vis and FT-IR spectra patterns of the isolate showed similarities with ciprofloxacin as well as its physical characteristics which were hygroscopic yellowish crystal, and fluorescence property. Therefore, the isolated compound is thought to have a similar structure with ciprofloxacin.

Keyword: Bebuas; Anti-inflammatory; Alkaloid; Ciprofloxacin

INTRODUCTION

Bebuas is a shrub that belongs to the verbenaceae family [1] which is traditionally used by the Malay community as a vegetable, as well as a traditional medicine to cure various diseases such as colds, eliminating bad breath, treating intestinal worms, treat diarrhea, lung infections, rheumatism, headaches, febrifuge and can help restore the health of women after childbirth [2,3]. This indicates that bebuas contains bioactive chemical compounds.

The phytochemical screening of the ethanol extract of bebuas leaves showed that these leaves contain secondary metabolites from flavonoid, tannin, alkaloid, phenolic, and saponin groups [4]. Meanwhile, the secondary metabolite compounds that are active as anti-inflammatory are mostly derived from alkaloid, phenolic, and steroid groups [5]. This shows that bebuas leaves contain a class of compounds that are active as anti-inflammatory. The plant of the same genus, *Premna cordifolia*, has also been reported to be active as an anti-inflammatory [6]. This supports the notion that bebuas leaves also contain active compounds as anti-inflammatory. This is because chemotaxonomically, a plant that is in the same genus will contain the same chemical compounds [7]. The fact that bebuas leaves

Corresponding author.
E-mail address: m.irhash@unja.ac.id (Muhammad I.S)
DOI: 10.29238/teknolabjournal.v11i2.275
Received 06 October 2021; Received in revised form 16 February 2022; Accepted 31 October 2022

ethnobotanically can reduce fever and restore women's health after childbirth also reinforces the notion that bebuas leaves contain active anti-inflammatory compounds.

Inflammation is a natural response to tissue injury or infection [8]. The inflammatory process is mediated by arachidonic acid, prostaglandins, histamines, and eicosanoids. Although it is a natural process, inflammation must be addressed immediately because if it prolongs it can cause rheumatoid arthritis, atherosclerosis, fever and ischemic heart disease [9]. In Indonesia itself, the death rate due to inflammation, namely ischemic heart disease in 2017 reached 10,408 people. This makes inflammation one of the top 50 causes of death in Indonesia [10]. Therefore an effective anti-inflammatory drug is needed.

Anti-inflammatory drugs are compounds that can treat diseases caused by inflammation. Anti-inflammatory drugs are divided into steroid and non-steroidal anti-inflammatory drugs. Steroid anti-inflammatory drugs work by inhibiting the formation of arachidonic acid. Meanwhile, non-steroidal anti-inflammatory drugs work by inhibiting the formation of prostaglandins. These anti-inflammatory drugs are commercially available today. However, these anti-inflammatory drugs still have side effects in the form of stomach ulcers and muscle development disorders when consumed in a long term [11]. Therefore, the search for new anti-inflammatory drug compounds that work better is still being continued.

MATERIAL AND METHOD

Materials

The plant material used in this study was the leaves of bebuas (*Premna serratifolia*) obtained from the Tanjung Jabung Timur Regency, Jambi Province, Indonesia. The chemicals used during the research included ethanol, n-hexane, ethyl acetate, silica gel, methanol, ammonia 0.05 N, chloroform, 2N sulfuric acid, Mayer's reagent, concentrated hydrochloric acid, concentrated sulfuric acid, anhydrous acetic acid, Mg powder, 1% ferric chloride solution, 1% carrageenan, Na diclofenac, Na CMC 1%, Aquadest.

Sample Preparation

Two kilograms of bebuas fresh leaves were cleaned and washed. Furthermore, the leaves were cut into small pieces to increase their surface area, and then the leaves were dried for several days to reduce the moisture content.

Extraction of Sample

Five hundred grams of dried leaves were macerated with hexane (nonpolar) and ethanol (polar) for 3 days and carried out several times. The macerate obtained was concentrated by using a rotary evaporator to 1/10 of its original volume. The concentrated extract obtained from each solvent was combined and evaporated on a water bath to evaporate the solvent, then the dry extract was weighed.

Phytochemical Screening

Alkaloid Test. A total of 1 mL of sample was dissolved in a few drops of 2N sulfuric acid, then tested with three alkaloid reagents, namely Dragendorff's reagent, Meyer reagent and Wagner reagent. The test results are stated positive if with Dragendorff's reagent a red to orange precipitate is formed, with Meyer reagent a yellowish-white precipitate is formed and with Wagner's reagent a brown precipitate is formed [12].

Flavonoid Test. A few samples were mixed with a few drops of concentrated HCl and then Mg powder is added. A positive result is shown by the formation of foam and the change in color of the solution to orange [12].

Saponin Test. Saponins were detected by a foam test in hot water. A stable foam that can last a long time and does not disappear when 1 drop of 2N HCl is added indicates the presence of saponins [12].

Tannin Test. A number of samples were mixed with $FeCl_3$ then the mixture was homogenized. A positive reaction is shown by the formation of a greenish black color in the mixture [12].

Steroid and Triterpenoid Test. A few samples were added with anhydrous acetic acid and concentrated sulfuric acid (Liebermann-Burchard reagent). If it forms a blue or green color it indicates the presence of steroids. If a purple or orange color is formed, this indicates triterpenoids [12].

Compound Separation and Purification

Alkaloid Extraction. The concentrated ethanol extract was further separated using the acid-base method of liquid-liquid extraction. The concentrated ethanol extract was dissolved in 500 mL of water, then acidified with 2 M HCl until the pH of the solution became 3. The acidic solution was partitioned using 100 mL hexane for 5 repetitions. The partition gave 2 layers, namely the acidic water layer below and the hexane layer above. Then the two layers were separated. The acidic water layer was re-partitioned using 100 mL ethyl acetate for 5 repetitions. The partition provided 2 layers, namely the acidic water layer below and the ethyl acetate layer above. After the two layers were separated, the acidic water layer was basified by adding 2 M NH_4OH until the pH of the solution became 9. Then it was re-extracted using 100 mL of ethyl acetate for 5 repetitions. The partition provided 2 layers, namely the basic water layer below and the ethyl acetate layer above. After being separated, the ethyl acetate layer was combined and concentrated using a rotary evaporator to obtain crude alkaloid extract. The crude alkaloid extract was then weighed and further separated using VLC [13].

Thin Layer Chromatography (TLC). A 1 x 5 cm TLC plate was prepared with a lower limit of 0.5 cm and an upper limit of 0.5 cm so that the eluent distance traveled was 4 cm. Then the eluent was made by using multilevel polarity of organic solvent. The extract was spotted at the lower boundary of the plate with a capillary tube, then eluted with the mobile/eluent phase. After the developer solution moved to the upper limit, the elution process was stopped. Then the shape of the stain was noted directly under UV light of 254 and 395 nm. After the column chromatography was carried out, all fractions were subjected to a TLC test to see the stain components. The fractions having the same spots were put together and re-analyzed by TLC.

Column Chromatography. Liquid vacuum column chromatography (VLC) was performed using the stationary phase of silica gel with a ratio sample to silica gel 1:20. The extract was impregnated with silica gel, then added to the column which already contained the stationary phase. The mobile phase used was ethyl acetate - methanol with various ratios. The fraction obtained was collected in vials, the eluate was collected based on each band obtained and then evaporated. The fractions from the column chromatography were monitored with TLC. Eluates that having identical stain patterns were combined based on the R_f value on the chromatogram. The fraction which had one spot was then tested using 3 different eluents to see the stain pattern. Isolates were purified by recrystallization using n-hexane, ethyl acetate and ethanol as solvents. Furthermore, phytochemical screening, characterization, and anti-inflammatory activity evaluation were performed.

Anti-Inflammatory Activity Evaluation

Preparation of Extract Suspensions. The ethanol and hexane extracts were suspended with Na CMC in distilled water. Na CMC was sprinkled over hot water in the mortar using water as much as 20 times the weight of Na CMC and left for 15 minutes until the Na CMC developed. Then the extract was inserted gradually into the mortar while being crushed homogeneously and distilled water was added until the total volume was 10 mL [14].

Anti-Inflammatory Activity Evaluation. Anti-inflammatory activity evaluation was carried out on positive control (formulated drug of Na diclofenac), negative control (Na CMC), ethanol extract, hexane extract, VLC fraction, and the isolate.

Na diclofenac was used for the positive control as it is a medication for inflammation that has been used commercially. Before the testing, the rats were fasted for 18 hours (not eating but still given a drink). Each group consisted of 4 rats. The categories of each group, namely, C0 = negative control (-) for 1% Na CMC; C1 = control (+) for 10 mg Na diclofenac; C2 = hexane extract 250 mg/kgbw; C3 = hexane extract 500 mg/kgbw; C4 = hexane extract 1000 mg/kgbw; C5 = ethanol extract 250 mg/kgbw; C6 = ethanol extract 500 mg/kgbw; and C7 = ethanol extract 1000 mg/kgbw. Anti-inflammatory evaluation was also performed on the five fractions of VLC with code F.1; F.2; F.3; F.4; and F.5 and the test dose of each was 10 mg/kgbw. Meanwhile, the anti-inflammatory activity of the isolate was evaluated at doses of 3, 5, and 10 mg/kgbw.

At the time of testing each animal was weighed and marked on the tail. After that, the rat's left paw was subjected into a pletysmometer, then the volume was recorded as the initial volume (V_0), namely the volume of the paw before being given the test substance. Each rat's paw was injected subplantarly with 0.1 ml carrageenan 1% solution. After thirty minutes, measurements were taken by dipping the rats' paw into a plethysmometer tube and each rat was given a suspension of the test substance orally according to its group. The changes in fluid volume that occurred were recorded as the volume of the rats' paw at each observation time (V_t). Measurements were carried out every 60 minutes for 300 minutes [15]. After the measurement, the volume of rat paw edema and AUC (Area Under the Curve) was calculated from the average edema against time curve and the percent of inflammation inhibition [16].

Calculation of volume of rat paw edema, AUC from the time-average edema curve, and the percent anti-inflammatory effect [16] are as follows:

$$Vu = V_t - V_0$$

Where:
V_u : volume of rat paw edema each time t
V_t : volume of rat paw after 1% carrageenan induction at time t
V_0 : Initial volume of rat paw before induced by carrageenan 1%

$$AUC_{t_{n-1}}^{t_n} = \frac{Vu_{n-1} + Vu_n}{2}(t_n - t_{n-1})$$

Where:
V_{un-1} : volume average edema at t_{n-1}
V_{un} : volume average edema at t_n

$$\%\ the\ percentage\ of\ inflammation = \frac{AUC_k - AUC_p}{AUC_k} \times 100\%$$

Where:
AUC_k : AUC of time-to-mean edema volume curve for negative control
AUC_p : AUC of the edema volume versus time curve for the treatment group in each individual

The data were then tested with One-Way ANOVA and Post Hoc LSD test with a 95% confidence level by using SPSS 25 software [17].

ED_{50} Determination.

The percentage of inflammation inhibition of each dose variation was transformed into a probit (probability unit). Meanwhile, the dose value was converted into the logarithmic form. The probit of inhibition was then plotted against the logarithm value of the dose. The linear equation of the graph was determined using the Microsoft Excel 2010 software. From the linear equation, the ED_{50} value was calculated by entering 5 as y and x as the calculated variable. The value of x obtained was then converted into its anti-algorithmic value. The antilogarithmic value of x obtained is the ED_{50} value [18].

RESULTS AND DISCUSSION

The extractIon of bebuas leaves resulted in 5.12 grams of dry extract, with a yield of 1.024%. Dried hexane extract of bebuas leaves had a sticky and tough character like sap and had a yellowish green color. Meanwhile, the ethanol extract gave a dry extract of 30.31 grams with a yield of 6.062%. The dry ethanol extract had a resin-like sticky character and was blackish green color. The extraction results showed that the percent yield of ethanol extract was higher than that of hexane extract. This can happen because ethanol can dissolve almost all organic compounds from various groups of compounds, both polar and nonpolar. Meanwhile, hexane can only dissolve organic compounds which tend to be nonpolar [19].

Phytochemical screening was carried out on both dry extracts obtained. The results of phytochemical screening can be seen in table 1.

Table 1. Results of Phytochemical Screening of Bebuas leaf extract

	Hexane Extract	Ethanol Extract
Alkaloids		
Meyer	-	-
Dragendorff	-	+
Flavonoids	-	+
Phenolics/Tannins	-	+
Saponins	-	+
Steroids	+	+
Terpenoids	-	-

Note: - : negative, + : positive

The results of the phytochemical screening in this study gave the same results as the results obtained by Oktaviani et al. [20]. Phytochemical screening showed that the compounds extracted in ethanol solvent were more diverse than those extracted in hexane solvents, because hexane tends to only extract nonpolar compound groups such as steroids.

Plants belong to the *premna* genus have several characteristic secondary metabolites, which consist of diterpenoids, iridoid glycosides, and flavonoids as the most common secondary metabolites, followed by sesquiterpenes, lignans, phenylethanoids, megastigmanes, glyceroglycolipids, and ceramides [21]. Based on the phytochemical screening, the ethanol extract positively contained phenolic and flavonoid compounds, according to the typical compound groups contained in the genus of *premna*. Phytochemical screening also showed that the extract contained classes of compounds that have anti-inflammatory activity, including alkaloids, flavonoids, and steroids. This data provides scientific evidence and supports the fact that bebuas leaves can be used as anti-inflammatory drugs, as is often used by the Malay community to cure various diseases associated with inflammation.

Based on the results of the anti-inflammatory evaluation (Fig. 4), the ethanol extract had a lower ED_{50} value than the hexane extract. Therefore, the extract that was continued to the isolation stage was ethanol extract. Since most of the active anti-inflammatory NSAID compounds come from the alkaloid group [22], and in accordance with the results of phytochemical screening that ethanol extract contained alkaloids, so the targeted compound isolated was an alkaloid. Therefore, a specific method to isolate alkaloids was used. The concentrated ethanol extract was dissolved in distilled water and was acidified by adding 4 M HCl dropwise until the pH became 3. Before acidification, the initial pH of the extract solution was 4. This indicated that the ethanol extract of bebuas leaves was acidic, which can be caused by the presence of acidic phenolic compounds. Acidification using HCl to pH 3 aimed to convert alkaloids into alkaloid salt, so that their solubility in water increased, and their solubility in organic solvents decreased.

From the results of this acidification, a reddish black extract solution was obtained. Meanwhile, there was an insoluble fraction in acidic water, which was a sticky substance such as resin. The resin was then separated from the acid aqueous solution. The acid water extract was then partitioned using a hexane solvent. This partition aimed to separate polar compounds that are soluble in acidic water from non-polar compounds such as steroids and terpenoids. From the results of this partition, a green hexane layer and a reddish black acidic water extract were obtained (Fig. 1 a).

(a) (b) (c)

Fig. 1. Partition Results (a) acidic water extract with hexane (b) acidic water extract with ethyl acetate (c) alkaline water extract with ethyl acetate

After partitioning with hexane, then the acidic water extract was partitioned using ethyl acetate. Ethyl acetate was used to attract compounds that are semipolar and tend to be acidic, such as flavonoids, phenolics, and tannins. This can happen because in acidic water extracts these compounds tend to be in their neutral (uncharged) molecular form, so they are more soluble in semipolar organic solvents such as ethyl acetate. Meanwhile, alkaline compounds, such as alkaloids, are in the ionic form (charged) so that they are more soluble in water than organic solvents. This partition gave a layer of ethyl acetate (above) which was reddish brown in color and acidic water which was reddish black (Fig. 1 b).

After partitioning with ethyl acetate, the acidic water extract was basified with a 4 M ammonia solution until the pH was 9. The purpose of this basification was so that the alkaloids that were previously present in ionic form change back into their free, uncharged molecular form. After obtaining a pH of 9, then the basic water extract was partitioned using ethyl acetate. In a basic state, alkaloids return to their neutral molecular form so that their solubility in semipolar organic solvents such as ethyl acetate increases. From the results of this partition, a yellow ethyl acetate layer (above) and a reddish black layer of basic water were obtained (Fig. 1 c). The partition was carried out several times until the ethyl acetate appeared colorless. The ethyl acetate fraction of basic water (EaBW) is then concentrated. From the results of this concentration, 3.513 g of concentrated EaBW was obtained which was orange in color.

The hexane fraction of acidic water (HAW), ethyl acetate fraction of acidic water (EaAW), and EaBW were then screened for phytochemicals. The results of the phytochemical screening of the three fractions can be seen in Table 2.

Table 2. Results of Fractions Phytochemical Screening

	HAW	EaAW	EaBW
Alkaloids			
Dragendorff	-	-	+
Flavonoids	-	+	-
Phenolics/Tannins	-	+	+
Saponins	-	-	-
Steroids	+	-	-
Terpenoids	-	-	-

Note: HAW=hexane fraction of acidic water; EaAW=ethyl acetate fraction of acidic water; EaBW=ethyl acetate fraction of basic water

The screening results of the three fractions showed that the HAW extract was only positive for steroids. This is because steroid compounds tend to dissolve in nonpolar solvents such as hexane. Steroid compounds also tend not to form ions in either acidic or alkaline conditions. Therefore, steroids remain in a neutral molecular state which is more soluble in nonpolar organic solvents. EaAW was positive for flavonoids and phenolic. This is because in acidic conditions, the flavonoid and phenolic molecules are not charged. The aromatic –OH groups present in the flavonoid and phenolic molecules give the compound semipolar properties. Therefore, flavonoids and phenolics have large solubility in semipolar solvents such as ethyl acetate. Meanwhile, the EaBW was positive for alkaloids and phenolics as was predicted. Yet, phenolics were extracted both in EaAW and EaBW. This was possible because there were compounds that contain both phenolic and alkaloids functional groups.

Isolation was continued by using VLC to separate compounds in EaBW. Gradient elution was carried out in the VLC process using 100% ethyl acetate to 100% methanol as the eluent. The eluent was used in accordance with the results of the TLC test, which gave the result that the compounds in EaBW could only be eluted using the two eluents. The elution process was monitored using a 395 nm UV lamp (Fig. 2). This was performed so that each compound can be separated according to the band/fluorescence of the compound observed.

Fig. 2. Vacuum liquid chromatography process

Gradient elution was used to increase the resolution of complex mixtures especially if the sample has a wide polarity range. This can be seen when VLC was carried out using ethyl acetate eluent, the second band cannot be eluted and was retained on silica. After the eluent polarity was increased by the addition of methanol, the bands can be eluted. From the VLC results, eleven vials were obtained. The solvent from each vial was evaporated and a TLC test was carried out with 100% ethyl acetate as the eluent. The vials that had the same stain pattern were combined. From the TLC test, it was obtained five fractions namely F.1; F.2;

F.3; F.4; and F.5 which were coded according to the VLC elution time sequence. The fraction mass obtained for F.1; F.2; F.3; F.4; and F.5, respectively were 35.35 mg; 164.85 mg; 18.3 mg; 859.95 mg; and 137.48 mg.

TLC test using ethyl acetate eluent showed that F.3 gave a single stain with R_f 0.3 (Fig. 3 a). The TLC test on F.3 was then followed by eluent ethyl acetate: methanol 1: 1 and ethyl acetate: methanol 1: 2, which gave a single stain with R_f values of 0.61 and 0.81, respectively. This indicated that F.3 was a single compound, or at least there was one dominant compound in it. F.3 was then characterized using FT-IR and UV-Vis to determine the functional groups and basic skeleton of this compound. Furthermore, F.3 and other fractions previously obtained were subjected to a phytochemical screening.

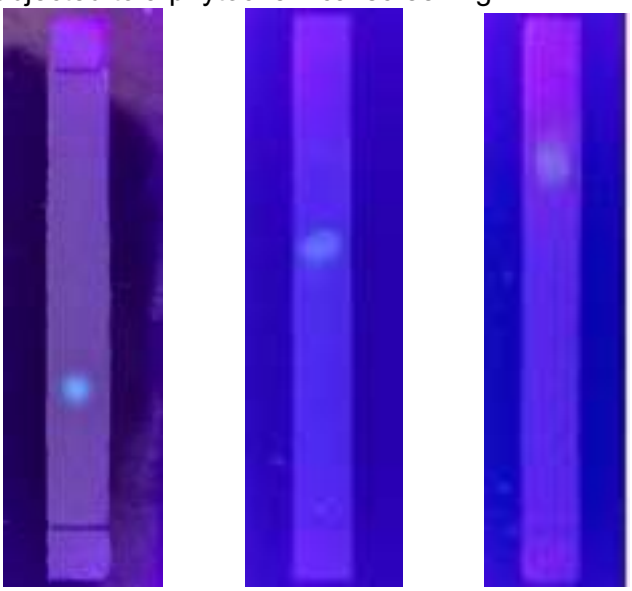

(a) (b) (c)

Fig. 3. TLC test results of F.3 with (a) ethyl acetate (b) ethyl acetate: methanol 1: 1 (c) ethyl acetate: methanol 1: 2 deluent

The results of the phytochemical screening of the five fractions are presented in Table 3. Phytochemical screening showed that all fractions were positively contained alkaloids. Meanwhile, in addition to alkaloids, F.1 was also positive to steroids and F.2 and F.3 were positive to phenolics. This might happen because there was a possibility that F.1; F.2; and F.4 was a mixture of compounds from different groups or the compounds in them had more than one functional group, thus giving positive results to more than two functional groups.

Table 3. Phytochemical Fraction Screening

	F.1	F.2	F.3	F.4	F.5
Alkaloids					
Dragendorff	+	+	+	+	+
Flavonoids	-	-	-	-	-
Phenolics/Tannins	-	+	-	+	-
Saponins	-	-	-	-	-
Steroids	+	-	-	-	-
Terpenoids	-	-	-	-	-

Note: F.1 to F.5 are the chromatography column factions of EaBW. The numbers represent the order in which the fractions are eluted from the chromatography column.

The five fractions were tested for their anti-inflammatory activity to determine which fraction had the best anti-inflammatory activity. The dose used to evaluate anti-inflammatory activity was 10 mg/kgbw, as the positive control dose used. The test results of the five fractions can be seen in Fig. 6.

From the test results, it can be seen that F.5 had the highest activity as an anti-inflammatory. However, based on the TLC test of F.5 using 1:1 methanol: water eluent, it consisted of several spots. This indicated that F.5 was still a mixture of compounds. Meanwhile, the TLC test on F.3 with various solvent ratios showed that F.3 consistently gave one spot, indicating that F.3 was a single compound. Therefore, characterization was carried out to F.3.

The anti-inflammatory activity evaluation was carried out on crude extract of hexane and ethanol from the leaves of bebuas. Tests were carried out on male albino rats (*Rattus norvegicus*). These rats were used as test animals because their genome is similar to the human genome (90%) and many human condition symptoms can be replicated on them [23]. Before being tested, the rats were not fed for 18 hours in order to avoid the influence of other substances on the test. The results of the anti-inflammatory evaluation are presented on the graph in Fig. 4.

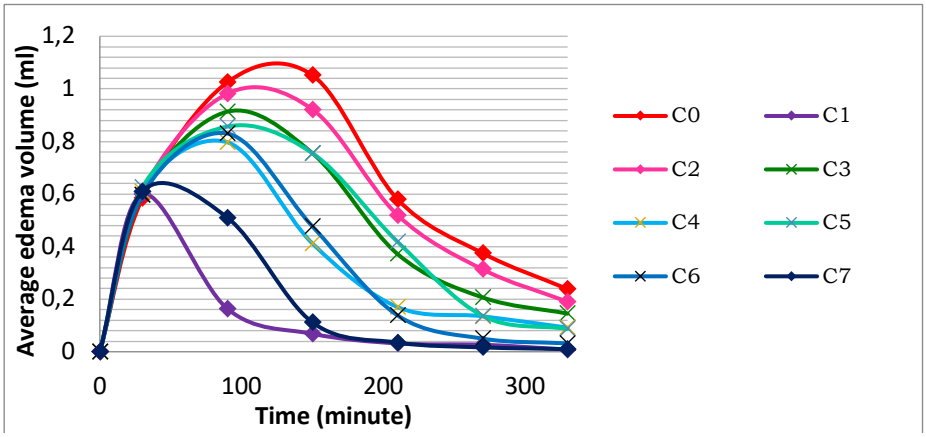

Fig. 4. Graph of edema volume against time

Note:
C0 = negative control (1% Na CMC); C1 = positive control (10 mg Na diclofenac); C2 = hexane extract 250 mg/kgbw; C3 = hexane extract 500 mg/kgbw; C4 = hexane extract 1000 mg/kgbw; C5 = ethanol extract 250 mg/kgbw; C6 = ethanol extract 500 mg/kgbw; and C7 = ethanol extract 1000 mg/kgbw.

The data in Fig. 4 shows that ethanol extract at 250, 500, and 1000 mg/kgbw doses could reduce swelling of the rats' paws at 60 minutes after induction. Hexane extract had a significant effect on reducing swelling at 60 minutes only at a dose of 1000 mg/kgbw. Meanwhile, hexane extracts at doses of 250 and 500 mg/kgbw were only able to significantly reduce swelling in 120 minutes after induction.

The average of percentage of inhibition of each dose was calculated based on the data in Fig. 4. The mean percentage of inhibition obtained for C1 was 79.30%. The average percentage of inhibition of hexane extracts, for C2, C3, and C4 were 8.37%, 22.90%, and 43.83%, respectively. Meanwhile, the average percent inhibition of ethanol extracts, for C5, C6, and C7 respectively were 25.35%, 45.42% and 68.35%. This showed that both hexane extract and ethanol extract have strong anti-inflammatory activity (percent inhibition is above 40%). However, the anti-inflammatory activity of ethanol extract was stronger than that of hexane extract. This can be seen from the percent inhibition of ethanol extract which was above 40% at a dose of 500 mg/kgbw (C6). Meanwhile, the percentage of inhibition above 40% was only achieved by hexane extract at a dose of 1000 mg/kgbw (C4).

The one-way ANOVA statistical test showed that there were significant differences between the groups of rats tested. Post Hoc LSD test shows that all doses statistically had significant differences in inhibition compared to the negative control. Meanwhile, it was also seen that there was no significant difference between the percent of inhibition of C4 and C6, which means that the two doses

had almost the same percentage of inflammation inhibition. However, for the percent inhibition value, the ethanol extract requires a lower dose. This showed that the ethanol extract was more active than the hexane extract. Compared to the positive control, all the doses given had a significant difference in the percentage inhibition value. This showed that the dose given had not been able to match the percent inhibition of C1. All doses also statistically had a significant difference with the C0 which meant that all extract showed anti-inflammatory activity.

Table 4. LSD Post Hoc Test Results on Bebuas Leaf Extracts

Sample	% Inhibition
C1	79.30 a
C7	68.35 b
C6	45.42 c
C4	43.83 c
C5	25.35 d
C3	22.90 e
C2	8.37 f
C0	0.00 g

Note:

The values followed by different letter notations indicate that there is a statistically significant difference.

The values followed by the same letter notation indicate that there is no statistically significant difference.

The percentage of inhibition of each dose was transformed into a probit (probability unit) form and plotted into a graph against the logarithmic value of the dose (Fig. *5*). From the graph, a linear equation of the probit of inhibition against the logarithm of the dose was obtained to calculate the ED_{50}. The ED_{50} for hexane and ethanol extract were 1,162.30 mg/kgbw and 571.56 mg/kgbw, respectively. This showed that the ethanol extract had a higher anti-inflammatory activity than the hexane extract because it had a lower ED_{50} value.

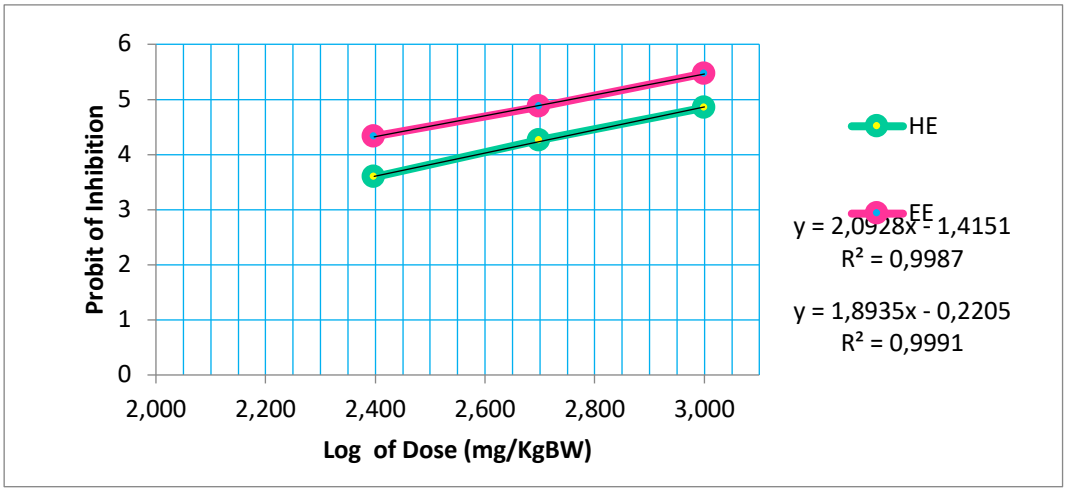

Fig. 5. Graph of Probit inhibition vs log of extract dose

Where: HE = Hexane Extract; EE = Ethanol Extract

The active anti-inflammatory compounds found in hexane extract could be steroid compounds which was detected in previous phytochemical screening. Meanwhile, the anti-inflammatory active compounds in ethanol extract could come from the phenolic or alkaloid groups [5].

Based on the anti-inflammatory evaluation, ethanol extract had a higher percent of inhibition than hexane extract for the same dose. Therefore, the extract that was continued to the isolation stage was the ethanol extract. Since most of the active NSAID compounds come from the alkaloid group [22], and in accordance with

the results of phytochemical screening that ethanol extract contained alkaloids, the targeted compound to be isolated was an alkaloid. Therefore, special extraction and isolation methods for alkaloids were used. From the method, the EaBW was obtained and it was positive for alkaloids.

Each fraction resulting from VLC of EaBW was evaluated for anti-inflammatory to determine which fraction has the best activity as anti-inflammatory. The dosage used for all fractions was 10 mg/kgbw, as the dose used for positive control. The results of the anti-inflammatory evaluation for each fraction can be seen in Fig. 6.

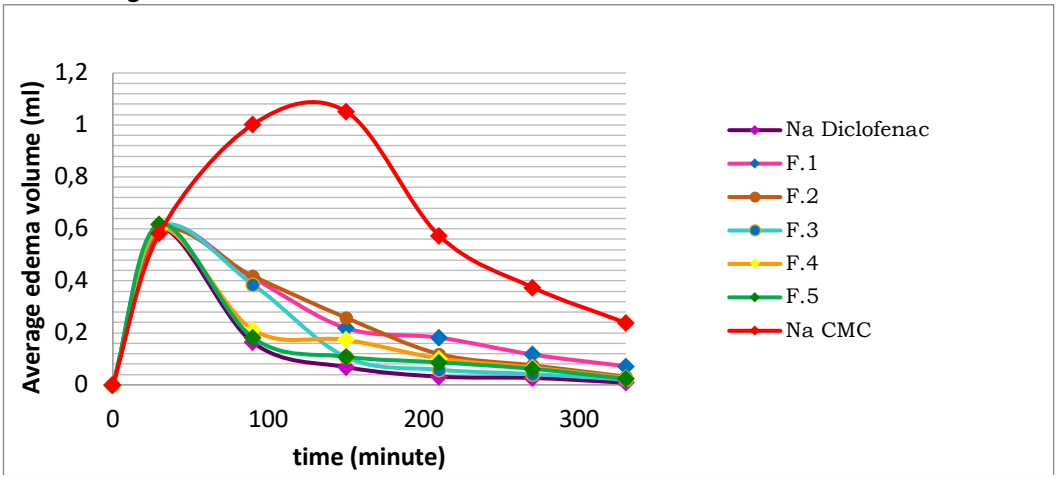

Fig. 6. Fraction's anti-inflammatory evaluation curve

From the results of the anti-inflammatory evaluation, the percent of inhibition for F.1; F.2; F.3; F.4; and F.5, respectively were 60.26%, 62.78%, 70.29%, 71.43% and 74.32%. It showed that all fractions had strong anti-inflammatory activity (% inhibition > 40%).

The one-way ANOVA statistical test showed that there were significant differences between the groups of rats tested with the five fractions. This can be seen from the calculated F value which was greater than the $F_{0.05\ (6.35)}$ table (889.408 > 2,372) and the p value was smaller than the α value (0,000 < 0.05).

Table 5. Post Hoc LSD test results for each EaBW fraction from VLC

Sample	% Inhibition
C1	79.30 a
F.5	74.54 b
F.4	71.67 c
F.3	70.53 c
F.2	63.09 d
F.1	60.59 d
C1	0.00 e

Note:

The values followed by different letter notations indicate that there is a statistically significant difference.

The values followed by the same letter notation indicate that there is no statistically significant difference.

The post hoc LSD test data in Table 5 shows that all fractions statistically had a significant difference in percentage of inhibition compared with negative controls. This shows that all fractions were active as anti-inflammatory agents. There was also no significant difference between the percentage of inhibition of F.1 and F.2, as well as the percentage inhibition of F.3 and F.4. This indicates that F.1 and F.2 as well as F.3 and F.4 have the same inflammation inhibition strength. This similarity of inhibitory strength occurred because there was the possibility that

the same chemical compound spread in F.1 and F.2, as well as in F.3 and F.4, which is possible because the fractions were in close order according to their separation in VLC.

Based on the TLC test, F.3 gave one single stain. This showed that F.3 was a pure compound (isolate). Therefore, the anti-inflammatory activity evaluation with various doses was carried out on F.3, hereinafter referred to as isolates. The results of the isolate anti-inflammatory evaluation is depicted in Fig. 7.

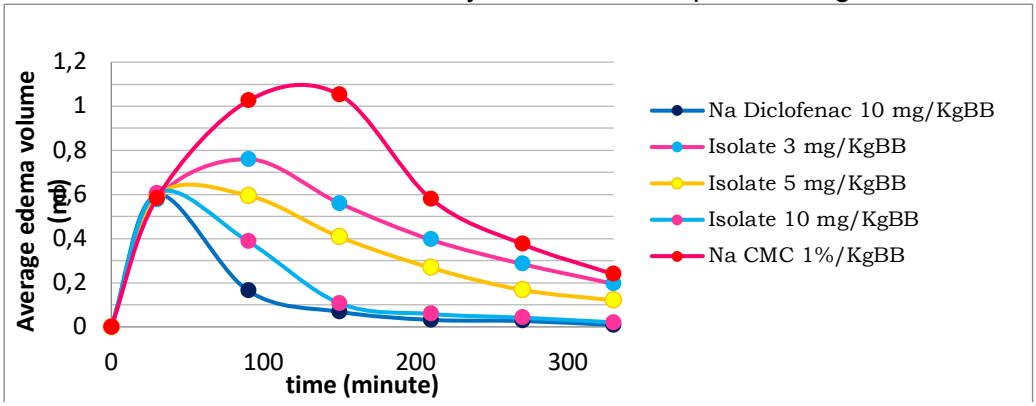

Fig. 7. The isolate anti-inflammatory evaluation curve

Based on the anti-inflammatory evaluation, the percentage of inhibition of isolates for doses of 3, 5, and 10 mg/kgbw, respectively were 29.48%, 45.88% and 70.53%. The graph of the probit of inhibition against the logarithm of dose can be seen in Fig. 8. Based on the calculation of the linear equation in Fig. 8, the ED_{50} value of the isolate was 5.45 mg/kgbw.

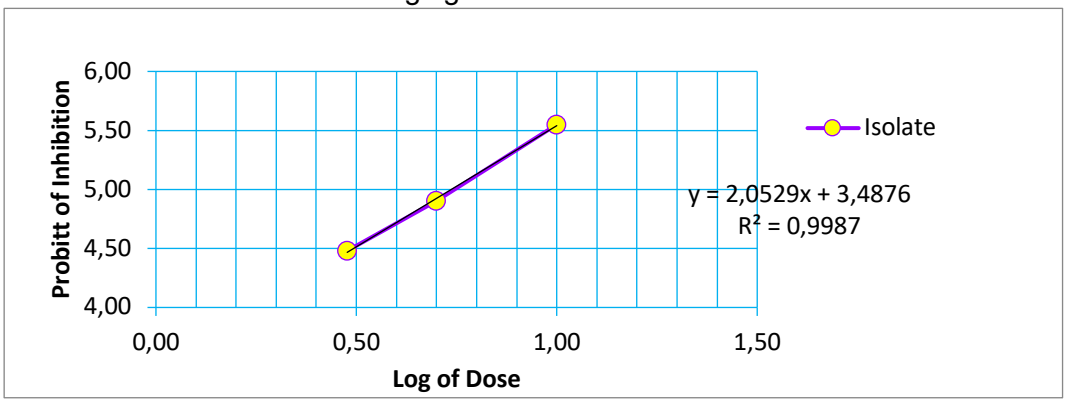

Fig. 8. Graph of probit vs log dose of the isolate

One-way ANOVA statistical test showed that there was a significant difference between the groups of rats tested and the isolates. This can be seen from the calculated F value which was greater than the $F_{0.05(4,21)}$ table (1847.997 > 2.840) and the p value was smaller than the α value (0.000 < 0.05). Based on the LSD post hoc test data presented in Table 6, it can be seen that all isolate doses were statistically significantly different in inhibition compared to the negative control.

Table 6. LSD Post Hoc Test Results on the Isolate

Sample	% Inhibition
C1	79.30 a
Isolate 10 mg/kgbw	70.53 b
Isolate 5 mg/kgbw	45.88 c
Isolate 3 mg/kgbw	2948 d
C0	0.00 e

Note:

The values followed by different letter notations indicate that there is a statistically significant difference.

The values followed by the same letter notation indicate that there is no statistically significant difference

The isolate was characterized using FT-IR and UV-Vis instruments. UV-Vis characterization was carried out to determine the basic skeleton of the compounds from these isolates. The UV-Vis spectrum (Fig. 9) showed that the isolate gave two absorption peaks at λ = 281 nm and λ = 307 nm. The absorption at 281 nm indicates the presence of a conjugated diene/double system in the structure. Meanwhile, the absorption at 307 indicates the presence of an aromatic system with certain substituents [24].

The UV-Vis spectrum of the isolates has a similar pattern to the spectra of compounds containing the quinolone skeleton. The two UV absorption bands of the isolate approach the typical quinolone absorption area, specifically the presence of two peaks at λ around 269 nm and 314 nm [25]. Based on the literature, the UV spectrum of the isolate has a similar pattern to the UV spectrum of ciprofloxacin, and both absorption bands are close to each other. This shows that isolate and ciprofloxacin have the same basic skeleton. However, the absorption peak of the isolates did not appear to be too intense. This could be due to the relatively low concentration of the isolate when characterized by using UV-Vis.

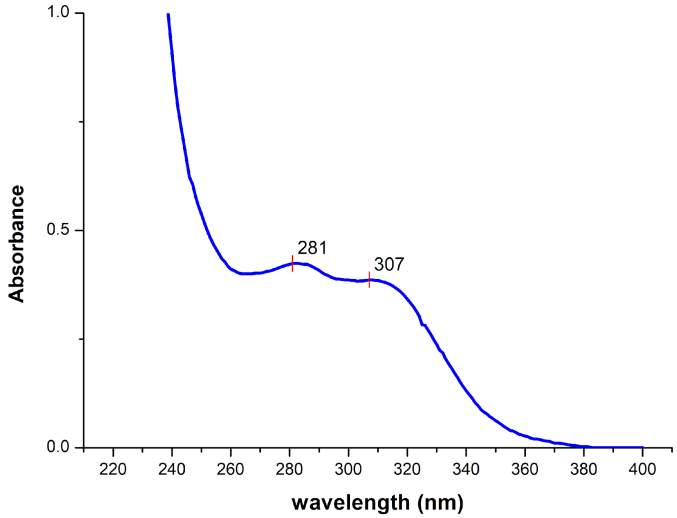

Fig. 9. UV-Vis spectrum of the isolates, λ = 281 nm and 307 nm

FT-IR characterization was carried out to determine the functional groups contained in the isolate (Fig. 10). Based on the comparison with literature [26,27], the FT-IR spectrum pattern of the isolates is similar to the IR spectrum of ciprofloxacin. This strengthens the notion that the isolate is a compound that has a structure similar with ciprofloxacin.

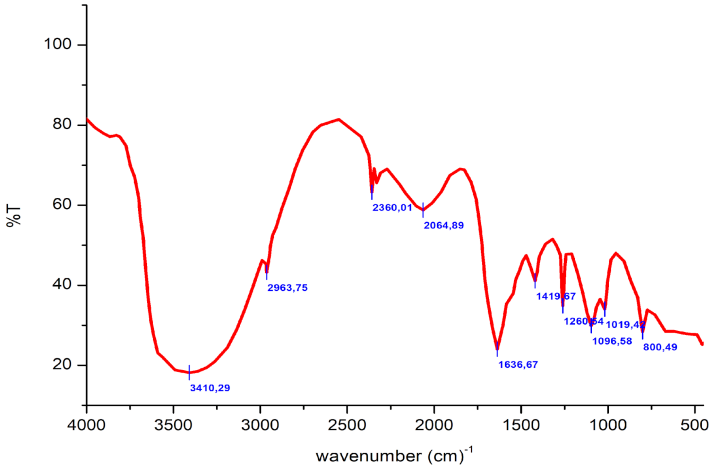

Fig. 10. FT-IR spectrum of the isolate

Ciprofloxacin is an alkaloid compound derived from quinolone which has been widely used as an antibiotic. The quinolone skeleton in the isolate can be seen clearly based on the UV-Vis and FT-IR spectra. In FT-IR, the presence of absorption at wave number 1260.54 indicated the presence of aromatic C-N bonds, which is a characteristic of the basic quinolone skeleton.

The interpretation of functional groups based on the FT-IR spectrum is presented in Table 7. An alkaloid compound that has the same FT-IR spectrum pattern with this compound is ciprofloxacin (Fig. 11). The functional groups presented in the FT-IR spectrum of the isolate corresponded to the characteristic of functional groups presented in ciprofloxacin.

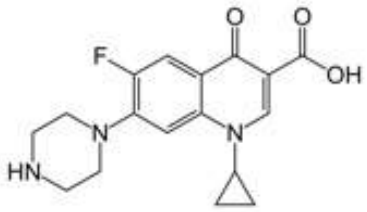

Fig. 11. Structure of Ciprofloxacin

The assumption that the isolate was a compound with characters like ciprofloxacin is also supported by the compatibility of their physical forms. Ciprofloxacin is known to be in the form of yellowish crystals which are hygroscopic. This is in accordance with the physical form of the isolate in the form of yellowish crystals when it was freshly dried from the solvent, but after being exposed for a long time by air, the isolate changed into a liquid like oil due to absorbing water vapor from the air.

Table 7. Interpretation and Comparison of IR Spectra

Interpretation	Adsorption (cm^{-1})		
	Isolate	Ciprofloxacin [26]	Ciprofloxacin [27]
O-H	3410,29	3342.64	3308.70
C-H Alkane/aromatic	2963,75	-	2974.33
C=N, C=C	1636,67	1635.64	1577.8
O-H Bending	1419,67	-	1413.87
C-N aromatic	1260,54	1204.56	1288.49
C-H aromatic	800,49	-	-

The unique characteristic that was also observed from the isolate was that they could fluoresce under a 395 nm UV lamp, which emitted a blue light as can be seen in Fig.12.

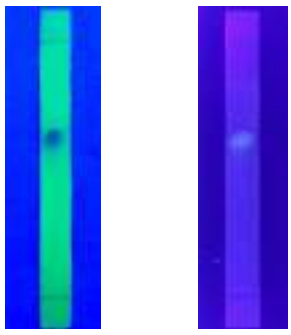

(a) (b)

Fig. 12. TLC plate resulted from the isolate elution when observed under a UV light (a) 254 nm (b) 395 nm

Ciprofloxacin has also been reported to provide fluorescence [19,28]. The fluorescence of the ciprofloxacin compound occurs due to the quinolone skeleton in its structure. Ciprofloxacin has a maximum absorption at a wavelength of 280 nm and 331 nm [29]. Meanwhile, the wavelength emitted by ciprofloxacin when it glows is 445 nm. The wavelength corresponding to the range of visible light blue is in the range of 435-500 nm [30]. This shows that the nature of the isolate which could glow blue under a UV lamp of 395 nm further strengthens the notion that the isolate was a compound with a basic skeleton similar to ciprofloxacin.

CONCLUSION

The study showed that bebuas leaves contain compounds that are active as anti-inflammatory agents. The ED_{50} values of hexane extract, ethanol extract, and F.3 (isolate), as anti-inflammatory agents were 1,162.30 mg/kgbw, 571.56 mg/kgbw, and 5.45 mg/kgbw, respectively. Compounds that are active as anti-inflammatory agents in bebuas leaves are best extracted with ethanol. The anti-inflammatory active compound that was isolated from the ethanolic extract was an alkaloid. The isolate had similar characters with ciprofloxacin, namely yellow color, hygroscopic crystal, and containing quinolone scaffold as interpretated from UV-Vis and FT-IR spectra.

Further characterization of the isolate using LC-MS/MS and NMR instrument to ensure the purity as well as to determine the exact structure of the isolate might be needed for future research.

ACKNOWLEDGEMENT

Thank you to the Major of Chemistry, Faculty of Science and Technology, Jambi University for the support of laboratory facilities as a place for conducting the research and thanks to the late Dr. Dra. Yusnelti, M.Si, for all her support and guidance during her lifetime so that this research can be completed.

AUTHOR'S CONTRIBUTION STATEMENT

all authors have equal responsibility in the research and preparation of the manuscript.

FUNDING INFORMATION

-

DATA AVAILABILITY STATEMENT

The utilized data to contribute to this investigation are available from the corresponding author on reasonable request.

DISCLOSURE STATEMENT

The views and opinions expressed in this article are those of the authors and do not necessarily reflect the official policy or position of any affiliated agency of the authors. The data is the result of the author's research and has never been published in other journals.

REFERENCE

1. Vadivu R, Suresh A, Girinath K, Kannani P, Vimala R, Kumar N. Evaluation of Hepatoprotective and In-vitro Cytotoxic Activity of Leaves of *Premna serratifolia* Linn. *J Sci Res*. 2009;1:145-152. doi:10.3329/jsr.v2i3.4899
2. Saim. Pendayangunaan Sumber Daya Hutan Bagi Suku Talang Mamak di Daerah Seberrida Riau. *Pros Semin Nas dan Lokarya Etnobotani 1 Cisar Bogor*. 1992:381-389.
3. Padua LS de, Bunyapraphatsara N, Lemmens RHMJ. *Plant Resources of*

South-East Asia 12 (3): Medicinal and Poisonous Plants 3. Vol 87. Bogor: Backhuys Publishers; 1999. doi:10.1016/s0378-8741(03)00056-4
4. Parawansah, Nuralifah, Akib N, Antrie G. Uji Toksisitas Akut Ekstrak Etanol Daun Buas-Buas (*Premna serratifolia* Linn.) Terhadap Larva Udang (*Artemia salina* Leach) dengan Metode Brine Shrimplethality Test (BLST). 2017;(April):171-177.
5. Katzung BG, Masters SB, Trevor AJ. *Basic and Clinical Pharmacology*. 12th ed. New York: Mc Graw Hill; 2012.
6. Adyttia A, Untari EK, Wahdaningsih S. Efek Ekstrak Etanol Daun *Premna cordifolia* terhadap Malondialdehida Tikus yang Dipapar Asap Rokok. *Pharm Sci Res*. 2017;1(2):104-115. doi:10.7454/psr.v1i2.3302
7. Setyaningrum PA. Isolasi dan Identifikasi Senyawa Fenolik dari Fraksi Etil Asetat Kulit Batang Tumbuhan Turi (*Sesbania grandiflora*) serta Uji Bioaktivitas Antibakteri. *Skripsi Univ Lampung*. 2016.
8. Ikawati Z. *Farmakoterapi Penyakit Sistem Saraf Pusat*. Yogyakarta: Bursa Ilmu; 2011.
9. Black PH, Garbutt LD. Stress, inflammation and cardiovascular disease. *J Psychosom Res*. 2002;52(1):1-23. doi:10.1016/S0022-3999(01)00302-6
10. World Health Expectancy. Indonesia: Life Expectancy. World Health Expectancy. https://www.worldlifeexpectancy.com/indonesia-life-expectancy. Published 2018. Accessed December 10, 2019.
11. Tjay TH, Rahardja K. *Obat-Obat Penting Khasiat, Penggunaan Dan Efek-Efek Sampingnya*. 6th ed. Jakarta: PT. Elex Media Komputindo; 2007.
12. Harbone JB. *Metode Fitokimia : Penuntun Cara Modern Menganalisis Tumbuhan*. 2nd ed. (Padmawinata K, Soediro I, eds.). Bandung: ITB Press; 1987.
13. Titis M, Fachriyah E, Kusrini D. Isolasi, Identifikasi dan Uji Aktifitas Senyawa Alkaloid Daun Binahong (*Anredera cordifolia* (Tenore) Steenis). *Chem Info J*. 2013;1(1):196-201.
14. Emrizal, Fernando A, Suryani F, Ahmad F, Sirat HM, Dayar Arbain D. Isolasi senyawa dan uji aktivitas anti-inflammasi Isolasi Senyawa dan Uji Aktivitas Anti-inflammasi Ekstrak Metanol Daun Puwar Kincung (*Nicolaia speciosa* Horan). *J Penelit Farm Indones*. 2012;1(1):1-5.
15. Hasanah F, Hidayah N. Uji Aktivitas Antiinflamasi Ekstrak Air Daun Salam (*Sygyzium polyanthum* Wight.) Terhadap Tikus Wistar Jantan yang Diinduksi dengan Karagenan 1%. *J Pharm Sci*. 2018;1(1):16-22.
16. Apridamayanti P, Sanera F, Robiyanto R. Aktivitas Antiinflamasi Ekstrak Etanol Daun Karas (*Aquilaria malaccensis* Lamk.) Antiinflammatory Activity of Ethanolic Extract from Karas Leaves (*Aquilaria malaccensis* Lamk.). 2018;5(3):152-158.
17. Luliana, S., Susanti, R. dan Agustina E. Uji Aktivitas Antiinflamasi Ekstrak Air Herba Ciplukan (*Physalis angulata* L.) terhadap Tikus Putih (*Rattus norvegicus* L.) Jantan Galur Wistar yang diinduksi Karagenan. *Maj Obat Tradis*. 2017;22(3):199. doi:10.22146/mot.31556
18. Ross GJS, Finney DJ. Probit Analysis. *Stat*. 1972;21(3):222. doi:10.2307/2986688
19. Aslamiah S, Haryadi. Identifikasi Kandungan Kimia Golongan Senyawa daun pohon kapuk. *Anterior J*. 2014;53(9):1689-1699. doi:10.1017/CBO9781107415324.004
20. Oktaviani E, Wibowo MA, Idiawati N. Penapisan Fraksi Antioksidan Daun Buas-buas (*Premna serratifolia* Linn). *J Kim Khatulistiwa*. 2015;4(3):40-47.
21. Dianita R, Jantan I. Ethnomedicinal uses, phytochemistry and pharmacological aspects of the genus Premna: A review. *Pharm Biol*. 2017;55(1):1715-1739. doi:10.1080/13880209.2017.1323225
22. Wibowo S, Gofir A. *Farmakoterapi Nyeri Inflamasi: Farmakoterapi Dalam Neurologi*. 1st ed. Jakarta: Salemba Medika; 2001.

23. Vandamme TF. Use of Rodents as Models of Human Diseases. 2014;6(1):2-9. doi:10.4103/0975-7406.124301
24. Dachriyanus. *Analisis Struktur Senyawa Organik Secara Spektroskopi*. Padang: Lembaga Pengembangan Teknologi Informasi dan Komunikasi (LPTIK) Universitas Andalas; 2004.
25. Abdou MM. Chemistry of 4-Hydroxy-2 (1 H)-quinolone. Part 1 : Synthesis and reactions. *Arab J Chem*. 2018; 10 (December): S3324-S3337. doi:10.1016/j.arabjc.2014.01.012
26. Khan ZH, Aziz A, Hasan R, Al-mamun R. The role of drug as corrosion inhibitor for mild steel surface characterization by SEM, AFM, and FTIR. 2016;(May 2017). doi:10.1108/ACMM-11-2015-1597
27. Sunitha P, Amareshwar P, Kumar MS, Chakravarti P. Study on Effect of Solvents & Nonsolvents on Microspheres of Ciprofloxacin: Coacervation Phase Separation. 2015;(January 2010).
28. Pagare S, Bhatia M, Tripathi N, Pagare S, Bansal YK. Secondary metabolites of plants and their role: Overview. *Curr Trends Biotechnol Pharm*. 2015;9(3):293-304.
29. Zuyun H, Houping H, Ruxiu C, Yun Z. Study on the Fluorescence Properties of Some Fluoroquinolones in Various Media. 1997;2(3):2-7.
30. Malacara D. *Color Vision and Colorimetry: Theory and Applications*. New York: SPIE Press; 2002.

JTL 11 (2) December 2022
Page: 95-104
Contents list available at Jurnal Teknologi Laboratorium

JURNAL TEKNOLOGI LABORATORIUM

Journal Homepage: www.teknolabjournal.com
ISSN 2580-0191(Online) I ISSN 2338 – 5634(Print)

Original Study

Effectiveness of temulawak (*Curcuma* xanthorrhiza) ointments *as wound healing agents in wistar rats*

Jessica Panjaitan, **Ermi Girsang**, **Linda Chiuman***
Department of Biomedical Sciences, Faculty of Medicine, Universitas Prima Indonesia, Medan, Indonesia.

Abstract: Temulawak is known for its potential as a powerful antioxidant, anti-inflammatory, and anti-aging. Numerous studies have been reported on how temulawak extract components minimize wrinkles, boost collagen production, and prevent degradation. This study aims to determine whether temulawak ointment promotes wound healing in Wistar rats. Pure experimental laboratory research and only post-test control group design observations have been done. Our results showed changes in the macroscopic appearance of wounds, particularly in the look of closed, dry wounds, which were exclusively observed in patients who received ointments containing 15%, 20% and 25% temulawak ointments after 14 days. Based on the histopathology observation there was a significant difference in the mean comparison of the area of epithelialization, the number of fibroblasts, and the quantity of angiogenesis. We conclude that temulawak ointment benefited incision wound healing in Wistar rats.

Keyword: Temulawak; Wound healing; Epithelialization; Fibroblasts; Angiogenesis

INTRODUCTION

The skin is a complicated organ that shields the body from the environment. Approximately 15% of body weight is comprised of skin, making it the heaviest organ [1]. The skin has multiple roles, including providing a physical permeability barrier, protecting against pathogenic agents, thermoregulation, sensation, ultraviolet radiation protection, regeneration, and wound healing [2]. Various skin aging phenotypes are age, gender, ethnicity, air pollution, nutrition, smoking, and sun exposure [3]. Skin aging changes physiological functions, skin structure, and age. Signs of skin aging are reduced skin barrier function, slowed epidermal cell turnover, and reduced skin vascularity [4]. The decrease in keratinocytes and fibroblasts during the aging process will degrade the skin functions such as protection, excretion, secretion, absorption, thermoregulation, and decreased sensory perception [5]. In addition, a decrease in the number of *Langerhans* cells and melanocytes will cause a decrease in skin pigmentation, and a decreased number of collagen cells, elastic fibers, mast cells, and macrophages will cause changes in skin texture [5].

Recently, many antioxidant agents have been used, both synthetic and herbal antioxidant agents [6,7]. Anti-aging agents may help to prevent degenerative processes with visible symptoms such as wrinkles, rough skin, and dark spots [8]. One of Indonesian herbal widely used in traditional medicine is temulawak (*Curcuma xanthorrhiza*). Temulawak has been reported for its bioactive compound called *Curcumin* [9], which is efficacious as an antioxidant, anti-inflammatory, and anti-aging[10]. The bioactive components of temulawak extract can reduce wrinkles, increase collagen synthesis and suppress collagen degradation [11]. There is a relationship between temulawak extract and anti-aging on the skin by inducing a

Corresponding author.
E-mail address: lindachiuman@unprimdn.ac.id (Linda Chiuman)
DOI: 10.29238/teknolabjournal.v11i2.376
Received 31 August 2022; Received in revised form 07 October 2022; Accepted 14 November 2022

cellular response in normal human skin fibroblasts, which causes the induction of peroxides and other antioxidant enzymes to modulate aging and improve cell function [12]. Oxidative stress and inflammation mostly contribute to aging and age-related conditions including skin aging [13,14].

To the best of our knowledge, the literature on the effect of temulawak ointments on wound healing in non-diabetic Wistar rats based on the comparison of the area of epithelialization, the number of fibroblasts, and the quantity of angiogenesis are still rarely reported. Recently, a study reported that temulawak extract has increased the number of fibroblasts, tissue granulation, blood vessel density and wound contraction in diabetic Wistar rat induced by Streptozotocin (STZ) [15]. The results of other studies showed that temulawak extract was able to accelerate wound closure by 15.262%/day compared to the untreated group by 13.54%/day [16]. Previous study on curcumin bioactivities have revealed that there were neovasculogenesis and expressions of CD31, VEGF, TGF-b1, hypoxia-inducible growth factor-1alpha, stromal cell-derived growth factor-1alpha, and heme oxygenase-1, and western blotting studies [17]. The wound healing potential of curcumin has been proposed regarding its antioxidant and antiinflammation bioactive compounds [18]. However, there is no report of the study on the tipical non-diabetic rats to date.

This research is supposed to fill the gap in the literature on the wound healing effect of temulawak ointments based on microscopic observation, wound appearances, number of fibroblasts, neovascularization points, and epithelialization area of non-diabetic Wistar rats. Hence, this experimental research is highly recommended to fill the gap in this field of study.

MATERIAL AND METHOD

This study was an experimental laboratory with a post-test-only control group design of observations of male Wistar rats. Experimental research was conducted at the animal house laboratory of FMIPA USU Medan for approximately three months (September to November 2021). The protocol of animal research has been approved by Animal Research Ethics Committees/AREC FMIPA USU No. 0763/KEPH-FMIPA/2021.

Temulawak extract was obtained via maceration method using 96% ethanol to separate solid-liquid mixtures from temulawak simplicia. Maceration was followed by rotary evaporation to get the crude extract.

To get temulawak ointments, we have prepared by following the formulation described in Table 1 below:

Table 1. Ointment Formulation

Group Treatment	Temulawak Extract (g)	Vaseline Album (g)	Adeps Lanae (g)	Ointment (g)
15%	1.5	7.225	1.275	10
20%	2	6.8	1.2	10
25%	2.5	6.375	1.125	10
Ointment base	-	8.5	1.5	10

Wistar rats were placed in cages made of a plastic material covered with a cover made of wire mesh and placed separately according to each treatment. All test animals under the same conditions were acclimatized for one week and fed in an adlibitum way. The incision was made in the back area of the Wistar rats that had been disinfected with 70% alcohol. Anesthesia was performed using a lidocaine injection of 0.1-0.3 ml/kg BW intramuscularly. About 2 cm incision with a depth of 0.5 cm to the subcutis layer on the back using a sterile scalpel. Cuts in rats were smeared with ointment with a predetermined concentration twice/day, at 08.00 am and 05.00 pm, based on the group. The cuts in the negative control group (K(-)) were only cleaned with normal saline in the positive control group (K(+)). The

wound was smeared with povidone-iodine. Treatment group I (PI), treatment II (PII), and treatment III (PIII) were smeared with temulawak extract ointment with concentrations of 15%, 20%, and 25%, respectively.

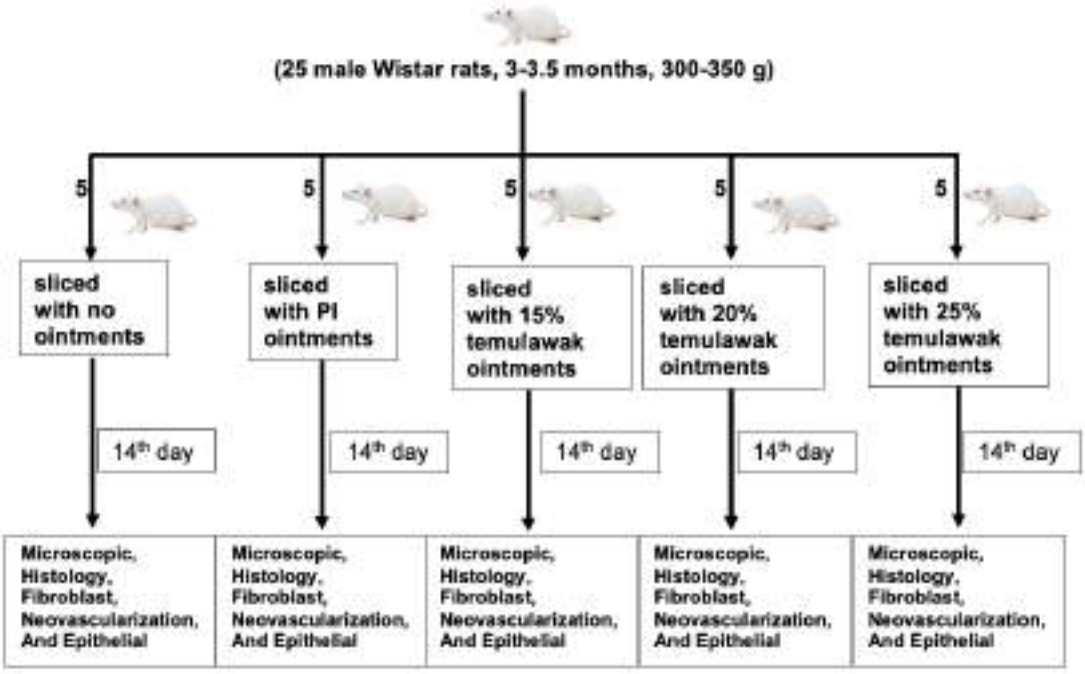

Fig.1 Scheme of animal experiments

After 14 days treatments, observations were carried out macroscopically and microscopically. The macroscopic observation parameters were Mb (red swelling), M (Red), Kt (dry open), and Km (dry closed, healed), and observe the length of the wound healing day between the control and the ginger extract ointment with each concentration. Microscopic observations were conducted by observing rats' skin on the 14th day. The histology preparations used the paraffin method. The number of fibroblast cells, neovascularization, and epidermal epithelial thickness was assessed by taking rat skin samples at the time of wound care and by *Hematoxylin-eosin* staining under a light microscope.

The normality test uses the *Shapiro-Wilk* test with α = 0.05 because the number of samples is less than 30. The data is normally distributed if the data shows the *p*-value > 0.05. *Levene Statistic test* used to determine homogeneity with α = 0.05. When the *p*-value > 0.05, the data is homogeneous and has the same variance, then a parametric test using one-way ANOVA is applied. If a *p*-value < 0.05 was obtained after statistical testing with one-way ANOVA, then there was a significant difference in the number of fibroblast cells, neovascularization, and epidermal thickness on day 14th. *Post-Hoc test* was applied to determine the most significant among the experimental groups with a *p*-value <0.05.

RESULTS AND DISCUSSION

The treatment groups with cuts and administration of temulawak ointments were 15%, 20%, and 25% showed no dead animals. There were no infected wounds in the experimental animals. All experimental animals were observed in a safe and clean environment and fed without distinction. During the surveillance period, the experimental animals were active, not in pain and suffering. Microscopic observations of fibroblast cells, neovascularization, and epidermal epithelial thickness on the 14th day were shown in Figure 2.

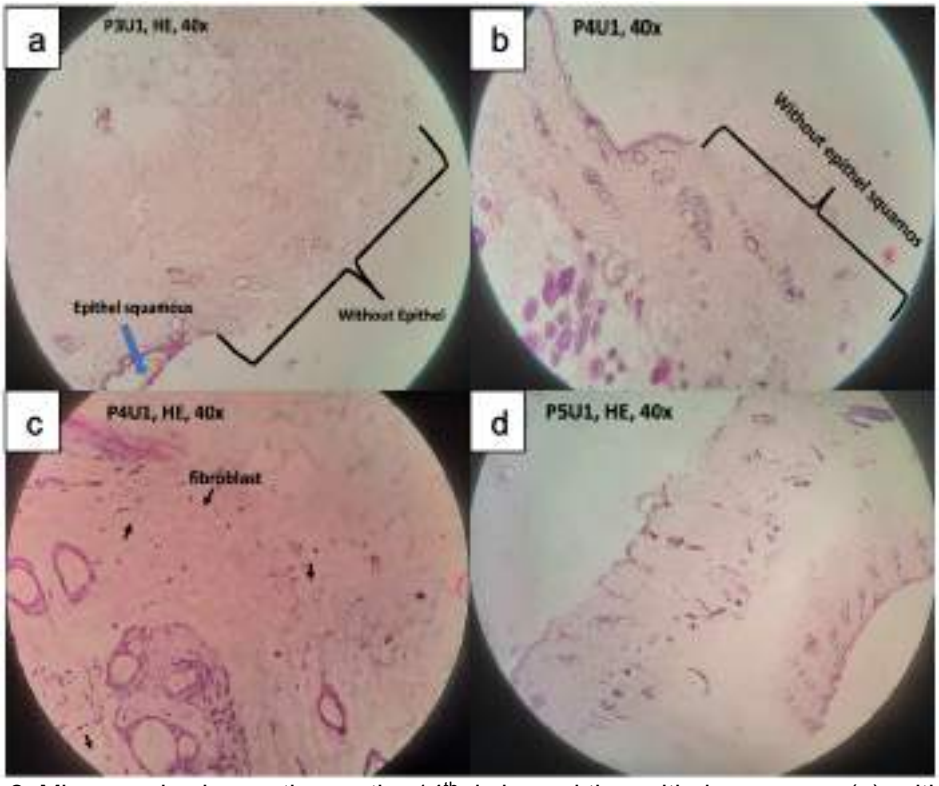

Fig. 2. Microscopic observation on the 14th d showed the epithel squamous (a), without epithel squamous (b) fibroblast cells (c), and neovascularization (d).

Several studies have examined the wound healing ability of temulawak extract regarding the macroscopic appearance of wounds. Previous studies have shown that wounds in experimental animals treated with temulawak extract experienced faster-wound healing or wound closure [15]. Temulawak was also reported to inhibit *methicillin-resistant staphilococcus aureus* (MRSA) [19]. The area of erythema in rats given 20% temulawak extract was much smaller than standard treatment with saline and vaseline, namely 81.87±8.01. The results of the one-way ANOVA test in this study showed a significant value (p = 0.000). A bioactive compound, namely *Xanthorrhizol*, which has bioactivity as antidiabetic, anti-inflammatory, and antioxidant that can counteract free radicals so that the inflammatory phase does not expand and the wound healing process improves better [19]. Another study also reported that temulawak extract could accelerate wound closure in white rats by 15,262% per-day compared to the group that was not treated [20]. Pieces of literature reveal that the treatment with antioxidants strengthens cellular antioxidant defense mechanisms, can reduce free radical-mediated damage and minimize tissue damage during burn injury, and can accelerate the wound healing process [21,22].

In the experimental group with normal saline (NS); 2 out of 5 rats (40%) had swollen red wounds (MB), 1 out of 5 (20%) had red sores (M), 2 out of 5 (40%)) had an open dry wound (KT). In the experimental group with povidone-iodine, 1 out of 5 rats (20%) had a swollen red wound (MB), and 4 out of 5 (80%) had an open dry wound (KT).

In the experimental group treated with 15% ointment; 1out of 5 mice (20%) had red sores (M), and 4 out of 5 (80%) had open dry results (KT). In the experimental group of animals that were treated with 20% ointment; 2 out of 5 (40%) had an open dry wound (KT), and the remaining 3 out of 5 (60%) had a closed dry wound (KM). In the group of experimental animals treated with 25% ointment; 3 out of 5 (60%) had an open dry (KT), and the remaining 2 out of 5 (40%) had a closed dry wound (KM). The *p-value* shows the result of 0.126 under

the *Fisher-Exact test,* as shown in Table 2, indicating no statistical significance between groups.

Table 2. Macroscopic Appearance of Wounds in Experimental Animals

Group Treatment	Macroscopic Appearance					*p-value*
	MB	M	KT	KM	Total	
NS	2 (40%)	1 (20%)	2 (40%)	0 (0%)	5 (100%)	
P. Iodine	1 (20%)	0 (0%)	4 (80%)	0 (0%)	5 (100%)	
S15%	0 (0%)	1 (20%)	4 (80%)	0 (0%)	5 (100%)	0.126
S20%	0 (0%)	0 (0%)	2 (40%)	3 (60%)	5 (100%)	
S25%	0 (0%)	0 (0%)	3 (60%)	2 (40%)	5 (100%)	

**Fisher-Exact test*

We further analyze the dry wound closure (KM) only found in the experimental group of animals treated with temulawak ointment, either with a concentration of 20% or 25%. The *Fisher-Exact test* showed that $p = 0.04$ indicated statistical significance, as shown in Table 3.

Table 3. Closed-Dry Macroscopic Appearance (KM) in Experimental Animals

Group Treatment	Dry Close (KM)			*p-value*
	Yes	No	Total	
NS	0 (0%)	5 (100%)	5 (100%)	
P. Iodine	0 (0%)	5 (100%)	5 (100%)	
S15%	0 (0%)	5 (100%)	5 (100%)	0.04*
S20%	3 (60%)	2 (40%)	5 (100%)	
S25%	2 (40%)	3 (60%)	5 (100%)	

**Fisher-Exact test*

There was no significant difference between the wound sizes in each group on day 14^{th,} as shown in Table 4. Significant differences were found in the other three microscopic parameters. Epidermal area and total area were calculated using IC Measure® software. Here, we compare the epidermis area against the total area of each experimental treatment.

Table 4. Comparison of Wound Size on Day 14th in Each Treatment Group

Treatment (n=25)	Mean ± SD (cm)	Min-Max	95%CI	*p-value*
NS	1.86±0.11	1.70-1.98	1.72-2.00	
P. Iodine	1.77±0.12	1.60-1.88	1.62-1.77	
S15%	1.76±0.39	1.70-1.80	1.71-1.81	0.91*
S20%	1.66±0.08	1.58-1.78	1.56-1.76	
S25%	1.68±0.17	1.40-1.85	1.68-1.90	

**One-way ANOVA*

The variable number of fibroblasts found that the highest mean number of fibroblasts was 65.20 ± 6.38, as shown in Table 5. The highest mean value was found in the experimental group of animals that received ointment treatment with

a concentration of 20% temulawak extract. The lowest mean number of fibroblasts was obtained from the experimental group that received normal saline, which was 55.40 ± 3.21. The smallest number of fibroblasts was found in the normal saline (NS) group. After performing the one-way ANOVA test, it was found that the *p-value* = 0.008 indicated a significant difference in the number of fibroblasts.

Table 5. Comparison of the number of fibroblasts in each treatment group

Treatment (n=25)	Mean ± SD	Min-Max	95%CI	*p-value*
NS	55.40 ± 3.21	52 – 60	51.42 – 59.38	
P. Iodine	58.60 ± 5.13	52 – 65	52.23 – 64.97	
S15%	61.60 ± 2.70	59 – 65	58.25 – 64.95	0.008*
S20%	65.20±6.38	58 – 73	57.28 – 73.12	
S25%	64.60±2.51	61 – 67	58.84 – 63.32	

**One-way ANOVA*

The highest mean value of neovascularization points was 39.00 ± 5.52, as shown in Table 6. It was found in the experimental group of animals that received ointment treatment with a concentration of 20% temulawak extract. The lowest mean neovascularization was obtained from the experimental group that received normal saline (NS), which was 31.80 ± 1.48. The distribution normality test was carried out using the *Shapiro–Wilk test*. It was found that the *p-value* > 0.05 means the data was normally distributed, so the multivariate analysis was then carried out using the one-way ANOVA test. It was found that the value of *p* = 0.003 indicated a significant difference in the amount of neovascularization.

Table 6. Comparison of Neovascularization Points in Each Treatment Group

Treatment (n=25)	Mean ± SD	Min-Max	95%CI	*p-value*
NS	31.80±1.48	30 – 34	29.96 – 33.64	
P. Iodine	34.80 ± 3.11	32 – 40	30.93 – 38.67	
S15%	30.60±3.36	27 – 35	26.43 – 34.77	0.003*
S20%	39.00 ± 5.52	30 – 45	32.14 – 45.86	
S25%	39.20±4.09	34 – 45	34.13 – 44.27	

**One-way ANOVA*

The highest mean area ratio of epithelialization area against total skin area was 23.90 ± 2.52 $mm^{2,}$ as shown in Table 7. The highest mean value was found in the experimental group of animals that received ointment treatment with 25% temulawak extract. The experimental animal group receiving normal saline obtained the lowest mean area ratio, 18.12 ± 1.13 mm^2. The distribution normality test was carried out using the *Shapiro–Wilk test*. It was found that the *p*-value > 0.05 means the data was normally distributed, so the multivariate analysis was carried out using the one-way ANOVA test. The *p*-value = 0.001 indicated a significant difference in the number of fibroblasts.

Table 7. Comparison of New Epithelialization Area with Total Skin Thickness

Treatment (n=25)	Mean ± SD	Min-Max	95%CI	*p-value*
NS	18.12 ± 1.13	16.88 – 19.67	16.71 – 19.52	
P. Iodine	18.31 ± 1.33	16.86 – 20.31	16.67 – 19.97	
S15%	19.78 ± 2.28	17.56 – 23.57	16.94 – 22.61	0.001*
S20%	21.88 ± 2.65	17.88 – 24.59	18.59 – 25.17	
S25%	23.90 ± 2.52	20.77 – 26.48	20.77 – 27.03	

**One-way ANOVA*

The homogeneity test showed a *p*-value > 0.05 for the three variables, so the *Tukey-LSD post-hoc test* was carried out. In the fibroblast, it was found that there were significant differences in the mean between the normal saline (NS), povidone-iodine treatment groups, S15%, S20%, and S25% treatment groups. There was a mean difference of -6,200 (p = 0.032) between NS and S15%; -9,800 (p = 0.002) between NS and S20%; -9,200 (p = 0.003) between NS and S25%; -6,600 p = 0.024) between povidone-iodine and S20%; and -6,000 (p = 0.038) between povidone-iodine and S25%.

In the neovascularization variable, it was found that there were significant differences in the mean between several variables. There was a mean difference of -7.20 (p = 0.007) between NS and S20%; -7.40 (p = 0.005) between NS and S25%; -8.40 (p = 0.002) between S15% and S20%; - 8.60 (p = 0.002) between S15% and S25%; and -6,000 (p = 0.038) between povidone-iodine and S25%.

In the comparison between the area of epithelialization and the total skin area, it was found that there were significant differences in the mean between several variables. There was a mean difference of -3.7640 (p = 0.01) between NS and S20%; -5.7880 (p = 0.00) between NS and S25%; -4.1260 (p=0.005) between NS and S25%; -3, 5620 (p = 0.014) between povidone-iodine and S20%; and -5.5860 (p = 0.0001) between povidone-iodine and S25%.

The wound healing process may be explained by the number of fibroblasts, neovascularization, and epithelialization. A study showed that a mouse model that had been intentionally injured, when treated with turmeric extract, experienced a much more significant increase in fibroblasts [23]. When a *Post-Hoc* analysis was performed, the mean difference between the control group and the topical curcumin extract group was found to be -20.11 (p = 0.021). Epithelialization has been reported in an animal model treated with 5% temulawak gel. It has produced the highest re-epithelialization among the other modeling groups (1.67 ± 0.36 mm). The 1% and 3% temulawak gels also produced good re-epithelialization compared to the control (1.49 ± 0.4 mm and 1.24 ± 0.47 mm, respectively) [19]. *Curcumin* has been reported to accelerate wound healing by triggering more TGF-β1 formation [23]. Elevated levels of TGF-β1 and growth factors in the region of a wound stimulate fibroblast proliferation and migration and induce extracellular matrix creation. The TGF-β1 can also trigger the proliferation of epithelial cells, thereby accelerating re-epithelialization [24].

However, *Curcumin* inhibits the production of *Tumor Necrosis Factor-alpha* (TNF-α) and Interleukin-1 (IL-1) as the two central cytokines released by monocytes and macrophages, thereby inducing an inflammatory response [24]. Inflammatory cells, such as polymorphonuclear cells, will reduce the wound area by inhibiting the production of proinflammatory cytokines, thereby shortening the length of the inflammatory phase and accelerating the wound healing process to enter the next healing phase, namely the proliferation phase with the formation of fibroblasts [25]. Angiogenesis will allow the delivery of oxygen and nutrients to the wound area resulting in suppression of ROS activity, facilitating local collagen synthesis and repelling processes. In this study, we found angiogenesis in the form of capillary dots or endothelium in the microscopy significantly increased, especially in the treatment group that received 20% and 25% extract. This is also in line with the previous studies that curcumin application caused markedly fast wound closure with well formed granulation tissue dominated by fibroblast proliferation, collagen deposition, and complete early regenerated epithelial layer [17].

CONCLUSION

Temulawak ointments was found to be effective for incision wound healing in non-diabetic Wistar rats during the 14th day of observation. The treated groups showed significant differences based on microscopic observation, wound

appearances, number of fibroblasts, neovascularization points, and epithelialization area compared to the untreated groups with normal saline and povidone-iodine. Based on literature studies, the wound healing activity was proposed due to the curcumin compound involved in the temulawak ointmentst, which may induce the TGF-β1 formation and inhibit the TNF-α and IL-1, respectively.

ACKNOWLEDGEMENT
We would like to thank Arlen H.J, head of the animal house laboratory of FMIPA USU Medan, for all the support regarding this study.

AUTHOR'S CONTRIBUTION STATEMENT
JP has conducted the experiment, data analysis, and wrote the manuscript. EG dan LC have supervised the experiment, and revised the manuscript.

FUNDING INFORMATION
-

DATA AVAILABILITY STATEMENT
The utilized data to contribute to this investigation are available from the corresponding author on reasonable request.

DISCLOSURE STATEMENT
The views and opinions expressed in this article are those of the authors and do not necessarily reflect the official policy or position of any affiliated agency of the authors. The data is the result of the author's research and has never been published in other journals.

REFERENCE
1. Gilaberte Y, Prieto-Torres L, Pastushenko I, Juarranz Á. *Anatomy and Function of the Skin*. Elsevier Inc.; 2016. doi:10.1016/B978-0-12-802926-8.00001-X
2. Abdo JM, Sopko NA, Milner SM. The applied anatomy of human skin: A model for regeneration. *Wound Med*. 2020;28(September 2019):100179. doi:10.1016/j.wndm.2020.100179
3. Wong QYA, Chew FT. Defining skin aging and its risk factors: a systematic review and meta-analysis. *Sci Rep*. 2021;11(1):1-13. doi:10.1038/s41598-021-01573-z
4. Farage MA, Miller KW, Eisner P, Maibach HI. Functional and physiological characteristics of the aging skin. *Aging Clin Exp Res*. 2008;20(3):195-200. doi:10.1007/BF03324769
5. Gruber F, Kremslehner C, Eckhart L, Tschachler E. Cell aging and cellular senescence in skin aging — Recent advances in fibroblast and keratinocyte biology. *Exp Gerontol*. 2020;130:110780. doi:10.1016/j.exger.2019.110780
6. Hayati W, Raif MA, Ginting CN, Ikhtiari R. Antioxidant and Wound Healing Potential of Persea Americana Mill. Leaves extract. *AIMS 2021 - Int Conf Artif Intell Mechatronics Syst*. 2021:1-5. doi:10.1109/AIMS52415.2021.9466076
7. Arfani, Raif A, Novalinda Ginting C, Ikhtiari R. Evaluation of wound healing potential of a sea cucumber (Actinopyga mauritiana) extract in mice (Mus. *J Nat*. 2020;20(3):61-65. doi:10.24815/jn.v21i3.19953
8. Adewale Ahmed I, Abimbola Mikail M, Hisam Zamakshshari N, Rais Mustafa M, Mohd Hashim N, Othman R. Trends and Challenges in Phytotherapy and Phytocosmetics for Skin Aging. *Saudi J Biol Sci*. 2022;29(8):103363. doi:10.1016/j.sjbs.2022.103363
9. Carvalho AC, Gomes AC, Pereira-Wilson C, Lima CF. *Mechanisms of*

Action of Curcumin on Aging: Nutritional and Pharmacological Applications. Elsevier Inc.; 2016. doi:10.1016/B978-0-12-801816-3.00035-2
10. Zia A, Farkhondeh T, Pourbagher-Shahri AM, Samarghandian S. The role of curcumin in aging and senescence: Molecular mechanisms. *Biomed Pharmacother*. 2021;134(December 2020):111119. doi:10.1016/j.biopha.2020.111119
11. HWANG J-K. The use of xanthorrhizol for anti-wrinkle treatment. 2008.
12. Lima CF, Pereira-Wilson C, Rattan SIS. Curcumin induces heme oxygenase-1 in normal human skin fibroblasts through redox signaling: Relevance for anti-aging intervention. *Mol Nutr Food Res*. 2011;55(3):430-442. doi:10.1002/mnfr.201000221
13. Ganceviciene R, Liakou AI, Theodoridis A, Makrantonaki E, Zouboulis CC. Skin anti-aging strategies. *Dermatoendocrinol*. 2012;4(3). doi:10.4161/derm.22804
14. Makrantonaki E, Zouboulis CC. Molecular mechanisms of skin aging: State of the art. *Ann N Y Acad Sci*. 2007;1119(1):40-50. doi:10.1196/annals.1404.027
15. Kristianto H, Khotimah H, Sholeh RA, Mardianto EW, Sani HC, Paratiwi HA. The Effects of Javanese Turmeric (Curcuma xanthorriza Roxb) on Fibroblasts, Granulation, Blood Vessel Density, and Contraction in Wound Healing of STZ-Induced Diabetic Rats. *Kuwait J Sci*. 2006;(December):1-6.
16. Barung EN, Wungow R, Kalonio DE. Percepatan Penutupan Luka Sayat pada Tikus Putih Akibat Pemberian Perasan Rimpang Temulawak (Curcuma xanthorrhiza Roxb.). *J Pharmascience*. 2021;8(1):1. doi:10.20527/jps.v8i1.9333
17. Kant V, Gopal A, Kumar D, et al. Curcumin-induced angiogenesis hastens wound healing in diabetic rats. *J Surg Res*. 2015;193(2):978-988. doi:10.1016/j.jss.2014.10.019
18. Kant V, Gopal A, Pathak NN, Kumar P, Tandan SK, Kumar D. Antioxidant and anti-inflammatory potential of curcumin accelerated the cutaneous wound healing in streptozotocin-induced diabetic rats. *Int Immunopharmacol*. 2014;20(2):322-330. doi:10.1016/j.intimp.2014.03.009
19. Kesumayadi I, Almas AI, Rambe INH, Hapsari R. Effect of curcuma xanthorrhiza gel on methicillin-resistant staphylococcus aureus-infected second-degree burn wound in rats. *Nat Prod Sci*. 2021;27(1):1-9. doi:10.20307/nps.2021.27.1.1
20. Weta IW, Nadia HD, Weta IW, Aman IGM. Topical virgin red palm oil improved wound healing by increasing fibroblasts , neovascularization and epithelialization in male Wistar rats (Rattus norvegicus). 2020:24-27.
21. Surya KE, Khu A, Raif A, Ikhtiari R. Papaya Latex for Healing the Second Degree of Burn Wound in Male Mice. *InHeNce 2021 - 2021 IEEE Int Conf Heal Instrum Meas Nat Sci*. 2021. doi:10.1109/InHeNce52833.2021.9537269
22. Aidah N, Nyoman Ehrich Lister I, Ginting CN, Ikhtiari R. Evaluation of Honey Effectivity on Burned-Wound Contraction in Rattus Norvegicus. In: *InHeNce 2021 - 2021 IEEE International Conference on Health, Instrumentation and Measurement, and Natural Sciences*. IEEE; 2021. doi:10.1109/InHeNce52833.2021.9537239
23. Yahya EB, Setiawan A, Wibowo MD, Danardono E. The effect of topical curcumin extract on fibroblast count and collagen density as an indicator on accelerating clean wound healing process: A study on wistar rats. *Syst Rev Pharm*. 2020;11(5):567-570. doi:10.31838/srp.2020.5.74
24. Mohanty C, Sahoo SK. Curcumin and its topical formulations for wound healing applications. *Drug Discov Today*. 2017;22(10):1582-1592. doi:10.1016/j.drudis.2017.07.001
25. Barchitta M, Maugeri A, Favara G, et al. Nutrition and wound healing: An

overview focusing on the beneficial effects of curcumin. *Int J Mol Sci*. 2019;20(5). doi:10.3390/ijms20051119

JTL 11 (2) December 2022
Page: 105-113

Contents list available at Jurnal Teknologi Laboratorium

JURNAL TEKNOLOGI LABORATORIUM

Journal Homepage: www.teknolabjournal.com
ISSN 2580-0191(Online) I ISSN 2338 – 5634(Print)

Original Research

The effects of IR-Bagendit rice leaf infusions from Blora on renal tubular degeneration and necrosis: (Study on Wistar albino rats covered with plumbum acetate)

Budi Santosa*, **Erick Erianto Arif, Ana Hidayati Mukaromah**

Magister Program of Clinical/Medical Laboratory Science, Universitas Muhammadiyah Semarang, Indonesia

Abstract: Plumbum exposure still becomes a health problem in Indonesia. Plumbum (Pb) is widely used in various industries; thus, it can cause health problems, including impaired kidney functions. The accumulation of Pb rise to degeneration and necrosis of renal tubule cells. Therefore, preventive efforts are necessary to inhibit renal function deterioration. Infused extract of IR Bagendit rice leaf from Blora contains protein metallothionein which could bind PB covalently. This study aims to determine the supplementation of IR Bagendit rice leaf infusion to inhibit degeneration and necrosis of renal tubular cells exposed to Pb. The experimental research method was conducted using Wistar albino rats divided into five groups: negative control group, positive group, and treatment groups 1, 2, and 3. Each group consisted of six rats. The negative control group only received a placebo, and the positive group only received Pb acetate 60 mg/kg BW/day. Meanwhile, treatment groups 1, 2, and 3 received 0.2 ml, 0.4 ml, and 0.8 ml IR Bagendit rice leaf infusions successively and Pb acetate 60 mg/kg BW/day. The experiment was conducted for 60 days. Histological preparations of tubular cells were colored using hematoxylin-eosin. Normal cell differences, degeneration, and necrosis of each group were tested using Kruskal Wallis and Mann Whitney tests.This study has revealed that the average normal cells in the positive control group are lower than those in the negative control group and treatment groups 1, 2, and 3. This difference is insignificant with the p = 0.477. Moreover, treatment groups 1, 2, and 3 show decreased cell degeneration and necrosis with significant differences of p = 0.000 and 0.001. IR Bagendit rice leaf infusions could inhibit degeneration and necrosis of renal tubular cells exposed to Pb.

Keywords: IR Bagendit; Degeneration; Necrosis; Pb; Metallothionein

INTRODUCTION

Plumbum (Pb) exposure still becomes a health problem in Indonesia and is widely used in various industries, such as battery, accumulator, paint, and coloring material industries. Thus, Pb could be toxic to humans. Pb enters the human body through three pathways: the gastrointestinal tract (gastrointestinal), respiratory tract (inhalation), and penetration through skin (topical). PB toxicity of 5 ug/dL could poison adults.[1] The accumulation of Pb in the body could cause loss of appetite, weak muscles, anemia, intellectual disability, behavioral disorders, renal physiology disorders, liver disease, and death. [2,3]

Pb toxicity can form free radicals and degrade endogenous antioxidant enzymes, such as superoxide dismutase (SOD), catalase (CAT), and glutathione transferase (GSH), that cause organ dysfunctions. An imbalance number

Corresponding author.
E-mail address: budisantoso@unimus.ac.id (Budi Santosa)
DOI: 10.29238/teknolabjournal.v11i2.352
Received 19 August 2022; Received in revised 01 September 2022; Accepted 28 October 2022

between free radicals and antioxidants will lead to oxidative stress.[4,5] Oxidative stress is the excessive production of reactive oxygen species (ROS), such as hydroxyl, superoxide, and hydroperoxyl, which react with fats, proteins, and cellular nucleic acids; this condition results in local damage (glomerulus dysfunction) and renal tubular cells.[6,7,8] Acute PB poisoning (Pb levels in the blood >80-100 µg/dL) disrupts the structure and functions of the renal tubules.[9] The kidney damage due to Pb toxicity is in the form of degeneration and necrosis.[10]

Cell degeneration refers to damage that occurs in cytoplasm, but not in nucleus cells, and could repair damage to be normal and reversible. Cell degeneration that lasts a long time and continuously will disable cells to conduct metabolism properly; consequently, the cells death or cell necrosis occurs. Cell necrosis can be characterized by damage in the form of irreversible karyolysis, pycnosis, or cariorexis.[11,10]

Various efforts through curative and preventive measures have been made to prevent Pb toxicity. Preventive measures are done with the chelating agent principles and are still considered the best choice. One of the chelating ingredients is IR Bagendit rice leaves that contain a lot of protein metallothionein. This protein is rich in sulfhydryl groups that could covalently bind heavy metals (Pb).[12,13] The content of metallothionein proteins in IR Bagendit rice leaves from various locations in Northern Java has been investigated, and the investigation has revealed that R Bagendit rice from Blora has the highest content.[14] The metallothionein gene is located on chromosome 3 of IR Bagendit rice leaves **(***Oryza Sativa***)** and functions as stress-inducible proteins in drought conditions as well as soil and water-containing metals. Therefore, metallothionein can be used as a biomarker of heavy metal exposure.[15] This study aims to determine the functions of IR-Bagendit rice leaf infusion from Blora to prevent degeneration and necrosis of renal tubular cells.

MATERIAL AND METHOD

Rice leaves of various varieties had been cleaned and washed with running water before they were chopped into smaller pieces. Afterward, they were weighed as much as 100 g and put into pot A. Then, a liter of aquades was added. Finally, the pot was closed. Meanwhile, pot B (as a water bath) was added with sufficient water until the upper pot (A) was submerged partially. The pots were heated for 15 minutes until the temperature inside pot A reached 90^{o}C while being stirred occasionally. The infusion was sprayed while it was hot using a fabric flannel, supernatants are infusions. This process is summarized Figure 1, the produced infusions were labeled according to their regions. Meanwhile, the infusions' protein metallothionein was examined using the Elisa method.

Microplate coated with specific antibodies MT. Standards and samples were added to microwells and were corresponding to specific polyclonal antibodies-conjugated biotin for MT. Furthermore, peroxidase conjugated-avidin was added to each well and incubated. Then, substrate solution was added to each well. Discoloration occurs in wells containing MT, antibodies-conjugated biotin, and enzymes-conjugated avidin. Enzyme-substrate reactions end with adding a sulfuric acid solution and color changes that were measured spectrophotometrically with a wavelength of 450 2 nm. The concentration of MT in the samples was determined by comparing their OD to the standard curve.

This study examined 30 male rats aged 2-3 months and weighed 170-200 grams. These rats were divided into five groups: the negative control group, the positive control group, and treatment groups 1, 2, and 3. Each group consisted of six rats. The negative control group only received a placebo while the positive

control only received PB acetate 60 mg/kg BW/day for 60 days, that given in the form of a solution through a sonde. Treatment group 1 (P1) received 0.2 ml of IR-Bagendit rice leaf (*Oryza sativa L*) infusion, treatment group 2 (P2) received 0.4 ml of infusion, and treatment group 3 (P3) received 0.8 ml of infusion for 10 days. Afterward, the infusions were subsequently administered while exposing PB acetate of 60 mg/kg BW/day until the 60th day. Meanwhile, 100 g/L = 100,000 mg/1000 mL IR of Bagendit rice leaf infusion was produced from 100 mg/mL for various concentrations of 0.2 ml (P1), 0.4 ml (P2), and 0.8 ml (P3).

The surgical stage was performed on the 61st day. Moreover, at this stage, anesthesia was performed. The anesthetic induction used in this research was a combination of ketamine and xylazine with a dose of 40 mg/kg and 10 mg/kg; this induction was administered intraperitoneally (IP). Surgery was performed in the abdomen horizontally and vertically. Afterward, the kidney organ was taken to make histopathological preparations. The preparations were made using the paraffin method with the hematoxylin-eosin (HE).

The quality of kidney tissue preparations resulting from staining hematoxylin-eosin (HE) was assessed macroscopically and microscopically. Then, the number of normal cells, degenerative cells, and renal tubular necrosis cells in the control and treatment groups was calculated. the number of normal, degenerative, and necrotic cells was calculated in percent units which were read using a microscope with a magnification of 400x. The data were analyzed by comparing the results of each group using the Kruskal-Wallis test.

This research received the ethical clearance No: 503 503/KEPK-FKM/UNIMUS / 2021 from the Health Committee of the Faculty of Health, Universitas Muhammadiyah Semarang. Moreover, the head of the Integrated Research and Testing Laboratory (LPPT) of Universitas Muhammadiyah Semarang approved this research by considering research ethics.

RESULTS AND DISCUSSION

Metallothionein Content

The metallothionein protein levels of the obtained infusions were checked using the ELISA. The 0.321 absorbances with the obtained concentration have resulted in 380.636 ng/L. Based on this result, the treatment groups receiving rice leaf infusion of 100 g/L = 100,000 mg/1000 mL have produced 100 mg/mL with concentration variations of 0.2 ml, 0.4 ml, and 0.8 ml.

Microscopic Pictures of Renal Tubular Cells of Wistar Rats

The results of laboratory tests provide pictures of normal, degenerative, and necrosis renal tubular cells of all treatment groups can see at figure 2.

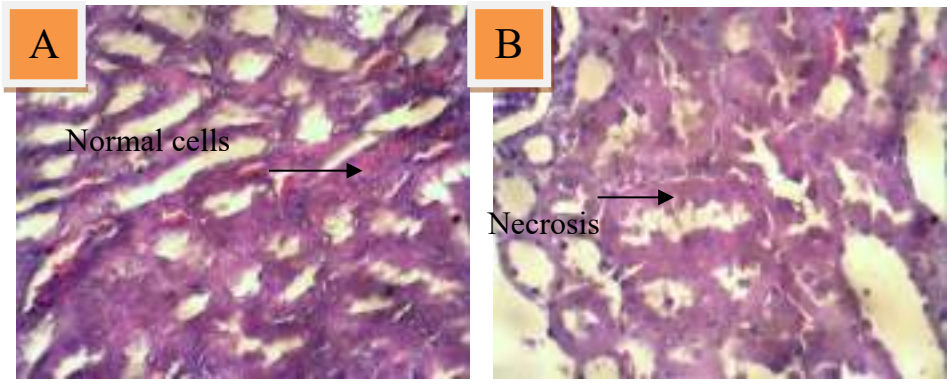

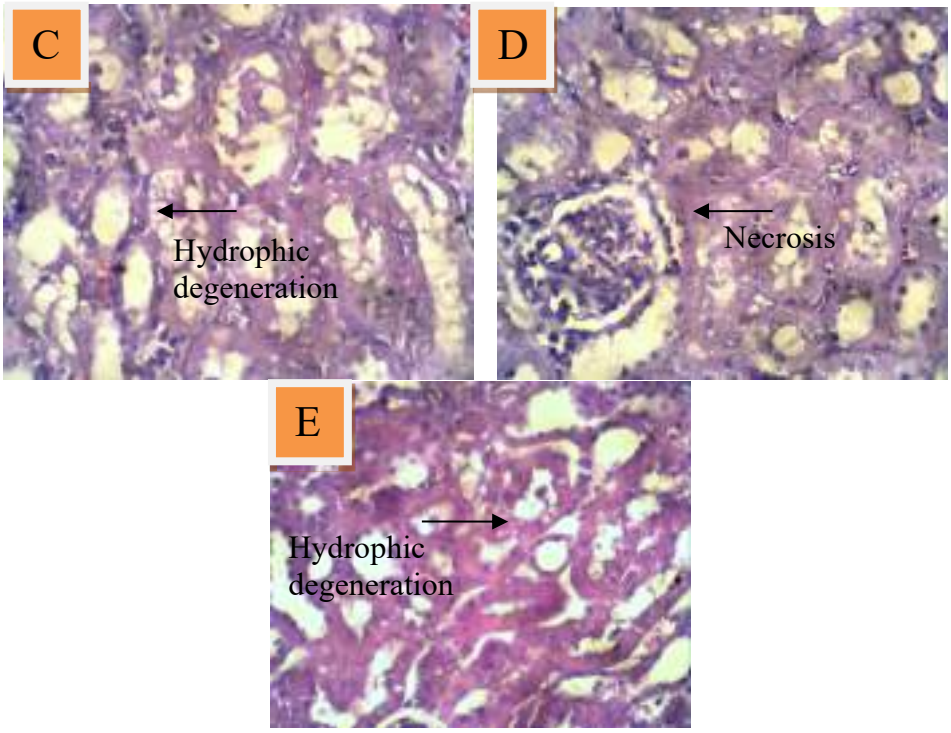

Figure 2. Microscopic picture of renal tubular cells of Wistar albino rats with 400X of magnification; A = Negative control; B = Positive control; C = Treatment 1; D = Treatment 2; E = Treatment 3

Meanwhile, the mean scores of normal, degenerative, and necrosis cells in the negative control group, positive control group, and treatment groups 1, 2, and 3 are summarized in Table 1. Table 1 shows that the body weights of rats in all treatment groups are not significantly different. All groups have gained weight from the beginning to the end of the treatment. The mean of normal cells of the positive control group has decreased, but that of the treatment groups 1, 2, and 3 has increased and is nearly equal to that of the negative control group. The highest mean of degenerative and necrosis cells is found in the positive control group. Meanwhile, P1 and P2 treatment groups have experienced a decrease in both cell groups, but the P3 treatment group has not. The data show significant differences between the positive group and the treatment control groups (Table 2). The calculation results in Table 2 are related to Figure 2 presenting degenerative and necrosis cells of renal tubules in Figures C, D, and E. The degenerative and necrosis cells are significantly different; to determine the differences between groups, the Mann-Whitney test was conducted. The results of this statistical test are presented in Table 2.

The results of the statistical test denote that the negative and positive control groups have significantly different degenerative cells from the treatment groups. The negative control group has significantly different necrosis from the positive control group and treatment group 1. Meanwhile, the positive control group has significantly different necrosis from all treatment groups (P1, P2, and P3).

Moreover, the weight of Wistar albino rats has met the inclusion criteria and group average in each homogeneous group. The average number of normal cells in each group is not significantly different. However, the average number of normal cells in the positive control group is descriptively lower than that in the negative control group and the treatment groups 1, 2, and 3. In contrast, all groups show a significantly different average number of degenerative cells. This study has discovered that necrosis cells in the control groups 1, 2, and 3

decrease, but not in the positive control group. Moreover, their differences are significant.

This study has revealed that IR Bagendit rice leaves from Blora contain high metallothionein protein that meets the requirement for this research.[14] This study has deployed that Plumbum acetate is a toxic heavy metal that causes impaired functions characterized by the increasing amount of damage in renal tubule cells. Plumbum acetate can cause oxidative stress that can increase the formation of free radicals, such as superoxide, hydrogen peroxide, hydroxyl, and lipid peroxide, as well as decrease endogenous antioxidant systems, such as superoxide dismutase, catalase, glutathione peroxidase, and glutathione reductase. Such conditions could damage kidney cells.[15,5] The decrease in the body's antioxidants and the increase in free radicals will cause oxidation and escalate lipid peroxidation. Unstable lipid peroxidation can damage three types of compounds that significantly maintain cell integrity; they are cell membranes, proteins, and DNA.[7,8] Cell degeneration constitutes damage that occurs in cell membranes. This damage will trigger the oxidation of amino acids and increase the permeability of cell membranes. As a result, cellular reactions do not work perfectly and could become reversible and irreversible (cell death).[5,16] Degenerative cells could have the adaptability to reach new conditions and maintain their viability. To a certain extent, the cells return to a stable state that enables them to divide by responding to injury through hypertrophy. Afterward, adaptation and proliferation of the cells are performed with re-eptelization.[10] If the stress is severe or persistent, irreversible injury occurs, and the cells will die (necrosis).[5] The provision of IR Bagendit rice leaf infusion could reduce the degeneration of renal tubule cells.

Necrosis of renal tubule cells occurs due to a higher level of cell damage after the membrane permeability is disrupted by the emergence of turbid swelling followed by lysis.[17] Irreversible damage (necrosis) is characterized by the loss of nucleus and cell fragmentation as well as the release of cytoplasmic contents in the renal tubules.[18] Such conditions occur because tubule cells have a weak epithelium and leak easily.[19] This study has proven that necrosis is characterized by more basophilic and disappearing nucleus cells (karyolysis).

Protein metallothionein is mostly found in various plants, such as IR-Bagendit rice leaves (*Oryza sativa L*). The leaves of IR-Bagendit rice (*Oryza sativa L*) contain the highest protein metallothionein among other leaves of other types of rice.[20] Protein metallothionein in (*Oryza sativa L*) IR-Bagendit rice leaves has a sulfhydryl group and can bind PB acetate; thus, this protein metallothionein is stable for the detoxification process.[21,22] This study has found that the provision of IR-Bagendit rice (*Oryza sativa L*) leaf infusion of 0.2 ml/day, 0.4 ml/day, and 0.8 ml/day can successively decrease necrosis cell damage up to 75% in P1, 90% in P2, and 100% in P3. These numbers show that the intervention groups have significantly different improvements from the positive control group. The greater the dose of R-Bagendit rice (*Oryza sativa L*), the greater the decrease in degenerative and necrosis cell damage. It shows that protein metallothionein has a nephroprotective activity against nephrotoxicity induced by Plumbum acetate.

CONCLUSION

The provision of IR Bagendit rice leaf infusion from Blora can inhibit renal tubular cell damage (degeneration and necrosis) and has been proven effective for the treatment groups 2 (0.4 ml = 40 mg) and 3 (0.8 ml = 80 mg). The metallothionein protein could bind plumbum so that renal tubular degeneration and necrosis can be prevented.

AUTHORS' CONTRIBUTIONS

BS formulated the research design, conducted experiments, analyzed data, and compiled, revised, and reviewed the manuscripts critically. The EEA collected and analyzed the data. AHM prepared the reagents and materials and analyzed the data. All of the researchers read and approved the final manuscript.

ACKNOWLEDGEMENT

We would like to thank the Director-General of Higher Education of the Ministry of Education, Culture, Research, and Technology for supporting this research.

FUNDING INFORMATION

Not any information from author's

DATA AVAILABILITY STATEMENT

The utilized data to contribute to this investigation are available from the corresponding author on reasonable request.

DISCLOSURE STATEMENT

The data is the result of the author's research and has never been published in other journals and not any conflict of interest between authors and financial funding.

REFERENCE

1. Čadková Z, Száková J, Miholová D, et al. Faecal Excretion Dynamic during Subacute Oral Exposure to Different Pb Species in Rattus norvegicus. *Biol Trace Elem Res*. 2013;152(2):225-232. doi:10.1007/s12011-013-9609-8
2. Yabe J, Nakayama SM, Nakata H, et al. Current trends of blood lead levels, distribution patterns and exposure variations among household members in Kabwe, Zambia. *Chemosphere*. 2020;243(125412):125412. doi:10.1016/j.chemosphere.2019.125412
3. Kim KS, Lim H-J, Lim JS, et al. Curcumin ameliorates cadmium-induced nephrotoxicity in Sprague-Dawley rats. *Food Chem Toxicol*. 2018;114:34-40. doi:10.1016/j.fct.2018.02.007
4. Jiang S, Shang M, Mu K, et al. In vitro and in vivo toxic effects and inflammatory responses induced by carboxylated black carbon-lead complex exposure. *Ecotoxicol Environ Saf*. 2018;165:484-494. doi:10.1016/j.ecoenv.2018.09.040
5. Sugiharto Sugiharto, Darmanto W, Wahyuningsih SPA, et al. Antioxidant Activities of Curcumin to MDA Blood Serum Concentration and Lead Levels in Liver of Mice. *Malaysian J Sci*. 2019;38(3):21-29. doi:10.22452/mjs.sp2019no3.3
6. Koerniasari, Setiawan, Ngadino, Rustanti. Protective Effects of Ethanol Extract of Mangosteen (Garcinia mangostana L) Pericart Against Lead Acetate-Induces Acetate Induced Hepatotoxicity in Mice. *Int J Curr Res*. 2015;7(2):12518-12522. https://www.journalcra.com/article/protective-effects-ethanol-extract-mangosteen-garcinia-mangostana-l-pericarp-against-lead
7. Ishii C, Nakayama SMM, Kataba A, et al. Characterization and imaging of lead distribution in bones of lead-exposed birds by ICP-MS and LA-ICP-MS. *Chemosphere*. 2018;212:994-1001. doi:10.1016/j.chemosphere.2018.08.149
8. Flora G, Gupta D, Tiwari A. Toxicity of lead: a review with recent updates. *Interdiscip Toxicol*. 2012;5(2):47-58. doi:10.2478/v10102-012-0009-2
9. Rana MN, Tangpong J, Rahman MM. Toxicodynamics of Lead, Cadmium,

Mercury and Arsenic- induced kidney toxicity and treatment strategy: A mini review. *Toxicol Reports*. 2018;5(April):704-713. doi:10.1016/j.toxrep.2018.05.012
10. Soliman MM, Baiomy AA, Yassin MH. Molecular and Histopathological Study on the Ameliorative Effects of Curcumin Against Lead Acetate-Induced Hepatotoxicity and Nephrototoxicity in Wistar Rats. *Biol Trace Elem Res*. 2015;167(1):91-102. doi:10.1007/s12011-015-0280-0
11. Oyagbemi AA, Omobowale TO, Akinrinde AS, Saba AB, Ogunpolu BS, Daramola O. Lack of reversal of oxidative damage in renal tissues of lead acetate-treated rats. *Environ Toxicol*. 2015;30(11):1235-1243. doi:10.1002/tox.21994
12. Santoso B, Subagio HW, Suromo L, Sunomo HR. Zinc supplementation improves heme biosynthesis in rats exposed to lead. *Universa Med*. 2016;34(1):3. doi:10.18051/UnivMed.2015.v34.3-9
13. Santosa B, Sunoko HR, Sukeksi A. Aqueous IR Bagendit rice leaf extract decreases reticulocyte count in lead-exposed rats. *Universa Med*. 2018;37(1):57-64. doi:10.18051/UnivMed.2018.v37.57-64
14. Santosa B. Water Infusion of IR-Bagendit Rice Leaves from Various Locations in Central Java as a Candidate Material to Prevent a Heavy Metal Exposure. *J Hunan Univ Sci*. 2021;48(7):238-243. http://jonuns.com/index.php/journal/article/view/669
15. Santosa B, Darmawati S, Kartika AI, et al. Isolation, Identification Similarity and Qualitative Expression of Metallothionein Gene in IR-Bagendit Rice (Oryza sativa). *Pharmacogn J*. 2020;12(4):709-715. doi:10.5530/pj.2020.12.103
16. Shafiekhani M, Ommati MM, Azarpira N, Heidari R, Salarian AA. Glycine supplementation mitigates lead-induced renal injury in mice. *J Exp Pharmacol*. 2019;Volume 11:15-22. doi:10.2147/JEP.S190846
17. Mas'ulun MJ, Mustika A, Qurnianingsih E. The Effect of Dandang Gendis Extract (Clinacanthus nutans) on Kidney Histopathological Features of Diabetic Rats Model. *Heal Notions*. 2021;5(01):19-22. doi:10.33846/hn50104
18. Kumar, Abbas AR. *Basic Pathology*. 10th ed. (Kumar, Vinay. Abbas AKAJ, ed.).; 2018. https://www.elsevier.com/books/robbins-basic-pathology/kumar/978-0-323-35317-5
19. Vallon V. Tubular Transport in Acute Kidney Injury: Relevance for Diagnosis, Prognosis and Intervention. *Nephron*. 2016;134(3):160-166. doi:10.1159/000446448
20. Santosa B, Sunoko HR, Sukeksi A. The Analysis, Identification, and Formulation of Metallothionein Extract Available in Roots, Stems, Leaves , Flowers , and Grains of Rice, Corns, Beans , and Soybeans. *Int J Sci Eng - IJSE*. 2016;10(1):17-20. doi:10.12777/ijse.10.1
21. Santosa B, Sunoko HR, Sukeksi A. Ekstrak Air Daun Padi Memperbaiki Hematopoesis pada Tikus yang Terpajan Plumbum. *Maj Kedokt Bandung*. 2015;47(2):84-90. doi:10.15395/mkb.v47n2.458
22. Santosa B. Rice leaf Extract for Kidney Damage Prevention in Plumbum exposes rats. In: *The 12th International Conference On Lesson Study (ICLS-XII)*. Universitas Muhamadiah Malang Press; 2021. https://jurnal.unimus.ac.id/index.php/psn12012010/article/view/1956

Figure 1. Stages of making IR Bagendit rice leaf infusion: 1) cleaning and washing rice

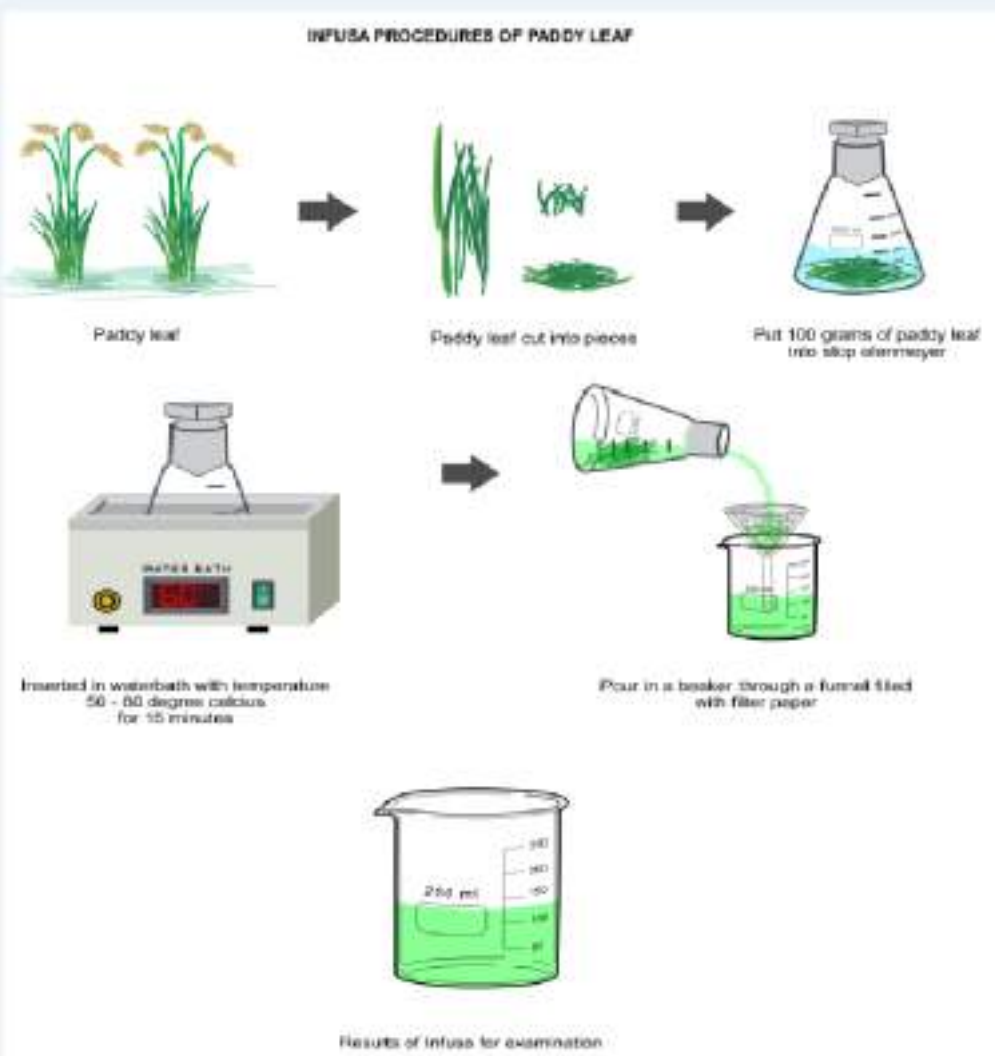

leaves from several varieties with running water; 2) chopping the leaves into small parts; 3) weighing the small parts as much as 100 g and putting them into pot A; 4) adding a liter of aquades; 5) closing the pot; 6) adding sufficient water on pot B (as a *water bath)* until the upper pot (A) partially submerged; 7) heating the pots while stirring the water inside occasionally for 15 minutes until the temperature inside pot A reaching 90^{o}C; 8) spraying the infusion while hot using a fabric flannel, supernatants are infusions.

Table 1. Average numbers of normal, degenerative, and necrosis cells and differences between initial weight and final weight after the 60-day intervention in the control and treatment groups

Variables	Treatment					p-value
	Control -	Control +	P1	P2	P3	
Initial BW (g)	178 ± 7.07	177 ± 9.20	180 ± 10.71	176.3 ± 4.96	184 ± 10.91	0.575
Final BW (g)	212 ± 20.01	215.8 ± 25.38	209.6 ± 10.89	200 ± 9.18	202.5 ± 32.18	0.310
Normal cells	604 ± 9.49	483 ± 9.49	608 ±9.9	608 ± 6.04	609 ± 6.33	0.477
Degenerative cells	0	2 ± 1.43	1.71 ± 0.9	1.55 ± 0.73	1.05 ± 0.35	0.000
Necrosis cells	0	2 ± 1.41	0.5 ± 1	0.2 ± 0.4	0	0.001

Table 2. Results of difference test on degenerative cells and necrosis cells of two treatment groups

Groups	P-value				
	Control-	Control+	P1	P2	P3
Degenerative cells					
K-	-	0.004*	0.005*	0.004*	0.004*
K+	0.004*	-	0.007*	0.005*	0.015*
Necrosis cells					
K-	-	0.005*	0.018*	0.134	1.000
K+	0.005*	-	0.008*	0.007*	0.005*

JTL 11 (2) December 2022
Page: 114-121
Contents list available at Jurnal Teknologi Laboratorium

JURNAL TEKNOLOGI LABORATORIUM

Journal Homepage: www.teknolabjournal.com
ISSN 2580-0191(Online) I ISSN 2338 – 5634(Print)

Original Study

Comparison between use courier transport with pneumatic tube system on the results of routine hematology test, Prothrombin Time (PPT), Activated Partial Thromboplastin Time (APTT), and potassium

Yoki Setyaji *[1], Kurnia Fitriasari [2], Tri Novitasari [2], Norma Agustin Palupi[2]
[1] Politeknik Kemenkes Semarang, Indonesia
[2] Rumah Sakit Akademik UGM, Yogyakarta, Indonesia

Abstract: Pneumatic tube system (PTS) is a transport medium that is widely used in hospitals. The samples transported via PTS would get vibrations due to changing air velocity and pressure. This unstable pressure could cause pre-analytic errors in laboratory measurements. It happened because it damages erythrocytes and lymphocytes and causes haemolysis. It has been demonstrated that these changes can alter the quality of samples and induce haemolysis by leading primarily to increase in lactate dehydrogenase (LDH) concentrations, and potassium concentration. Haemolysis is dined as the release of intracellular components of erythrocytes and other blood cells into the extracellular space of blood. It can also affect the results of in vitro platelet function test. Incorrect test results can affect the diagnosis and the treatment for patients Every hospital that uses PTS are advised to validate and investigate that PTS has the possibility of haemolysis and impacts laboratory results of blood specimens. The purpose of the study was to validate and know comparison between use courier transport with using PTS on the results of routine haematology tests, PPT, APTT, and potassium. This research was experimental research by using posttest without control. The research used statistical test which was paired t-test. The research was conducted at the Integrated Clinical Laboratory Installation of the Gadjah Mada University Academic Hospital in August – October 2020 with 30 preoperative patients. Data were analysed with Prism GraphPad 8 software. There was no significant difference between WBC, RBC, Hb, HCT, MCV, MCH, MCHC, PPT, and APTT. Moreover, there was a significant difference between the results of PLT and potassium in the samples transported via PTS and delivered by courier transport.

Keyword: APTT Evaluation; Pneumatic Tube System; Potassium; Routine Hematology

INTRODUCTION

Pneumatic tube system (PTS) is a transport medium that is widely used in hospitals. Delivery using PTS can help hospital services become faster and more efficient, especially for sending drugs, radiology results, tissue samples, and blood specimens from various units, both laboratory, radiology, pharmacy, and wards and poly services[1]. The use of PTS can reduce laboratory Turnaround Time (TAT). TAT is the period used for laboratory measurements starting from delivery, analysis up to the results come out[2]. During PTS transport, sample quality can be affected by the exposure to rapid acceleration, radial gravity forces, sudden decelerations, and other extreme temperature and physical forces. These violent forces may contribute to pre-analytical errors due to erythrocyte and lymphocyte rupture. A study by Weaver and colleagues compared the effects of PTS and manual transport on the results of 15 chemical tests and 6 hematologic

Corresponding author.
E-mail address: yokisetyaji@poltekkes-smg.ac.id (Yoki Setyaji)
DOI: 10.29238/teknolabjournal.v11i2.342
Received 13 May 2022; Received in revised form 31 May 2022; Accepted 31 October 2022

procedures. The only difference they observed in PTS specimens was that the activity of lactate dehydrogenase exceeded the precision of the test. However, the remaining tests - serum sodium, potassium, chloride, carbon dioxide, total protein, albumin, calcium, glucose, creatinine, total bilirubin, alkaline phosphatase, aspartate transaminase, acid phosphatase, uric acid, leukocyte count, erythrocyte count, hemoglobin, hematocrit, prothrombin time (PT), and activated partial thromboplastin time (APTT) - were not affected by PTS[3].

Preanalytical phase of clinical laboratory testing is the most vulnerable part to errors. This phase includes test ordering, collection of diagnostic specimens, handling, transportation, and storage of the specimen. Pneumatic tube system (PTS) provides rapid and efficient transportation of blood samples to the laboratory and has been widely adopted. It is widely used to reduce the expanding workloads and to lead to faster sample processing and decreased turnaround times. During transportation, however, samples are often exposed to fast acceleration and deceleration. It has been demonstrated that these changes can alter the quality of samples and induce hemolysis by leading primarily to increase in lactate dehydrogenase (LDH) concentrations, and potassium concentration[4]. Hemolysis is dined as the release of intracellular components of erythrocytes and other blood cells into the extracellular space of blood[5].It can also affect the results of in vitro platelet function test. Incorrect test results can affect the diagnosis and the treatment for patients[4].

PTS can cause small vibrations in the sample due to changes in air velocity and pressure during sample delivery. The unstable pressure can cause preanalytical errors in laboratory measurements. It is because it can damage erythrocytes and lymphocytes, causing hemolysis[6]. PTS's pressure and speed can increase potassium and Lactate Dehydrogenase (LDH) levels[7]. Sodi et al. emphasized that each laboratory should investigate the effects of the specific PTS used by the laboratory on the samples[5]. Every hospital that uses PTS are advised to validate PTS and investigate blood specimens for the possibility of hemolysis, activation of clotting factors that affect laboratory results[8].

MATERIAL AND METHOD

The research design was experimental research by using posttest without control[9]. The research was conducted at the Integrated Clinical Laboratory Installation of the Gadjah Mada University Academic Hospital in August – October 2020 with 30 preoperative patients. The sampling technique is purposive sampling. The criteria for the object of research were patients aged more than 18 years without comorbid diseases and not currently on blood-thinning drug therapy, and have a history of platelet disorders. Each research object was taken EDTA blood, citrate, and chemistry from two tubes each and then separated into two groups. The delivery of two groups of samples to the laboratory was conducted in two ways: Pneumatic Tube System and delivered by a delivery officer. Both groups of samples were processed for routine hematology tests, PPT, APTT, and laboratory measurements. The examination data was processed using the Paired t-test with the help of Prism GraphPad 8 software.

The research had been registered and obtained research ethics permit from the Health Research Ethics Commission of the Faculty of Medicine, Public Health and Nursing Universitas Gadjah Mada - Dr. Sardjito Hospital with registration number Ref.No. : KE/FK/1069/EC/2020.

RESULTS AND DISCUSSION

The research was conducted based on primary data from the routine hematological test. PTS and courier transport transported PPT, APTT, and potassium in September 2020.

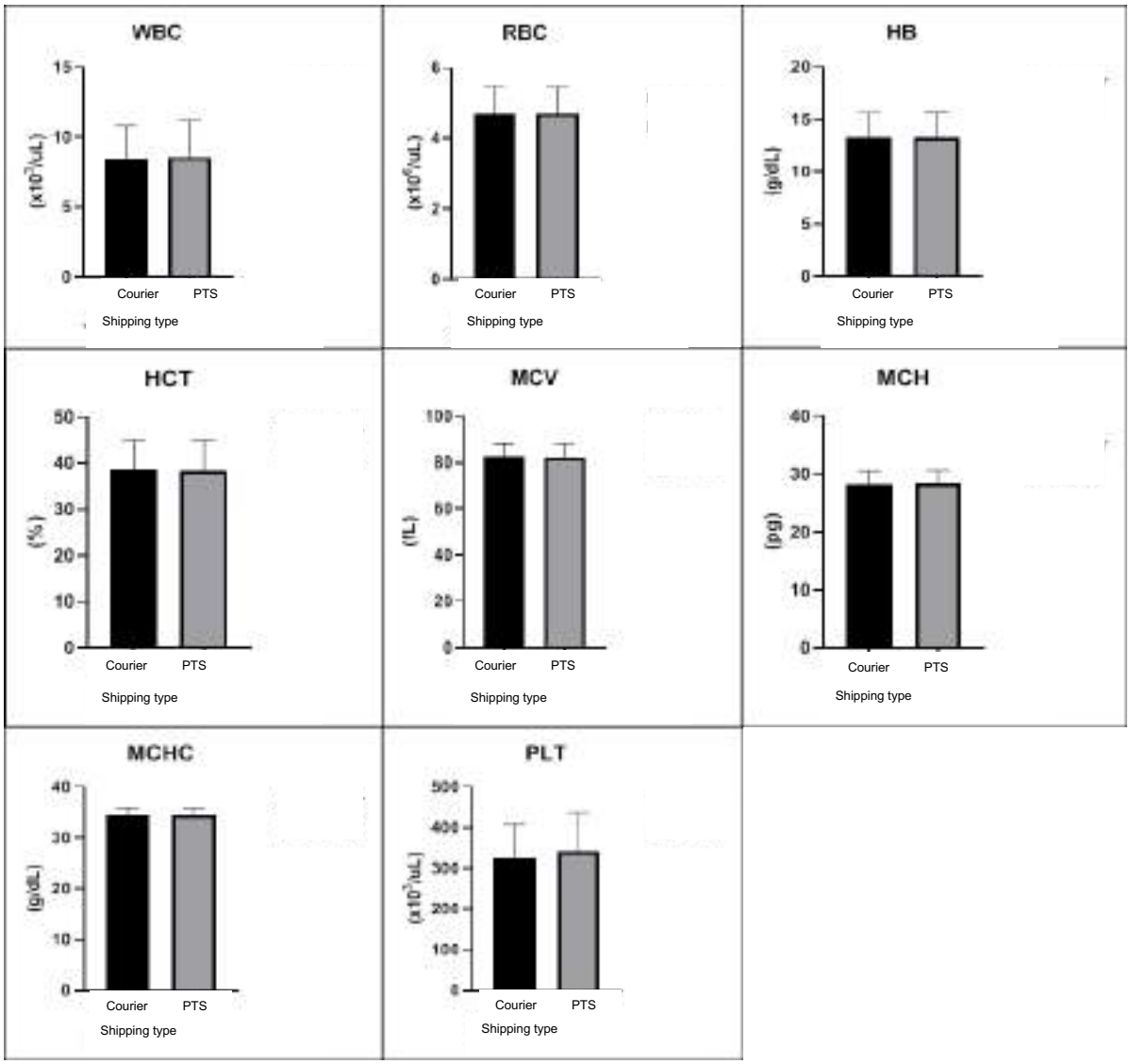

Figure 1. The comparison chart of Routine Hematology Test Results UsingSamples transported between by PTS and by Courier Transport

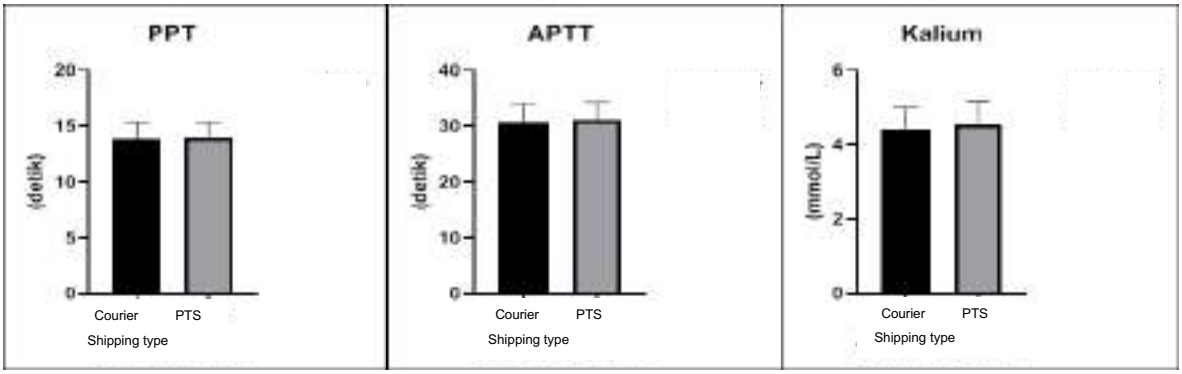

Figure 2. The comparison chart of PTT and APTT and Potassium Measurement Results Using Samples transported between by PTS and by Courier Transport)

The data was analyzed statistically by using paired t-test. The results were in the following:

Table 1. The Comparison of Hematology Test Results Transported between by

Parameter	*Mean*		*SD*		*P-value*
	Courier Transport	PTS	Courier Transport	PTS	
WBC	8.426	8.574	2.4099	2.6126	0.0556
RBC	4.687	4.687	0.7750	0.7733	0.9822
HB	13.24	13.28	2.4459	2.4585	0.1191
HCT	38.51	38.46	6.4492	6.4748	0.6857
MCV	82.28	82.17	5.8371	5.8237	0.1424
MCH	28.22	28.32	2.4502	2.4170	0.0896
MCHC	34.4	34.44	1.3736	1.3594	0.8007
PLT	326.1	340.9	82.4867	97.0115	0.0190

Based on table 1, the results of the PLT test between samples transported by PTS and by courier transport had significant differences with the SD difference is 32.64 and P-value 0.0190.

Table 2. The Comparison of PTT, APTT and Potassium Measurement Results Transported between by PTS and Courier Transport

Parameter	*Mean*		*SD*		*P-value*
	Courier Transport	PTS	Courier Transport	PTS	
PPT	13.85	14.02	1.5631	1.3895	0.4243
APTT	30.79	31.08	3.2293	3.2463	0.4212
Potassium	4.407	4.537	0.6047	0.6223	0.002

PTS is a transport medium that is being developed in hospitals. PTS is a fast and efficient automatic delivery system for sending drugs, patient medical record documents, X-Ray radiology results, tissue samples, and blood samples to laboratory units, pharmacies, wards, blood banks, and emergency units. The use of PTS can reduce waiting time for laboratory results and reduce manual labor. Reducing manual work can reduce the burden on workers and improve the quality of service to patients. However, PTS has a weakness as a transport medium for blood samples. Changes in velocity and pressure in the PTS vacuum system can cause the blood sample to be sent to hemolyze. Hemolysis is the disruption of the red blood cell membrane, which causes the release of hemoglobin and other intracellular components into the surrounding fluid. In vitro hemolysis caused by the use of PTS causes changes in the quality of specimens can affect the clinical laboratory measurements such as chemicals, especially potassium, lactate dehydrogenase (LDH), hematology, and coagulation parameters[8].

A routine hematology test was carried out using the Sysmex XP 100 tool. The Sysmex XP 100 tool is a tool used for routine hematology tests using the impedance method. This research's routine hematological tests consisted of some parameters such as WBC, RBC, HB, HCT, MCV, MCH, MCHC, and PLT. In this research, there were no significant differences between the results of WBC, RBC, HB, HCT, MCV, MCH, and MCHC in samples transported between by PTS and by courier transport. However, the results of the platelet (PLT) test showed a significant difference.

The use of PTS as a specimen transport medium did not have a negative impact[10]. The research conducted by Kurniawan et al. (2015) showed that delivery with PTS at Dr. Hospital. Wahidin Sudirohusodo did not affect the results of routine hematological tests when compared to transport by hand. The small vibrations that occurred during sample delivery could cause small changes in the lysis of blood and undetectable by direct sample observation. The distance and speed of samples travel also affect the incidence of hemolysis. It affects the results of routine hematological tests [11,12]. The results of this research were also in line with the research conducted by Quellec et al. (2017). The research stated no significant difference in the results of routine hematology transported between by PTS and by courier transporter. Another study also showed no statistically significant differences for CBC, reticulocyte count, and ESR transported by both methods [7]. Wallin et al. investigated the effects of PTS and manual transportation on routine hematology, coagulation, and platelet function with PFA-100, and they did not observe any differences in the results[13]. Another study also showed there were no statistically significant differences for CBC, WBC differential count, and ESR between both methods[14].

Pre-analytic factors strongly influenced the quality of the results of the hematology test. PTS was used to reduce waiting time for laboratory results. Thus, it could reduce pre-analytic errors due to delays in the tests between sampling and blood analysis. The waiting time for the results of laboratory tests between samples sent using PTS was shorter than the delivery by hand. The advantage of using PTS is that it can directly deliver blood samples after blood collection. At the same time, delivery by hand is usually done after collecting several samples so that there is storage and delay of sample processing[15].

Based on table 1, the results of the PLT test between samples transported by PTS and by courier transport had significant differences with the SD difference of 32.64. The results of this study are in line with research conducted by Subbarayan et al., where there was a significant difference between the results of the PLT sent by the PTS by courier transport. In this research, the p-value was <0.001, with an average difference of 0.135. Samples delivered PTS showed an increase in the number of PLT yields. The increase in PLT is due to pressure from PTS during delivery which causes PLT fragmentation[16].

The coagulation parameters test conducted in this research were PPT and APTT. The tool used in the research for coagulation test is the Stago Start.This research showed no significant difference between the results of the PPT and APTT test using samples transported between by PTS and by courier transport. This research is in line with Quellec *et al.* (2017), which reported that PPT results, Fibrinogen, PLT, and Factor VIII had no significant change between the samples transported PTS by courier transport. Kocak et al. (2012) also reported no significant difference in coagulation tests such as PPT and APTT between samples transported between by PTS and by courier transport. According to a study conducted by Handawi, there was no significant difference in the impact of using PTS and manual transportation by the courier transport for coagulation test. The clinical observations were also found to be insignificant. The PTS transport system does not cause activation of clotting factors in the PPT test, so it is safe for PPT test results[16]. The study by Enko et al. also stating that pneumatic transportation did not alter platelet function[17].

In this research, there was a significant difference in the potassium test results between samples transported by PTS and by courier transport. The tool used for the potassium test in the clinical pathology laboratory of UGM academic hospital was SmartLyte Plus. The serum used for potassium testing should not be hemolyzed.

PTS can cause hemolysis because of some aspects. There is the speed of delivery, the length of the system, acceleration or sudden deceleration of the system, changes in air pressure, and changes in the direction of motion of the PTS.

Hemolysis can cause false results on inspection LDH, potassium, and AST. Hemolyzed samples cannot be used for measurements and must use new samples, causing delayed laboratory results needed for diagnosis and treatment[18]. In this research, the hemolysis index level was not observed between samples transported by PTS and by courier transport but only observed by visual.

The significant differences in potassium results are possible because hemolysis micro is not perceivable by the eye. It was occurred due to delivery speed, system length, sudden acceleration or deceleration of the system, changes in air pressure, and changes in the direction of motion of the PTS causing micro hemolysis. In several types of research, the frequency of hemolysis in samples transported by PTS was 10.9% compared to 3.3% by manual labor, failure of the PTS system could also increase the frequency of hemolysis by 55%[19].

Different results were obtained by Cui et al., who reported that there was no difference between the potassium levels transported by PTS and by courier transport. On repeated deliveries with PTS, the potassium level increased slightly. Research by Kurniawan et al. shows no significant difference between samples transported by PTS and by courier transport[9]. LDH and K levels also were not significantly different in centrifuged samples transported by PTS and human carrier, regardless of rate and distance in the previous study[20].

The weakness in this research is that it is not known how the tool vendor sets much PTS speed. This research also did not evaluate the level of hemolysis of the sample. The waiting time for the test results from taking samples until the result comes out is also not counted. The effect of PTS on blood samples was not investigated at the location of other units delivered to the laboratory, such as the Arjuna ward, Yudistira, Nakula IGD, and Yudistira ER.

CONCLUSION

There were no significant differences in the measurement result of WBC, RBC, HB, HCT, MCV, MCH, MCHC, PPT, and APTT in this research. However, it was found that there were significant differences in the results of the PLT and Potassium test using samples transported by PTS and courier transport. The research can be continued by using PTS distance variations, PTS speed variations, and other laboratory examination parameters to evaluate PTS use. Measurements of platelet and potassium are not recommended with the use of PTS as a transport medium. Evaluation of the use of PTS as a delivery medium for Packed Red Cell (PRC) and Platelet Concentrate (TC) also needs to be conducted.

ACKNOWLEDGEMENT

The researchers want to thank UGM Academic Hospital.

AUTHOR'S CONTRIBUTION STATEMENT

Tri Novitasari and Norma Agustin Palupi prepared the samples, designed the protocols, executed the protocols. Kurnia Fitriasari and Tri Novitasari wrote the manuscript. Kurnia Fitriasari and Yoki Setyaji perform data processing and reviewed the manuscript. Yoki Setyaji supervised the manuscript. All authors have read and approved the final manuscript.

FUNDING INFORMATION

research funding assistance through the RKAT Grant Fund for the 2020 Fiscal Year with the research contract number 96/H/RSA-UGM/VIII/2020.

DATA AVAILABILITY STATEMENT

The utilized data to contribute to this investigation are available from the corresponding author on reasonable request.

DISCLOSURE STATEMENT

The views and opinions expressed in this article are those of the authors and do not necessarily reflect the official policy or position of any affiliated agency of the authors. The data is the result of the author's research and has never been published in other journals.

REFERENCE

1. Shibani W., Zulkafli.M., Basuno.B. Methods of transport technologies: a review on using tube/tunnel systems. IOP Conference Series: Materials Science and Engineering. IOP Conference SeriesMaterials Science and Engineering, 2016,160(1), DOI:10.1088/1757-899X/160/1/012042
2. Simundic A.M. The effect of transport by pneumatic tube system on blood cell count, erythrocyte sedimentation, and coagulation tests. Biochem Med 2013;23:206-10. http://dx.doi.org/10.11613/BM.2013.024.
3. Koçak F.E, Mustafa Yöntem, Yücel Ö, Çilo M, Genç Ö. The effects of transport by pneumatic tube system on blood cell count, erythrocyte sedimentation and coagulation tests., Ayfer Meral. Biochemia Medica 2013;23(2):206–10. http://dx.doi.org/10.11613/BM.2013.024
4. Streichert T,Otto B, Schnabel C, Nordholt G, Haddad M, Maric M, Petersmann A, Jung R , Wagener C. Determination of Hemolysis Thresholds by the Use of Data Loggers in Pneumatic Tube Systems. American Association for Clinical Chemistry. Clinical Chemistry 57:10 1390–1397 (2011)
5. Sodi R, Darn S.M, Stott A. Pneumatic tube system induced hemolysis: assessing sample type susceptibility to hemolysis. Ann Clin Biochem 2004; 41:237-40. http://dx.doi. org/10.1258/000456304323019631.
6. Felder, RA. Preanalytical errors introduced by sample transportation systems: a means to assess them. Clin Chem 2011; 57:1349-50. http://dx.doi.org/10.1373/clinchem.2011.172452.
7. Lee AJ, Suk Suh H, Jeon CH, Kim SG. Effects of one directional pneumatic tube system on routine hematology and chemistry parameters A validation study at a tertiary care hospital. Pract Lab Med. 2017; 9: 12-1. https://dio.org/10.1016/j.plabm.2017.07.002
8. Kapoula G V., Kontou PI, Bagos PG. The Impact of Pneumatic Tube system on laboratory parameters: A systematic review and meta-analysis. Clin Chem Lab Med. 2017; 55(12): 1834-44.
9. Kurniawan, LB. , Aswin N & Uleng B. Pneumatic tube against routine blood and lactate dehydrogenase Indonesian Journal of Clinical Pathology and Medical Laboratory, 2015, 21(2), ISSN 0854-4263.
10. Sandgren, P., Larsson, S., Waisan, P., & Diedrich, B,A. 2014. The effects of pneumatic tube transport on fresh and stored platelets in additive solution. Blood Transfus 2014; 12: 85-90 DOI 10.2450/2013.0097-13
11. Evliyaoqlu O, Toprak G, Tekin A, Basarali MK, Kilinc C, --. Effect of Pneumatic Tube Delivery System Rate and Distance on Hemolysis of Blood Samples. J Clin Lab Anal. 2012; 26(2): 66–69.
12. Tiwari AK, Pandey P, Dixit S, Raina V. Speed of Sample Transportation by A Pneumatic Tube System Can InfluenceThe Degree of Hemolysis. Clin Chem Lab Med. 2011; 50(3): 471–474.
13. Wallin O, Söderberg J, Grankvist K, Jonsson PA, Hultdin J. Preanalytical eff ects of pneumatic tube transport on routine haematology, coagulation parameters, platelet function and global coagulation. Clin Chem Lab Med 2008; 46:1443-9. http://dx.doi.org/10.1515/CCLM.2008.288
14. Oliveira G. Lima, Lippi, Salvagno, Dima, Brocco, Picheth, Guidi. Management of preanalytical phase for routine hematological testing: is the pneumatic tube system a source of laboratory variability or an important facility tool? Int. J. Lab. Hematol. 36 (2014) e37–e40

15. Quellec, S., Paris, M., Nougier, C., Sobas, F., Rugeri, F., Girard, A., Bordet, J.C., Negrier, C., & Dargaud., Y. 2016. Preanalytical Effects Of Pneumatic Tube System Transport On Routine Hematology And Coagulation Test, Global Coagulation Assays And Platelet Function Assays. Elsevier. Thrombosis Research 153 (2017) 7-13.http://dx.doi.org/10.1016/j.thromres.2016.12.022
16. Subbarayan, D. The Effects of Sample Transport by Pneumatic Tube System on Routine Hematology and Coagulation Tests. NCBI. Advances in Hematology, 2018 https://doi.org/10.1155/2018/6940152.
17. Enko D., Mangge M., Munch A., Niedrist T., Mahla E., Metzler H., Pruller F. Pneumatic Tube System Transport Does Not Alter Platelet Function in Optical and Whole Blood Aggregometry, Phrotrombin Time, Activated Partial Thromboplastin Time, Platelet Count and Fibrinogen in Patients on Anti-Platelet Drug Therapy. Biochem Med (Zagreb). 2017; 27(1):217-224
18. Cakirca, G. & Erdal, H. 2017. The Effect of Pneumatic Tube System on the Hemolysis of Biochemistry Blood Samples. Journal of Emergency Nursing. 2016;43:255-8. http://dx.doi/10.1016/j.en.2016.09.007
19. Kara, H., Bayir, A., Ak, A., Degirmenci, S., Akinci, M., Agacayak, A., Marcil, E., & Azap, M. 2014. Hemolysis associated with Pneumatic Tube System Transport for Blood Samples. Pak J Med Sci: 30(1). http://dx.doi.org/10.12669/pjms.301.4228
20. O. Evliyaoğlu, G. Toprak, A. Tekin, M.K. Başarali, C. Kilinç, L. Çolpan, Effect of pneumatic tube delivery system rate and distance on hemolysis of blood specimens: pneumatic system rate and length on hemolysis, J. Clin. Lab. Anal. 26 (2012) 66–69

JTL 11 (2) December 2022
Page: 122-128
Contents list available at Jurnal Teknologi Laboratorium

JURNAL TEKNOLOGI LABORATORIUM

Journal Homepage: www.teknolabjournal.com
ISSN 2580-0191(Online) I ISSN 2338 – 5634(Print)

Original Study

Alcian blue as a kidney staining in diabetic mice: An overview after administration of Loctabacillus plantarum

Sri Sinto Dewi[*], **Suci Indah Astuti**, **Fitri Nuroini**, **Aprilia Indra Kartika**
[1] Department of Medical Laboratory Technology Universitas Muhammadiyah Semarang, Indonesia

Abstract: One of the complications of DM is damage to the kidneys, with oral administration of *L. plantarum,* it can reduce glucose levels so that it is also possible to repair damaged kidney structures. The process of repairing the kidney structure by *L plantarum* can be seen microscopically in the glomerulus with Alcian Blue staining (AB). The purpose of the study was to determine the differences in the microscopic results of DM rat kidney after treatment of *L. plantarum* with AB staining. The study sample used the kidneys of DM rats. The kidney of DM rats that were given *L. plantarum* at a dose of 1.0 ml/rat in each treatment, T1 (dose 1×1 times a day), T2 (dose 1×2 times a day), T3 (dose 1×3 times a day), then performed AB staining. The results of cytoplasmic cells in the glomerulus in negative controls/sick rat are stained dark blue/concentrated (strong intensity) with a score of 4, normal controls/healthy rat are not stained blue (negative) with a score of 1. T1 is stained light blue score of 3, T2 is stained light blue score of 3, T3 is colored pale blue score of 2. Based on these results, it was found that the color intensity of the AB kidney treatment of DM rats was the best in reducing glucose residues.

Keyword: Alcian Blue staining; *Lactobacillus plantarum; Diabetes mellitus*

INTRODUCTION

Type 1 diabetes occurs due to destruction of pancreatic cells (autoimmune reaction)[1,2]. DM caused 1.6 million deaths in 2016, while in 2015 there were 415 million of the number of adults diagnosed with DM, an increase of 4 times from 108 million in 1980, in Southeast Asia in 2014, there were 96 million adults with diabetes in 11 countries[3]. DM is a disease that affects almost all organs of the body, including the heart, blood vessels, eyes, nerves, and kidneys.

Kidneys are excretory organs with a fairly high level of vascularity (Price and Wilson, 2006). Diabetic nephropathy (ND) is a complication that occurs in 40% of all patients with type 1 DM and type 2 DM and is the main cause of kidney disease in patients receiving kidney therapy which is characterized by an increase in blood pressure resulting in decreased glomerular filtration [4].

The decrease in glomerular filtration is caused by the accumulation of blood glucose residues that accumulate in the glomerular part of the kidneys, with the accumulation of kidney residues causing the organ to be fragile so that the connective tissue that connects cells is also fragile. The conversion of carbohydrates to lipids increases the amount of intracellular glycogen through increased glycogen synthesis, or impaired glycogenolysis causes an increase in glucose, in uncontrolled hyperglycemic conditions, can trigger hyperfiltration and renal hypertrophy resulting in reduced glomerular filtration area. These changes cause impaired kidney function to become glomerulosclerosis [5].

Corresponding author.
E-mail address: sintomun@unimus.ac.id (Sri Sinto Dewi)
DOI: 10.29238/teknolabjournal.v11i2.386
Received 16 November 2022; Received in revised form 01 December 2022; Accepted 15 December 2022

Alcian Blue (AB) is a histochemical stain used to detect carbohydrate content in tissues. Administration of L. plantarum can reduce glucose levels so that it is also possible to repair damaged kidney structures in DM patients, which can be seen microscopically with AB staining [6]. L. plantarum has the potential to lower blood glucose and create hypoglycaemic conditions. The basic dye in AB is copper phthalocyanin which is soluble in water so it can be blue because of its copper content and has an affinity for acidic tissues, copper compounds carry a positive charge and are attracted to acidic carbohydrates with a negative charge to form a blue color [7].

This study aims to determine the differences in the microscopic results of the kidneys diabetic rats after treatment using Lactobacillus plantarum with AB staining. Lactobacillus can be used to lower blood sugar (Okta, 2019). One of the complications of diabetes is nephropathy. AB staining was used to determine whether the kidneys of DM rats treated with Lactobacillus had any improvement in kidney tissue. AB has an intensive color discrimination ability in kidney damage due to DM with healthy kidney conditions.

MATERIAL AND METHOD

The type of research used in this research is experimental. The research design was True experimental design with Post Test-Only Control Group Design method [6]. This study used 25 male Wistar rats aged 12-16 weeks with an average body weight of 150-200 g which were divided into 5 groups and each group contained 5 rats. Group I: No treatment/healthy rats (negative control), Group II: alloxan induced/DM rats (positive control), Group III (T1): DM rats and given *Lactobacillus plantarum* suspension at a doses of 1.0 ml/rat (dose 1 × 1 time a day), Group IV (T2): doses of 1.0 ml/rat (dose 1 × 2 times a day), Group V (T3): doses of 1.0 ml/rat (1×3 dose) times a day). Induction of alloxan monohydrate was performed on test animals intraperitoneally at a dose of 150 mg/kg BW after the adaptation process for 7 days in the laboratory. Diabetic rats fasting blood glucose levels ± 200 mg/dL. Rats that had diabetes were given *Lactobacillus plantarum* isolate from breast milk according to the dose that had been set in each group. Treatment was done orally for 7 days with an interval of 5 hours for *Lactobacillus plantarum*. During the treatment the rats were fed and watered ad libitum. The sample in this study amounted to 25 kidney preparations of DM rats.

The materials (reagents) used in the processing and staining were 9 rat kidneys, 10% BNF, AB staining, Nuclear Fast Red, Alcohol (70%, 80%, 96% and 100%), xylol, paraffin. Tissue samples were fixed with Buffered Neutral Formaldehyde (BNF), 10% BNF volume. The sample was removed from the fixation solution and then the tissue was cut with a size of 1x1 cm. The sample is put into a tissue processor machine, immersed in a tank containing 10% BNF for 2 hours, followed by immersion in a tank containing low to high concentration alcohol, starting from 70%, 80%, 96% (for 1 hour 30 minutes each steps) and absolute alcohol I, II and III for 1 hour each steps. The tissue immersed in a tank containing a solution of xylol I and xylol II for 1 h and 30 min each steps, then the tank was immersed in a tank containing a solution of paraffin I and II for 2 h each steps. The tissue is removed from the tissue processor and then transferred to a microwave oven, the paraffin used for blocking the melting point is the same as the paraffin used for paraffin infiltration. This blocking process is carried out by pouring a small amount of paraffin liquid at a temperature of 60-65°C into the mold. As soon as the tissue is inserted using heated tweezers (so that the paraffin is not frozen) and positioned in the mold, the liquid paraffin is then poured back to cover the entire mold and the mold is left to stand until the paraffin solidifies.

The solid block preparations were cut with a rotary microtome to make slide preparations such as ribbons measuring 3-4 µm. The ribbon formed was placed in a water bath filled with warm water with a temperature of 52° C. The slide preparations were observed under a microscope, if they were good, they were

continued to be dried on a hotplate and ready for staining (Anatomical Pathology Laboratory of RSI Sultan Agung).

The initial stage of staining is by removing paraffin from the preparation (deparaffinization) by immersing it in a solution of xylol I, xylol II for 2-5 min each steps, then giving water to the tissue (rehydration) using an alcohol series graded from 100%, 95% and 70 % each steps for 2-5 min, then washing with distilled water to remove residual alcohol for 2-5 min. The preparations were stained with AB pH 2.5 staining for 30 min, after a bluish color change (positive reaction) occurred, then washed with running water for 5 minutes, then rinsed with distilled water, then dripped with contrast stain (counterstain) using Nuclear Fast Red, then wait for 5 minutes, while looking at it with a microscope. The preparations were washed with distilled water for 2-5 min until clean, then dehydrated from the preparation with 70%, 95%, and 100% alcohol. followed by the clearing process using xylol I and xylol II each for 3 min until they were clear (Anatomical Pathology Laboratory, Moewardi Hospital).

The readings of the preparations were carried out by Anatomical Pathology Specialist. Tissue was observed on microscope with a magnification of 400x in the cytoplasmic cells contained in the glomerulus as many as 50 glomeruli according to the criteria, then the results of the assessment (scoring) were entered into the table of reading results. Data was collected from the reading of kidney tissue preparations with AB staining, all data obtained from the results of the assessment and analyzed by the Kruskal Wallis test.

RESULTS AND DISCUSSION

The higher intensity doses treatment of *Lactobacillus plantarum* in DM rats, the lower level of blue color in the kidney glomeruli (Table 1). AC staining produces a blue color which indicates the sugar content in the kidneys. Giving *Lactobacillus plantarum* can reduce sugar in the kidneys of DM rats that it can reduce nephropathy. Kidney preparations of DM rats were stained blue using AB staining on the mucin (nephron coating). Mucins are part of epithelial cells composed of glycoproteins (Figure 1a). Mucin is composed of protein in the core and surrounded by carbohydrate chains (80%). AB staining is a large planar phthalocyanine with a copper atom in the center. AB staining contains four basic isothiouronium groups that carry a positive charge. The positive charge exerted by these groups results in the attraction of the AB staining dye molecule to the anionic site in the mucin molecule. AB staining does not color the neutral mucin.

Table 1. Results of Average Color Intensity in Kidneys of DM Rats

Treatment groups	Mean score
Negative control	4
Normal control	1
T1	3
T2	3
T3	2

The use of AB staining to distinguish the sugar content in the renal glomerulus because the reaction of the AB staining solution at pH 2.5 can stain all mucins that are acidic or carboxylated or sulfated. Sugar in the kidney glomerulus will ionize at pH 2.5 to produce anionic groups (COO, SO3) so that a blue color is formed. Kidney preparations of DM rats treated with *Lactobacillus plantarum* (Figure 1e) had the same color as the kidneys of normal rats (Figure 1b). The kidneys of DM (T3) rats decreased the sugar content in the kidneys so they were not stained blue by AB staining. The more *Lactobacillus plantarum* was given, the less blue color formed on the kidney preparations, indicating that the sugar content was getting lower (Figure 1 c, d, e). The kidneys of DM treatment 1 rats obtained moderate intensity results with a score of 3 on the preparations. Kidney

preparations in DM treatment 1 mice in the glomerulus there was a lot of accumulation of glucose residues so that the cytoplasmic cells reacted a lot by AB stained light blue. The moderate intensity in treatment 1 was in accordance with the[8] variations of intensity in the AB staining caused by the content of a lot or less accumulation of glucose residues in the glomerulus, which was seen in the cytoplasmic cells in the glomerulus[9]. If the intensity is weak, the cytoplasm of the cell will be colored pale blue.

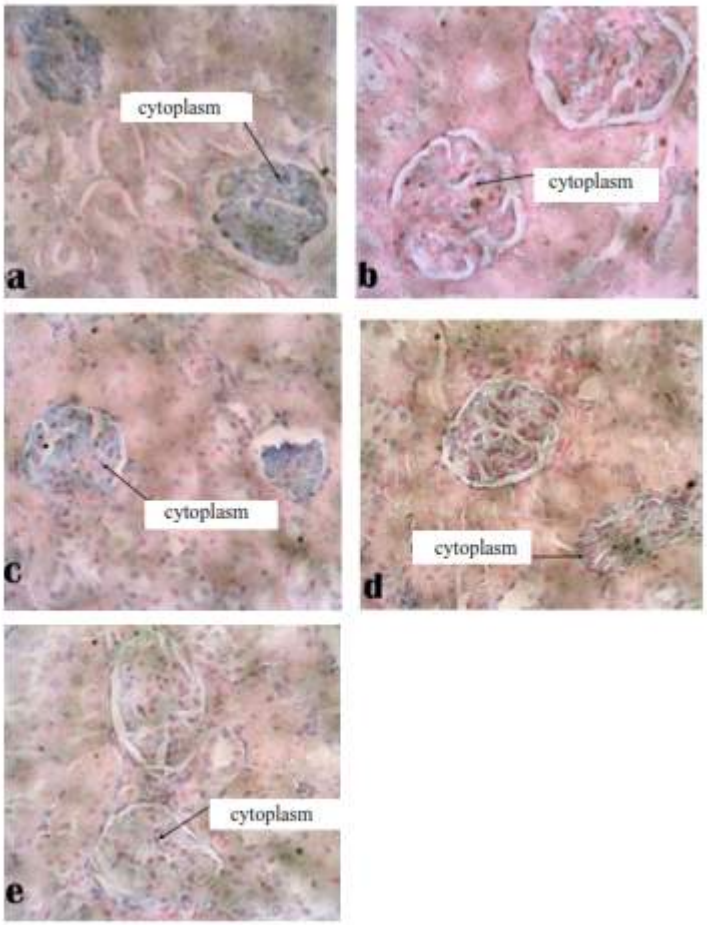

Figure 1. Microscopic results of AB staining at 400x magnification in the kidneys of DM rats at the glomerulus (a) Negative control; (b) Normal control; (c) Treatment 1; (d) Treatment 2; (e) Treatment 3

Treatment 2 obtained moderate intensity results with a score of 3, in the glomerulus there was a lot of accumulation of glucose residues so that the cytoplasmic cells reacted a lot by AB colored light blue. Treatment 3 obtained weak intensity results with a score of 2 on the preparations, in the glomerulus there was a slight accumulation of glucose residues so that the cytoplasmic cells reacted very little by AB stained with pale blue and light blue. Differences in color intensity that vary in the cytoplasm indicate differences in the amount of glucose in the glomerulus[10]. Carbohydrates are scattered in body tissues, these compounds are mainly found on the cell surface, in the cytoplasm (depending on the functional activity of the cell), AB staining pH 2.5 is used to detect mucopolysaccharides that are sour.

The microscopic results of the kidneys of DM with AB mice in this study showed that the treatment groups T1, T2, T3 showed a decrease in blood glucose levels after being given *L. plantarum* isolate from breast milk according to the dose of each treatment group but still above normal. Treatment using *L. plantarum* after the rats had diabetes had a significant effect on the average decrease in the rats' blood glucose levels[6]. *L. plantarum* administered to experimental animals was able

to improve HbA1C by decreasing glucose levels in prediabetic subjects [11]. *L. plantarum* could regulate glucose metabolism in the liver, protect islet beta cells, and restore gut microbiota[12,13,14]. *L. plantarum* has potential as an antihyperglycemic agent. *L. plantarum* recommended for food applications and pharmaceuticals products to prevent diabetes[15,16] because *L. plantarum* has the ability to inhibit the enzyme alpha glucosidase. The alpha glucosidase enzyme is an enzyme that plays a role in the breakdown of carbohydrates into glucose in the digestive tract[17]. The breakdown of carbohydrates into glucose results in higher blood glucose levels in diabetics so that the work of this alpha glucosidase enzyme in the intestine must be inhibited [13].

All three doses (T1,T2, and T3) had an equivalent glucose-lowering effect. The mean score was found to be of weak intensity at T3, so that the dose given 3 times a day is a good dose in reducing blood glucose efficiently. Lactobacillus plantarum identify potent anti-obesogenic and diabetic probiotics. Live probiotic orally in DM mice strongly attenuated weight gain and insulin resistance [18]. Administration of Lactobacillus (LAB) to determine the antidiabetic effect in addition to increasing insulin resistance, can also increase the level of expression of glucose transporter 4 (Glut4) and adiponectin genes in epididymic mice tissue. Glut4 and adiponectin are associated with increased insulin action. Upregulation of Glu4 and adiponectin expression is evidence that LAB can be used as an antidiabetic. Long-term research on LAB administration can restore the expression of genes associated with sugar metabolism that can downregulate obesity[12,19,20]. LAB is able to improve the composition of the microbiota in the gut. Lactobacillus given to mice can reduce blood sugar and body weight. Giving Lactobacillus is able to change the composition of the gut microbiota by suppressing opportunistic bacteria that can cause metabolic diseases[21].

CONCLUSION

Microscopic AB staining results based on the mean score on negative controls/sick mice stained dark blue/solid (strong intensity) with a score of 4, normal controls/healthy mice not stained blue (negative) with a score of 1, treatment 1 stained with light blue (medium intensity) with a score of 3, treatment 2 was stained light blue (medium intensity) with a score of 3, treatment 3 was stained pale blue (weak intensity) with a score of 2. Better microscopic results based on the intensity of the color binding to glucose residues were found in treatment 3 with weak intensity.

ACKNOWLEDGEMENT

We would like to thank the Department of Medical Laboratory Technology D4, the Molecular Biology laboratory team, and the UNIMUS Research and Community Service Institute.

AUTHOR'S CONTRIBUTION STATEMENT

Sri Sinto Dewi (construction of research ideas, design the research, analyzed data), Suci Indah Astuti (conducting lab-scale research, treating rats, making preparation for kidney tissue). Fitri Nuroini (contributing writing the manuscript), Aprilia Indra Kartika (contributing writing the manuscript).

FUNDING INFORMATION

-

DATA AVAILABILITY STATEMENT

The utilized data to contribute to this investigation are available from the corresponding author on reasonable request.

DISCLOSURE STATEMENT

The views and opinions expressed in this article are those of the authors and do not necessarily reflect the official policy or position of any affiliated agency of the authors. The data is the result of the author's research and has never been published in other journals.

REFERENCE

1. Dav G, Santilli F, Patrono C. Nutraceuticals in Diabetes and Metabolic Syndrome Diabetes Mellitus and Metabolic Syndrome : Role of Inflammation and Oxidative Stress. *Cardiovasc Ther*. 2010;28:216-226. doi:10.1111/j.1755-5922.2010.00179.x
2. Shin J, Lee J, Lim S, et al. Metabolic syndrome as a predictor of type 2 diabetes , and its clinical interpretations and usefulness. *J Diabetes Investig*. 2013;4(4). doi:10.1111/jdi.12075
3. CDC. *National Diabetes Statistics Report*.; 2020.
4. Sartika F, Purbayanti D, Safitri D. Gambaran laju filtrasi glomerulus pada penderita diabetes mellitus tipe 2 di RSUD DR. Doris Sylvanus Palangkaraya. *J Surya Med*. 2018;3(2):13-21.
5. Sari N, Hisyam B. Hubungan antara diabetes melitus tipe II dengan kejadian gagal ginjal kronik di Rumah Sakit PKU Muhammadiyah Yogyakarta periode Januari 2011-Oktober 2012. *JKKI*. 2014;6(1):11-18.
6. Kartikasari O, Astuti AD, Berkah M, Wabula M, Dewi SS. Aktivitas Lactobacillus plantarum Isolat Air Susu Ibu pada Tikus Galur Wistar Diabetes Mellitus. 2019;10(November):422-429.
7. Doan C. Special Stains-Which OOne, Why and HOw? Part 1: Mucins and Glycogen _ Leica Biosystems. https://www.leicabiosystems.com/knowledge-pathway/special-stains-which-one-why-and-how/.
8. Wahyuni S, Zuchri, Hamny, Jalaluddin M, Adnyane IKM. Studi Histokimia Sebaran Karbohidrat Usus Biawak Air (Varanus salvator). *Acta Vet Indones*. 2015;3(2):77-84.
9. Li X, Wang N, Yin B, et al. Effects of Lactobacillus plantarum CCFM0236 on hyperglycaemia and insulin resistance in high-fat and streptozotocin-induced type 2 diabetic mice. *J Appl Microbiol*. 2016;121:1727-1736. doi:10.1111/jam.13276
10. Teme ABY, Selan YN, Amalo FA. Gambaran anatomi dan histologi esofagus dan proventrikulus pada ayam hutan merah (Gallus gallus) asal Pulau Timor. *J Vet Nusant*. 2019;2(2):85-103.
11. Oh M, Jang H, Lee S, et al. Lactobacillus plantarum HAC01 Supplementation Improves Glycemic Control in Prediabetic Subjects: A Randomized, Double-Blind, Placebo-Controlled Trial. *Nutrients*. 2021;13:1-10.
12. Lee Y, Lee D, Park G, et al. Lactobacillus plantarum HAC01 ameliorates type 2 diabetes in high-fat diet and streptozotocin-induced diabetic mice in association with modulating the gut microbiota. *food func*. 2021;12:6363-6373. doi:10.1039/d1fo00698c
13. Panwar H, Calderwood D, Grant IR, Grover S, Green BD. Lactobacillus strains isolated from infant faeces possess potent inhibitory activity against intestinal alpha- and beta-glucosidases suggesting anti- diabetic potential. *Eur J Nutr*. 2014. doi:10.1007/s00394-013-0649-9
14. Sefidgari-abrasi S, Karimi P, Roshangar L, et al. Lactobacillus plantarum And Inulin : Therapeutic Agents to Enhance Cardiac Ob Receptor Expression and Suppress Cardiac Apoptosis in Type 2 Diabetic Rats. 2020:1-14.
15. Zhong H, Zhang Y, Zhao M, et al. Screening of novel ptential antidiabetic

Lactobacillus plantarum strains based on in vitro and in vivo investigations. *LWT - Food Sci Technol*. 2020. doi:10.1016/j.lwt.2020.110526
16. Liu W, Yang M, Wu Y, Chen P, Hsu C, Chen L. Lactobacillus plantarum reverse diabetes- induced Fmo3 and ICAM expression in mice through enteric dysbiosis-related c-Jun NH2- terminal kinase pathways. *PLoS One*. 2018:1-23.
17. Wardati Y, Deswati DA, Idayati. Uji aktivitas antidiabetes melitus tipe II infus buah kesemek (Diospyros kaki Linn.) terhadap tikus jantan putih galur wistar. *Kartika J Ilm Farm*. 2014;2(2):39-44.
18. Lee E, Jung S-R, Lee S-Y, Lee N-K, Paik H-D, Lim S. Lactobacillus plantarum Strain Ln4 Attenuates Diet-Induced Obesity, Insulin Resistance, and Changes in Hepatic mRNA Levels Associated with Glucose and Lipid Metabolism. *Nutrients*. 2018;10(643). doi:10.3390/nu10050643
19. Youn HS, Kim J, Lee S, et al. Lactobacillus plantarum Reduces Low-Grade In fl ammation and Glucose Levels in a Mouse Model of Chronic Stress and Diabetes. *Infect Immun*. 2021;89(8):615--620.
20. Meng X, Qian Y, Kang LJJ. Effects of Lactobacillus plantarum SCS2 on blood glucose level in hyperglycemia mice model. *Appl Biol Chem*. 2016;59(1):143-150. doi:10.1007/s13765-015-0135-6
21. Gulnaz A, Nadeem J, Han J, et al. Lactobacillus Sps in Reducing the Risk of Diabetes in High-Fat Diet-Induced Diabetic Mice by Modulating the Gut Microbiome and Inhibiting Key Digestive Enzymes Associated with Diabetes. *Biology (Basel)*. 2021;10(348):1-20.

JTL 11 (2) December 2022
Page: 129-139
Contents list available at Jurnal Teknologi Laboratorium

JURNAL TEKNOLOGI LABORATORIUM

Journal Homepage: www.teknolabjournal.com
ISSN 2580-0191(Online) I ISSN 2338 – 5634(Print)

Original Study

Potential of natural antioxidant compound in Cymbopogon nardus as anti-cancer drug via HSP-70 inhibitor: A bioinformatics approach

Rofiatun Solekha[1], Putri Ayu Ika Setiyowati[1], Eka Febrianti Wulandari[2], Lilis Maghfuroh[2]

[1] Department of Biology, Faculty of Science, Technology, and Education, Universitas Muhammadiyah Lamongan, Indonesia
[2] Department of Nursing, Faculty of Health Science, Universitas Muhammadiyah Lamongan, Indonesia

Abstract: Citronella grass (*Cymbopogon nardus)* is a plant containing many metabolite compounds which prevent and treat various diseases, one of which is cancer. Antioxidant compounds found in citronella have been shown to improve the immune system by increasing cytokines. The activity of changing homeostasis generates free radicals. Free radicals causing protein damage so that Heat Shock Protein-70 (HSP70) is overexpressed. HSP70 has a role as a chaperon. Mutations in the anti-apoptotic protein HSP70 are one of the causes of cancer. This current research aims to determine the potential of compounds present in the citronella plant stem as anti-cancer through inhibition of HSP-70. The method was a bioinformatics approach, namely the in-silico method which provided a simulation of binding protein ligands to HSP-70 as inhibitor mechanism. The results of this study indicated that there was a potential for citronella compounds, namely spathulenol binding to HSP-70. Spathulenol compounds interact with Hsp70 via the positions Thr204, Gly12, Gly203, Thr14, Lys71, Asp10, Val369, Asp199, Val337, Gly338, Asp366, Gly339, Pro365, Glys201, & Glys202 with Van der Waals bonds and hydrogen bonds on Thr13. In the complex, there was one unfavorable bond formed on the O atom of the query ligand. From the results above, it can be concluded that the Spathulenol compound is predicted to act as an inhibitor of Hsp70 protein activity because it inhibits the binding site of the native ligand on Hsp70. The stability of the binding interaction produced by Spathulenol allows a response to Hsp70 inhibitor activity. By inhibiting the activity of Hsp70 inhibitors, it is possible to inhibit the formation and proliferation of cancer cells.

Keyword: *Cymbopogon nardus; HSP70; cancer cells*

INTRODUCTION

Cancer is a complex disease that involves many types of biological interactions at various scales, physical, temporal and biological[1]. Cancer develops as a function of various biological interactions and events both in the domains between individual genes and proteins, and at the cellular and physiological levels between functionally diverse somatic cells[2]. At the genetic level, the genetic code interacts synergistically to achieve homeostasis. The genetic code is expressed into hundreds to thousands of proteins in cells[3].

Heat Shock Protein-70 (HSP-70) is a protein which plays a role in maintaining cell homeostasis and is also a molecular chaperone that maintains

Corresponding author.
E-mail address: lilisahza99@gmail.com (Lilis Maghfuroh)
DOI: 10.29238/teknolabjournal.v11i2.372
Received 10 August 2022; Received in revised form 12 August 2022; Accepted 14 November 2022

stability of protein levels, interactions between proteins and inhibit protein aggregation[4]. The presence of cancer is the result of an unbalanced biochemical reaction in the cells. In cancer patients, HSP70 is overexpressed so that HSP is used as an important prognostic factor in malignant diseases such as cancer[5]. Overexpression of HSP70 can inhibit apoptosis and prevent caspase activation in various cellular models through various cellular stressors[6], including accumulation of misfolded proteins, reactive oxygen species (ROS) or DNA damage[7].

Various ways of drug agents are used as anti-cancer in various fields, both in the pharmaceutical field and in the use of natural ingredients from plants. Research on traditional medicine has begun to develop, one of which is research on the citronella plant (Cymbopogon nardus L. Rendle.). Citronella grass is efficacious as a traditional medicine because it contains active compounds such as saponins, flavonoids, polyphenols, alkaloids, and essential oils (Rofi, 2021). These compounds function as antiprotozoal, anti-inflammatory, antimicrobial, antibacterial, anti-diabetic, anticholinesterase, molluscicide, and antifungal. Citronella grass is also easily cultivated and accessed by many people so it is flexible to be used as medicine[11]. Several studies have shown that compounds present in citronella have the potential to improve the immune system as protection from Sars Cov-1912. The geraniol compound of citronella essential oil also has the potential for anti-cancer chemoprevention, namely breast cancer MCF-713.

The potential of citronella compounds as anti-cancer through the inhibition of HSP70 can be seen through a mechanical model-based bioinformatics approach that explains the biochemical process using the in-silico method[14]. In silico is used to describe experiments performed with the aid of a computer. The in-silico test can be used to determine the interaction between a compound and the target molecule, one of which is the receptor[15]. Based on the information above, a bioinformatics technology is needed that shows the biochemical reaction of HSP70 as a target molecule with compounds from citronella.

MATERIAL AND METHOD

The PuChem database (https://pubchem.ncbi.nlm.nih.gov/) was used in this study for the preparation of chemical compounds samples from the results of GCMS analysis of citronella grass stems. Thirty-four compounds were successfully obtained from the database with PubChem Compound ID (CID) information. consisting of CID 7503, CID 460, CID 10329, CID 332, CID 7041, CID 1715136, CID 1146, CID 6432308, CID 92138, CID 92231, CID 95997 CID 12301996, CID 226486, CID 518516, CID 3084311, CID 521216, CID 5974, CID 592628, CID 9983, CID 26397, CID 527256, CID 75303, CID 594234, CID 554084, CID 12366, CID 565584, CID 606866, CID 548034, CID 543959, CID 15256789, CID 5363269, CID 7678, CID 123409, & CID 8791, other information was 3D structure with file structure data format (sdf). The process of energy minimization and conversion of sdf files to protein databank format (pdb) was carried out on all samples of compounds through OpeBabel 2.4.1 software. Minimization of energy in the compound aims to increase the flexibility of the molecule through positive bond energy. The 3D structure of the target protein, HSP70 (RCSB ID: 4IO8), was obtained from the RCSB PDB database (https://www.rcsb.org/), protein sterilization was carried out using PyMol 2.5 version software by removing water molecules and contaminant ligands [16,17].

The ability of inhibitor activity by query compounds from citronella grass stems on HSP70 in this study was predicted through molecular docking simulations. Molecular docking is used to measure the specific activity ability of the ligand and the pattern of molecular interactions through the value of binding affinity[18]. This study used PyRx 0.9.9 version software to identify the ability of inhibitor activity on Hsp70 & TNFR1 and activator on R by spathulenol compounds from citronella grass stems through molecular docking simulation with grid position Center (Å) X: 11,444 Y: -3.991 Z: 15,181 Dimension (Å) X: 36,592 Y: 38.011 Z:

35,415, Center (Å) X:6.891 Y: 30,858 Z:11,548 Dimension (Å) X:34,254 Y:29,278 Z:29,846, & Center (Å) X: 19,813 Y: 8.863 Z: 38,209 Dimension (Å) X: 39,358 Y: 37,212 Z: 53,400. Visualization of the 3D structure of the protein-ligand complex was carried out using PyMol 2.5 version software, the structure was displayed with cartoons, transparent surfaces, and selection coloring[19].

Identification of molecular interactions of compounds from citronella grass stems with all target proteins in this study were identified through the Discovery Studio 2016 version of the software. Types of chemical bond interactions such as Van der Waals, hydrogen, hydrophobic, electrostatic, and pi are present in molecular complexes. The interaction formed is a weak bond that plays a role in triggering the activity of the target protein[20].

The validation of the docking results was carried out through molecular dynamic (MD) simulation which aimed to identify the flexibility of ligand binding in the protein domain. The flexibility of the bond was shown by the RMSF plot on the CABS-flex 2.0ver server (http://biocomp.chem.uw.edu.pl/CABSflex2). Parameters used for MD simulation are RNG seed, temperature, side-chain, C-alpha, rigidity, & trajectory. A stable binding interaction on the ligand-protein complex should have an RMSF value <4Å[21].

The spatulenol compound from citronella grass stem extract with the strongest binding activity on Hsp70 was tested with the SwissADME server (http://www.swissadme.ch/) for the prediction of adsorption and distribution via Canonical SMILE. The prediction aims to identify physicochemical properties, bioavailability score, and prediction as a drug-like molecule using various methods such as Lipinski, Ghose, Egan, and Muegge[22]. Validation of inhibitory properties on specific compounds was further identified through the Molinspiration Chemoinformatics server (https://www.molinspiration.com/cgi-bin/properties), predictions with positive results as inhibitors on query compounds were shown through more positive values on probability scores[23].

RESULTS AND DISCUSSION

The simulation of the interaction of the ligand binding with the target specific domain in this study was carried out using the blind docking method. Blind docking aims to identify the ability of ligand binding activity on a specific domain by ignoring the functional position on the protein[24]. The most negative binding affinity for the ligand is used as a determinant of the ability of the ligand to affect the activity of the target protein. Binding affinity is the Gibbs energy formed when ligands and proteins interact and work according to the laws of Thermodynamics[25,26]. A negative value of binding affinity determines the binding activity, a more negative value indicates the ligand bond with the strongest bond. If the binding affinity value of the candidate compound is more negative, it is predicted to have activity on the target protein which refers to the response of inhibitors and activators[27,28].

The docking simulation in this study aimed to determine the inhibitory activity of compounds from citronella grass stem extract on Hsp70 via grid docking (Center (Å) X: 11,444 Y: -3.991 Z: 15,181 Dimension (Å) X: 36,592 Y: 38,011 Z: 35,415). The compounds from the citronella grass stem extract with the most negative binding affinity values for each target protein were Spathulenol (-7.9 kcal/mol), 10-epi-.gamma.-eudesmol (-8.3 kcal/mol), and Torreyol (-6.3) (Table 1). The compound with the most negative binding affinity value was predicted to trigger stronger activity on Hsp70 than other compounds. Visualization of the Spathulenol_Hsp70 molecular complex was carried out through rigid and transparent surfaces, cartoons, sticks structures with colored selection (Figure 1).

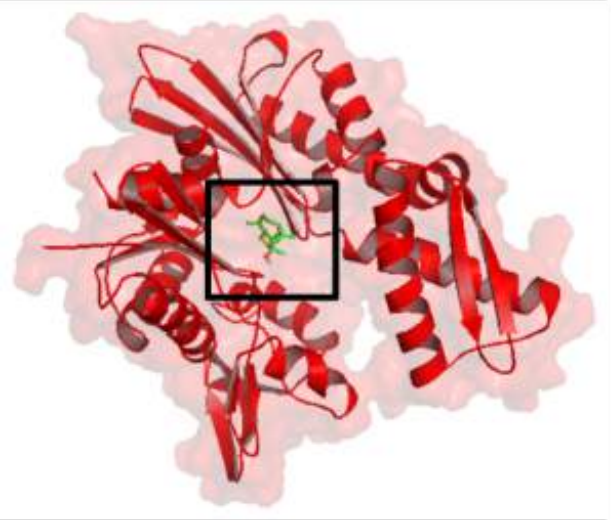

Figure 1. Structural visualization from the docking simulation Spathulenol_Hsp70.

The protein-ligand molecular complexes were formed by specific types of weak bonds that play a role in triggering the activation of specific biological responses such as inhibitory activities. The activity of the ligand as a protein activator was shown by binding to the cofactor region29. Hydrogen bonds and Van der Walls play a role in the stability of drug molecules to trigger the inhibitory activity of the target protein30. The unfavourable bond interactions formed in the molecular complex must be below three in order for the complex to remain stable31. Spathulenol compounds interacted with Hsp70 via the positions Thr204, Gly12, Gly203, Thr14, Lys71, Asp10, Val369, Asp199, Val337, Gly338, Asp366, Gly339, Pro365, Glys201, & Glys202 with Van der Waals bonds and hydrogen bonds on Thr13. In the complex, there is one unfavourable bond formed on the O atom of the query ligand (Figure 2).

Hsp70 activation was carried out by acetylation at the active site with lysine residues by the native ligand HOPX to produce a biological response to Hsp7032. Spathulenol compound was predicted to act as an inhibitor of Hsp70 protein activity because it inhibits the binding site of the native ligand on Hsp70.

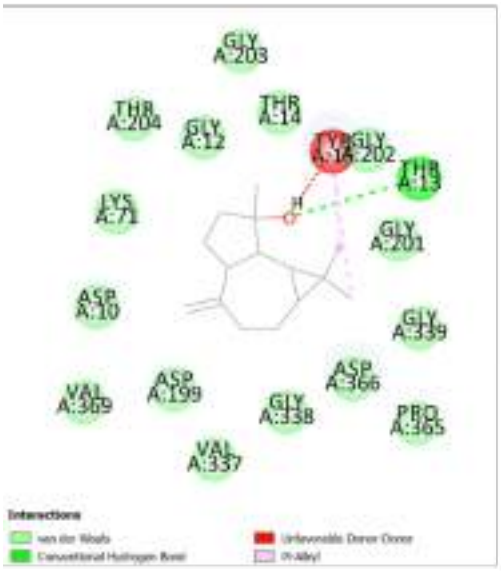

Figure 2. The ligand-protein interaction Spathulenol_Hsp70.

Table 1. The binding affinity from molecular docking simulation

No	Compound	PubChem CID	Binding Affinity (kcal/mol)
			Hsp70
1	Benzyl chloride	7503	-4.3
2	Phenol, 2-methoxy- (CAS)	460	-5.2
3	2,3-Dihydro-Benzofuran	10329	-5.2
4	2-Methoxy-4-vinylphenol	332	-5.5
5	Phenol, 2,6-dimethoxy- (CAS)	7041	-5.3
6	Phenol, 2-methoxy-4-(1-propenyl)-, (E)- (CAS)	1715136	-6.9
7	Methanamine, N,N-dimethyl- (CAS)	1146	-2.3
8	Naphthalene, 1,2,3,4,4A,5,6,8A-Octahydro-7-	6432308	-7.0
9	Elemol	92138	-6.4
10	Spathulenol	92231	-7.9
11	3',5'-Dimethoxyacetophenone	95997	-6.1
12	endo-1-bourbonanol	12301996	-5.7
13	Phenol, 2,6-dimethoxy-4-(2-propenyl)-	226486	-6.2
14	10-epi-.gamma.-eudesmol	518516	-7.6
15	Torreyol	3084311	-7.1
16	2-Naphthalenemethanol, 1,2,3,4,4a,5,6,8a-octahydro-	521216	-5.9
17	1-Hexadecanaminium, N,N,N-trimethyl-, bromide	2681	-5.5
18	1-Cyclohexanone, 2-methyl-2-(3-methyl-2-oxobutyl)	592628	-6.1
19	Phenol, 4-(3-hydroxy-1-propenyl)-2-methoxy- (CAS)	9983	-6.1
20	Heptadecanoic acid, ethyl ester (CAS)	26397	-5.4
21	Rosifoliol	527256	-7.7
22	1-Naphthalenamine, 4-bromo- (CAS)	75303	-6.3
23	6-Isopropenyl-4,8a-dimethyl-1,2,3,5,6,7,8,8a-octahydro-	594234	-7.3
24	Cyclopropanebutanoic acid, 2-[[2-[[2-[(2-pentylcyclopropyl)	554084	-6.3
25	Hexadecanoic acid, ethyl ester (CAS)	12366	-5.5
26	Longifolenaldehyde	565584	-7.1
27	4-(2,6,6-Trimethyl-cyclohex-1-enyl)-butyric acid	606866	-7.0
28	2-Methyl-5-(2,6,6-trimethyl-cyclohex-1-enyl)-pentane-2,3-diol	548034	-7.2
29	2H-Benzocyclohepten-2-one, decahydro-9a-methyl-, trans- (CAS)	543959	-7.1
30	1-Allyl-3-methylcyclohex-2-enol	15256789	-5.6
31	Ethyl Oleate	5363269	-5.6
32	1-Phenyl-2-propanone	7678	-5.3
33	Hexadecanoic acid, 2-hydroxy-1-(hydroxymethyl)ethyl ester (CAS)	123409	-5.4
34	Dodecanoic acid, phenylmethyl ester (CAS)	8791	-5.8

MD simulation was carried out to validate the docking results in this study. MD aimed to identify the stability of the protein-ligand molecular complex with reference to the RMSF33 value. The results of the MD analysis showed the stability of the RMSF in the complex produced by the compound Spathulenol_Hsp70 (Figure 3). The following is a link to the results of the molecular dynamic simulation from this study (http://212.87.3.12/CABSflex2/job/eb5d17d97cae2c3/) for Spathulenol_Hsp70. The stability of the binding interaction produced by Spathulenol allowed a response to Hsp70 inhibitor activity.

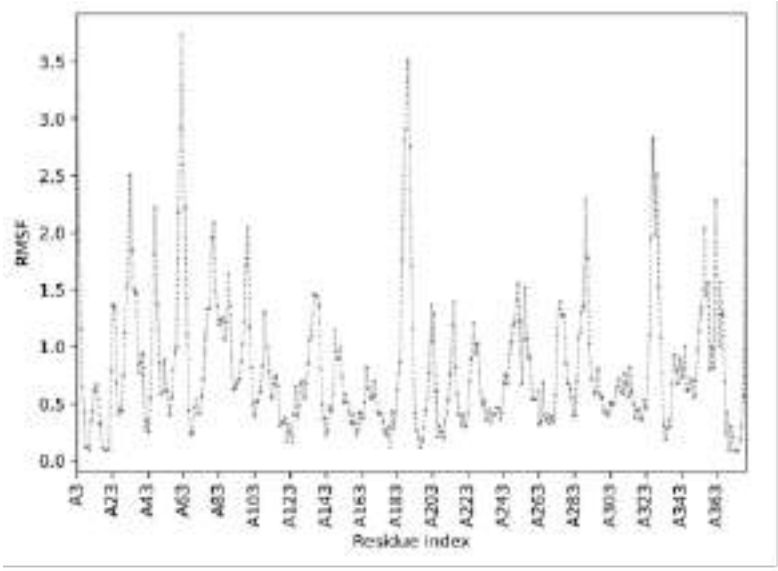

Figure 3. RMSF and residue index from MD simulation. (A) Spathulenol_Hsp70 (B) 10-epi.gamma.-eudesmol_AR (C) Torreyol_TNFR1.

Drug-like molecule analysis was used to determine the similarity of a candidate compound with a drug molecule. Similarity referred to the physicochemical properties through specific parameters such as molecular mass, high lipophilicity, hydrogen donor & acceptor bonds, and molar refractivity34. Drug-like molecule test can be done using Lipinski, Ghose, Veber, Egan, Muege, and bioavailability methods. These methods explain that candidate compounds are predicted to have similarities if they meet at least two rules and the bioavailability score of a drug candidate must be > 0.17 in order to trigger increased circulation drug molecule35. Physicochemical properties and solubility are important for early prediction of the absorption of drug candidate molecules, then prediction of bioactivity is carried out by referring to positive results as inhibitors on the query compound indicated by a more positive value on the probability score[36]. The results of the bioactivity analysis showed that Spathulenol compounds had bioactivity properties as inhibitors, the candidate compounds were drug-like and soluble (Table 2).

Heat shock protein 70 (Hsp70), one of the major stress-inducible members of the 70 kDa stress protein family (HSP70) whose expression is mainly regulated by Heat Shock Factor 1 (HSF-1) consists of at least 8 homologous members, exerts tumorigenic functions by sustaining proliferative cell signalling, increasing invasive and metastatic activity and migration and by preventing apoptotic signalling [37,38]. Hsp70 is frequently constitutively overexpressed in the cytosol and present on the plasma membrane of many different tumour types[39,40]. To promote cancer cell survival, tumorigenicity and anti-apoptotic activities such as interfering with the apoptosis signal regulating kinase 1 (ASK1) and the co-chaperone CHIP[41], blocking BAX translocation to the mitochondria[42] or by interfering with lysosomal membranes and thereby inhibiting their permeabilization[43]. Apart from its intracellular localization, Hsp70 could be transported to and anchored on the plasma membrane of tumor, but not normal cells, via tumor-specific lipid vesicular transport which was not completely unravelled[44]. Membrane Hsp70-positive tumors had been shown to actively release Hsp70 in exosomes[45] that could fuse with the plasma membrane. Since normal cells did not present Hsp70 on their cell surfaces, mHsp70 served as a tumor-specific targeting structure for in vivo imaging[46].

Table 2. Bioactivity analysis result of Spathulenol

Compounds	Activity Prediction	Physicochemical Properties	Water Solubility	Druglikeness
Spathulenol	GPCR ligand: -0.42 Ion channel modulator: -0.28 Kinase inhibitor: -0.68 Protease inhibitor: -0.36 Enzyme inhibitor: 0.06 Probable: Inhibitor	Formula: $C_{15}H_{24}O$ Weight: 220.35 g/mol Num. heavy atoms: 16 Num. arom. heavy atoms: 0 Fraction Csp3: 0.87 Num. rotatable bonds: 0 Num. H-bond acceptors: 1 Num. H-bond donors: 1 Molar Refractivity: 68.34 TPSA: 20.23 Å²	Log S (ESOL): -3.17 Class: Soluble Log S (Ali): -3.20 Class: Soluble Log S (SILICOS-IT): -2.96 Class: Soluble	Lipinski: Yes Ghose: Yes Veber: Yes Egan: Yes Muegge: No Bioavailability: 0.55 Probable: Drug-like Molecule

CONCLUSION

Compounds from citronella grass stem extract consisting of Spathulenol have the potential to inhibit the activity of Hsp70 protein. The candidate compound is proven by strong bonds through a more negative binding affinity that can form several types of weak bond interactions. The molecular complex is stable and has bioactivity as an inhibitor due to the drug-like nature of the molecule so that it is predicted to be a candidate as an anti-cancer drug.

ACKNOWLEDGEMENT

We appreciate and thank the governments Education Endowment Fund (LPDP) for funding this research.

AUTHOR'S CONTRIBUTION STATEMENT

RS and PAIS prepared the samples, designed and executed the protocol and also wrote the manuscript. LM and NFA reviewed the manuscript. NFA reviewed and supervised the manuscript.

FUNDING INFORMATION

This research received funding from a scientific research grant, an independent lecturer research scheme managed by LPDP.

DATA AVAILABILITY STATEMENT

The utilized data to contribute to this investigation are available from the corresponding author on reasonable request.

DISCLOSURE STATEMENT

The views and opinions expressed in this article are those of the authors and do not necessarily reflect the official policy or position of any affiliated agency of the authors. The data is the result of the author's research and has never been published in other journals.

REFERENCE

1. Gehrmann M, Specht HM, Bayer C, Brandstetter M, Chizzali B, Duma M, et al. Hsp70 - a biomarker for tumor detection and monitoring of outcome of

radiation therapy in patients with squamous cell carcinoma of the head and neck. Radiat Oncol. 2014;9:131. doi:10.1186/1748-717X-9-131.
2. Younas M, Hano C, Giglioli-Guivarc'h N, Abbasi BH. Mechanistic evaluation of phytochemicals in breast cancer remedy:current understanding and future perspectives. RSC Adv. 2018;8(52):29714-29744. doi:10.1039/C8RA04879G.
3. Nevins JR, Potti A. Mining gene expression profiles: expression signatures as cancer phenotypes. Nat Rev Genet 2007,8:601–609.
4. Lanneau D, Brunet M, Frisan E, Solary E, Fontenay M, Garrido C. Heat shock proteins: essential proteins for apoptosis regulation. J. Cell. Mol. Med. 2008;12(3):743-761. doi:10.1111/j.1582-4934.2008.00273.x.
5. Garrido C, Brunet M, Didelot C, Zermati Y, Schmitt E, Kroemer G. Heat shock proteins 27 and 70: antiapoptotic proteins with tumorigenic properties. Cell Cycle 2006;5:2592–601. doi: 10.4161/cc.5.22.3448.
6. Mosser DD, Caron AW, Bourget L, Meriin AB, Sherman MY, Morimoto RI, Massie B. The chaperone function of hsp70 is required for protection against stress-induced apoptosis. Mol Cell Biol. 2000;20:7146–59. doi:10.1128/MCB.20.19.7146-7159.2000.
7. Naderi A, Teschendorff AE, Barbosa-Morais NL, Pinder SE, Green AR, et al. A gene-expression signature to predict survival in breast cancer across independent data sets. Oncogene 2006, 26:1507–1516. doi:10.1038/sj.onc.1209920.
8. Solekha R, Setiyowati PAI, Sari CTU. Phytochemical Screening of Ethanol Extract on Stems, Leaves and Roots of Citronella Grass (Cymbopogon nardus L). 2022; 5(1);141-147. doi:10.30743/best.v5i1.5320.
9. Hartatie ES, Prihartini I, Widodo W, Wahyudi A. Bioactive Compounds of Citronella grass (Cymbopogon citratus) essential oil from different parts of the plant and distillation methods as natural antioxidant in broiler meat. IOP Conf Ser Mater Sci Eng. 2019;532(1). doi:10.1088/1757-899X/532/1/012018.
10. Li CC, Yu HF, Chang CH, Liu YT, Yao HT. Effects of citronella grass oil and citral on hepatic drug-metabolizing enzymes, oxidative stress, and acetaminophen toxicity in rats. J Food Drug Anal. 2018;26(1):432-438. doi:10.1016/j.jfda.2017.01.008.
11. Setiawati, A., Riswanto, F.D.O., Yuliani, S.H., Istyastono, E.P. Retrospective Validation of A StructureBased Virtual Screening Protocol To Identify Ligands For Estrogen Receptor Alpha and Its Application To Identify The Alpha-Mangostin Binding Pose. Indo J. Chem, 2014;14(2), 103-108. doi:10.22146/ijc.21245.
12. Setiyowati PAI, Solekha R, Negara SBSMK, Rosalina N. Immunomodulator Effect of Citronella grass Extract (Cymbopogon nardus L.) to Increase Immune Cells as a Precaution Against SARS-CoV-2. 2021. doi:10.20473/bhsj.v4i2.26619.
13. Amit Koparde A, Chandrashekar Doijad R, Shripal Magdum C. Natural Products in Drug Discovery. In: Pharmacognosy-Medicinal Plants. IntechOpen; 2019. doi:10.5772/intechopen.82860.
14. Saputra NA, Wibisono HS, Darmawan S, Pari G. Chemical composition of Cymbopogon nardus essential oil and its broad spectrum benefit. IOP Conf Ser Earth Environ Sci. 2020;415(1). doi:10.1088/1755-1315/415/1/012017.
15. Ansori ANM, Kharisma VD, Parikesit AA, Dian FA, Probojati RT, Rebezov M, Scherbakov P, Burkov P, Zhdanova G, Mikhalev A, Antonius Y, Pratama MRF, Sumantri NI, Sucipto TH, Zainul R. Bioactive Compounds from Mangosteen (Gracinia mangostana L.) as an Antiviral Agent via Dual Inhibitor Mechanism against SARS-CoV-2: An In Silico Approach. Pharmacogn J. 2022; 14(1): 85-90. doi: 10.5530/pj.2022.14.12.
16. Broni E, Kwofie SK, Asiedu SO, Miller WA 3rd, Wilson MD. A Molecular Modeling Approach to Identify Potential Antileishmanial Compounds Against

the Cell Division Cycle (cdc)-2-Related Kinase 12 (CRK12) Receptor of Leishmania donovani. Biomolecules. 2021;11(3):458.doi: 10.3390/biom11030458.
17. Dibha AF, Wahyuningsih S, Kharisma VD, Ansori ANM, Widyananda, MH, Parikesit AA, Rebezov M, Matrosova Y, Artyukhova S, Kenijz N, Kiseleva M, Jakhmola V, Zainul R. Biological activity of kencur (Kaempferia galanga L.) against SARS-CoV-2 main protease: In silico study. Int J Health Sci. 2022; 6(S1): 468-480. 10.1039/x0xx00000x.
18. Giordanetto F, Tyrchan C, Ulander J. Intramolecular Hydrogen Bond Expectations in Medicinal Chemistry. ACS Med Chem Lett. 2017; 8(2): 139-142. 10.1021/acsmedchemlett.7b00002
19. Kok BP, Ghimire S, Kim W, Chatterjee S, Johns T, Kitamura S, Eberhardt J, Ogasawara D, Xu J, Sukiasyan A, Kim SM, Godio C, Bittencourt JM, Cameron M, Galmozzi A, Forli S, Wolan DW, Cravatt BF, Boger DL, Saez E. Discovery of small-molecule enzyme activators by activity-based protein profiling. Nat Chem Biol. 2020 Sep;16(9):997-1005. doi: 10.1038/s41589-020-0555-4
20. Khan T, Dixit S, Ahmad R, Raza S, Azad I, Joshi S, Khan AR. Molecular docking, PASS analysis, bioactivity score prediction, synthesis, characterization and biological activity evaluation of a functionalized 2-butanone thiosemicarbazone ligand and its complexes. J Chem Biol. 2017; 10(3): 91-104. doi: 10.1007/s12154-017-0167-y.
21. Lee CM, Yen CH, Tzeng TY, Huang YZ, Chou KH, Chang TJ, Arthur Chen YM. Androgen response element of the glycine N-methyltransferase gene is located in the coding region of its first exon. Biosci Rep. 2013 Sep 17;33(5):e00070.
22. Luqman A, Kharisma VD, Ruiz RA, Götz F. In Silico and in Vitro Study of Trace Amines (TA) and Dopamine (DOP) Interaction with Human Alpha 1-Adrenergic Receptor and the Bacterial Adrenergic Receptor QseC. Cell Physiol Biochem. 2020; 54: 888-898. doi: 10.33594/000000276.
23. Nugraha AP, Rahmadhani D, Puspitaningrum MS, Rizqianti Y, Kharisma VD, Ernawati DS. Molecular docking of anthocyanins and ternatin in Clitoria ternatea as coronavirus disease oral manifestation therapy. J Adv Pharm Technol Res. 2021; 12 (4): 362-367. doi: 10.4103/japtr.japtr_126_21.
24. C, Nugraha AP, Kharisma VD, Ansori ANM, Devijanti R, Ridwan TPSP, Ramadhani NF, Narmada IB, Ardani IGAW, Noor TNEBA. A bioinformatic approach of hydroxyapatite and polymethylmethacrylate composite exploration as dental implant biomaterial. J Pharm & Pharmacogn Res. 2021; 9(5): 746-754. doi: 10. 21.1078_9.5.746
25. Proboningrat A, Kharisma VD, Ansori ANM, Rahmawati R, Fadholly A, Posa GAV, Sudjarwo SA, Rantam FA, Achmad AB. In silico Study of Natural inhibitors for Human papillomavirus-18 E6 protein. Res J Pharm Technol. 2022; 15(3):1251-6. doi:10.52711/0974-360X.2022.00209.
26. Rietman EA, Platig J, Tuszynski JA, Lakka Klement G. Thermodynamic measures of cancer: Gibbs free energy and entropy of protein-protein interactions. J Biol Phys. 2016; 42(3): 339-50. doi:10.1007/s10867-016-9410-y.
27. Rigsby RE, Parker AB. Using the PyMOL application to reinforce visual understanding of protein structure. Biochem Mol Biol Educ. 2016 Sep 10;44(5):433-7. doi:10.1002/bmb.20966.
28. Saddala MS, Huang H. Identification of novel inhibitors for TNFα, TNFR1 and TNFα-TNFR1 complex using pharmacophore-based approaches. J Transl Med. 2019 Jul 2;17(1):215. Doi:10.1186/s12967-019-1965-5.
29. Seo JH, Park JH, Lee EJ, Vo TT, Choi H, Kim JY, Jang JK, Wee HJ, Lee HS, Jang SH, Park ZY, Jeong J, Lee KJ, Seok SH, Park JY, Lee BJ, Lee MN, Oh GT, Kim KW. ARD1-mediated Hsp70 acetylation balances stress-induced

protein refolding and degradation. Nat Commun. 2016 Oct 6;7:12882. doi: 10.1111/all.13465.
30. Sharma P, Shanavas A. Natural derivatives with dual binding potential against SARS-CoV-2 main protease and human ACE2 possess low oral bioavailability: a brief computational analysis. J Biomol Struct Dyn. 2021; 39(15): 5819-5830. doi: 10.1080/07391102.2020.1794970.
31. Susanto H, Kharisma VD, Listyorini D, Taufiq A. Effectivity of Black Tea Polyphenol in Adipogenesis Related IGF-1 and Its Receptor Pathway Through In Silico Based Study. J Phys Conf Ser. 2019; 1093 (1): 012037. doi :10.1088/1742-6596/1093/1/012037.
32. Wijaya RM, Hafidzhah MA, Kharisma VD, Ansori ANM, Parikesit AA. COVID-19 In Silico Drug with Zingiber officinale Natural Product Compound Library Targeting the Mpro Protein. Makara J Sci. 2021; 25(3): 162-171. 10.7454/mss.v25i3.1244
33. Ciocca DR, Arrigo AP, Calderwood SK. Heat shock proteins and heat shock factor-1 in carcinogenesis and tumor development: an update. Arch Toxicol. 2013;87(1):19–48. doi:10.1007/s00204-012-0918-z.
34. Dakappagari N, Neely L, Tangri S, Lundgren K, Hipolito L, Estrellado A, et al. An investigation into the potential use of serum Hsp70 as a novel tumour biomarker for Hsp90 inhibitors. Biomarkers. 2010;15(1):31–8. doi:10.3109/13547500903261347.
35. Multhoff G, Botzler C, Wiesnet M, Müller E, Meier T, Wilmanns W, et al. A stress-inducible 72-kDa heat-shock protein (HSP72) is expressed on the surface of human tumor cells, but not on normal cells. Int J Cancer. 1995;61(2):272–9. doi: 10.1002/ijc.2910610222.
36. Ferrarini M, Heltai S, Zocchi MR, Rugarli C. Unusual expression and localization of heat-shock proteins in human tumor cells. Int J Cancer. 1992;51(4):613–9. doi: 10.1002/ijc.2910510418.
37. Hantschel M, Pfister K, Jordan A, Scholz R, Andreesen R, Schmitz G, et al. Hsp70 plasma membrane expression on primary tumor biopsy material and bone marrow of leukemic patients. Cell Stress Chaperones. 2000;5(5):438–42. PMC312874. 10.1379/1466-1268(2000)005<0438:hpmeop>2.0.co;2.
38. Aghdassi A, Phillips P, Dudeja V, Dhaulakhandi D, Sharif R, Dawra R, et al. Heat shock protein 70 increases tumorigenicity and inhibits apoptosis in pancreatic adenocarcinoma. Cancer Res. 2007;67(2):616–25. doi: 10.1158/0008-5472.CAN-06-1567.
39. Garrido C, Gurbuxani S, Ravagnan L, Kroemer G. Heat shock proteins: endogenous modulators of apoptotic cell death. Biochem Biophys Res Commun. 2001;286(3):433–42. doi:10.1006/bbrc.2001.5427.
40. Jäättelä M, Wissing D, Kokholm K, Kallunki T, Egeblad M. Hsp70 exerts its anti-apoptotic function downstream of caspase-3-like proteases. EMBO J. 1998;17(21):6124–34. doi:10.1093/emboj/17.21.6124. 11.
41. Gao Y, Han C, Huang H, Xin Y, Xu Y, Luo L, et al. Heat shock protein 70 together with its co-chaperone CHIP inhibits TNF-alpha induced apoptosis by promoting proteasomal degradation of apoptosis signal-regulating kinase1. Apoptosis. 2010;15(7):822–33. doi:10.1007/s10495-010-0495-7.
42. Yang X, Wang J, Zhou Y, Wang Y, Wang S, Zhang W. Hsp70 promotes chemoresistance by blocking Bax mitochondrial translocation in ovarian cancer cells. Cancer Lett. 2012;321(2):137–43. doi:10.1016/j.canlet.2012.01.030.
43. Kirkegaard T, Roth AG, Petersen NH, Mahalka AK, Olsen OD, Moilanen I, et al. Hsp70 stabilizes lysosomes and reverts Niemann-Pick disease-associated lysosomal pathology. Nature. 2010;463(7280):549–53. doi:10.1038/nature08710.
44. Bayer C, Liebhardt ME, Schmid TE, Trajkovic-Arsic M, Hube K, Specht HM, et al. Validation of heat shock protein 70 as a tumor-specific biomarker for

monitoring the outcome of radiation therapy in tumor mouse models. Int J Radiat Oncol Biol Phys. 2014;88(3):694–700. doi:10.1016/j.ijrobp.2013.11.008.
45. Stangl S, Varga J, Freysoldt B, Trajkovic-Arsic M, Siveke JT, Greten FR, et al. Selective in vivo imaging of syngeneic, spontaneous, and xenograft tumors using a novel tumor cell-specific Hsp70 peptide-based probe. Cancer Res. 2014;74(23):6903–12. doi:10.1158/0008-5472.CAN-14-0413.
46. Gehrmann M, Stangl S, Foulds GA, Oellinger R, Breuninger S, Rad R, et al. Tumor imaging and targeting potential of an Hsp70-derived 14-mer peptide. PLoS One. 2014;9(8):e105344. doi:10.1371/journal.pone.0105344.